11 33 3

IITRI Project No. G-6002

DEVELOPMENT OF LIGHTWEIGHT
THERMAL INSULATION MATERIALS
FOR RIGID HEAT SHIELDS

National Aeronautics and Space Administration
George C. Marshall Space Flight Center
Huntsville, Alabama 35812

IIT RESEARCH INSTITUTE
10 West 35th Street
Chicago, Illinois   60616

DEVELOPMENT OF LIGHTWEIGHT

THERMAL INSULATION MATERIALS

FOR RIGID HEAT SHIELDS

IITRI G-6002-27
Final Summary Report
for the period
June 25, 1964 to September 25, 1966
Contract No. NAS 8-11333

Prepared by

A. J. Mountvala
H. H. Nakamura

for

National Aeronautics and Space Administration
George C. Marshall Space Flight Center
Huntsville, Alabama   35812

Attention: Mr. V. Seitzinger
Project Manager
Propulsion & Vehicle Engineering Laboratory
Materials Division

October 1966

ACKNOWLEDGMENTS

IIT RESEARCH INSTITUTE

DEVELOPMENT OF LIGHTWEIGHT
THERMAL INSULATION MATERIALS
FOR RIGID HEAT SHIELDS

ABSTRACT

Exposed structural members at the base of large, high-thrust rocket engines are subject to excessive heating, largely radiative, from the engine exhaust. A program of engineering and scientific research has been carried out to develop light-weight ceramic foams which will provide adequate insulation and survive the mechanical environment associated with launch operations.

Castable ceramic foams of zircon, mullite, and calcium aluminate have been prepared and evaluated for use as rigid heat shields in launch vehicles. The effects of various additives, including fibers and opacifying materials, on zircon foams have been investigated. Comparative properties and the performance of silicate - and phosphate-bonded zircon foams have been investigated. Work has also been done on prefired zircon foams. Chemical and engineering factors critical to a "scaled-up" process for preparing the castable foams were investigated.

Chemically bonded, castable type zircon foams have been optimized to meet certain specific requirements. These foams of 1/2 in. thickness show good insulative and mechanical characteristics when subjected to a heat flux of 40 Btu/ft^2-sec with simultaneous vibration of 60 cps, 1/2 in. double amplitude displacement and 90 g's acceleration, as well as to a specific sinusoidal sweep-random vibrational test up to 2000 cps. Property measurements on an optimized zircon foam disclosed very high optical reflectance in the near-infrared wavelength region and an extremely low thermal conductivity to 2300°F.

A comprehensive literature survey on foamed ceramics was also carried out, which includes information on commercially available materials and their properties, as obtained from certain manufacturers. A computer program to theoretically evaluate the thermal analysis on foamed insulation is also presented.

CONTENTS

LIST OF ILLUSTRATIONS

LIST OF TABLES

LIST OF TABLES (Cont'd)

DEVELOPMENT OF LIGHTWEIGHT
THERMAL INSULATION MATERIALS
FOR RIGID HEAT SHIELDS

I. INTRODUCTION

This is the final summary report under NASA contract NAS 8-11333 for the development of lightweight thermal insulation materials for rigid heat shields.

The severity of radiation and convection heating from the engine plumes of high-thrust rocket engines requires the use of inorganic insulation materials that must meet certain specific requirements. Mechanical integrity is also a critical factor because of the acceleration and high vibrational forces that are present during lift-off and powered stages of flight. Therefore, the optimum insulation required for such applications should display certain characteristics such as low density, low thermal conductivity, good mechanical strength, thermal shock resistance, and good adhesion to metal substrates. Further, since the insulation is required primarily for applications in a radiant heating environment, the insulation material should have desirable reflective properties over the wavelength range of 1.0 to 2.4 microns.

Foamed ceramic composites, containing dispersed phases and fibers, have demonstrated a potential for use in rigid heat shields. Specifically, the foamed ceramics developed under this program have a bulk density not greater than 60 lb/ft^3. Further, the foam insulations that have been developed are such that the structures to be shielded do not exceed 400°F in 300 sec when subjected to a heat flux of 40 Btu/ft^2-sec and simultaneous vibrations of 60 cps with a double amplitude displacement of 1/2 in. and an acceleration level up to 90 g's. The foams were also successfully subjected to a specific sinusoidal vibration

profile, followed by random vibration simultaneous with a heat flux of 40 Btu/ft^2-sec.

Major emphasis has been on developing chemically bonded, castable type zircon foams containing fibers and other additives. These foams were prepared by mechanical whipping, using egg albumin as the foaming agent. Both silicate and phosphate binder systems were utilized. Although optimization to meet the program requirements was carried out on composite zircon foams, mullite and calcium aluminate foams were also investigated.

A computer program for predicting the performance of foamed ceramics as thermal insulators as a function of certain parameters was performed, and is presented in this report.

A comprehensive literature and technical survey on foamed ceramics was carried out. This includes information gathered from technical journals, reports, and patent literature, together with data gathered from prominent manufacturers by way of a technical questionnaire.

II. THERMAL ANALYSIS OF FOAMED CERAMIC INSULATORS

A. Introduction

The ability of a material to perform as a thermal insulator is dependent upon its thermal properties and the application in which it is used. Since the roles of thermal conductivity, specific heat, density, emittance, and absorptivity are not evident in determining the effectiveness of an insulator, a thermal analysis to determine the influence of these properties in the present application was undertaken.

The computer program for predicting the performance of foamed ceramics as insulators have been developed in the Fortran II language for use on the IBM 7090 computer. This program has been used to carry out a comprehensive parametric study of the heat-transfer system. The insulation performance has been

evaluated over a broad range of thermal properties, and the influence of various thermal properties upon performance has been determined.

B. Thermal Analysis

A numerical analysis of the thermal properties of foamed insulation was carried out. In this analysis, a one-dimensional steady-state equation was set up, together with the radiation boundary condition at the insulation-substrate interface. The nonsteady, radiant heating of a material has been analytically treated to determine the temperature distribution in an infinite plate subjected to a radiant heat flux. An insulation-substrate boundary condition has been assumed, wherein the substrate is uniform in temperature throughout. This is undoubtedly true since the substrate conductivity and diffusivity will be large in comparison to that of the insulation.

The functional variations of thermal conductivity, rate of change of thermal conductivity with temperature, and emittance and specific heat with temperature have been incorporated into four subroutines so that the functional relationships can be altered with ease for a particular material.

By non-dimensionalizing the differential equation and the boundary conditions for the case of constant thermal properties, pertinent groups of problem parameters are obtained. This procedure yields the following expression which relates insulation weight, density (ρ), specific heat (C_p), thermal conductivity (k), absorptance (α), incident heat flux (q), and emittance (ϵ).

$$\frac{W''}{\rho} = (\rho C_p k, \alpha q'', \epsilon)$$

where W'' = weight per unit area of insulation (W'' = ρL)

L = insulation thickness

A parametric study has been performed employing the computer program by allowing $\rho C_p k$, $\alpha q''$, and ε to vary over suitable ranges and calculating the corresponding values of W''/k. Thus, for a given material with known density and thermal properties, the thickness of insulation (and therefore its weight) required to yield the desired interface temperature after the prescribed heating time can be determined from this study. Alternately, for a prescribed thickness the values of absorptance, emittance, density, specific heat, and thermal conductivity required to provide the desired performance are delineated.

The parametric study was performed for the following conditions:

Initial temperature = 540°R = 80°F

Heating time = 150 sec

Interface temperature (at t = 150 sec) = 960°R = 500°F

Substrate parameter $(M''C_{p,s}) = 0.0662$ Btu/ft^2-°F

Results of the parametric study are presented in the following section.

C. Results of the Analysis

Results of the analysis have yielded a set of curves that indicate the dependence of the pertinent parameters involved in the thermal performance of foamed ceramic insulation. The parameters that have been considered are thermal conductivity, specific heat, density, emissivity, absorptance, thickness, and front and backface temperatures of the ceramic insulation for various heat fluxes.

In Fig. 1 the insulation on weight parameter $(W''/\rho k)$ is shown as a function of $\rho C_p k$ for various values of the absorbed heat flux ($\alpha q''$) and emittance (ε). The most obvious conclusion that can be made from Fig. 1 is that the surface emittance has very little influence in the determination of the required insulation thickness. However, the emittance is of

some consequence for very low values of $\rho C_p k$. It should be noted, however, since this study was performed for constant thermal properties, that the dependence of thermal conductivity of a foamed material upon emittance at high temperatures was not considered. Should the thermal conductivity of foam materials be greatly dependent upon emittance, a low-emittance material can be employed without suffering any significant weight penalties. The savings in weight that can be obtained for a given heat flux by employing a material with low absorptance is shown clearly in this figure. Given a material with known thermal properties, the thickness of insulation required can be determined from this figure.

Figure 2 shows the insulation surface temperature as a function of $\rho C_p k$ for various values of emittance and absorbed heat flux. Emittance plays a larger role in determining the magnitude of the surface temperature. Here again, for a given heat flux, a low absorptance is desirable to maintain lower surface temperatures.

In Figs. 3a and 3b the data have been replotted for the two pertinent heating rates to make the influence of absorptance upon the required insulation weight (or thickness) clear. Great savings in weight or reductions in the other thermal property requirements can be obtained by employing a material with low absorptance.

The minimum volumetric specific heat (ρC_p) required to produce the desired performance is shown in Fig. 4 as a function of thermal conductivity for an insulation thickness of 1 in. For the lower values of absorbed heat flux, little reduction in the specific heat requirement is obtained by reducing thermal conductivity until very low values of conductivity are approached. If the reductions in thermal conductivity are obtained by decreasing the insulation density, it is possible that no savings

will occur; a penalty may be incurred since the volumetric specific heat of a material decreases with density. To fully investigate the role of conductivity, an analytical relationship between thermal conductivity and density is required.

The data of Fig. 4 are replotted in Figs. 5a and 5b to show the reductions in the volumetric specific heat requirement that are obtained by reducing the absorptance of the two pertinent heating rates. For all values of thermal conductivity, significant savings in the volumetric specific heat requirements can be obtained by reducing the absorptance.

To investigate the influence of the substrate upon the insulation performance, the insulation weight parameter was calculated for various values of $\rho C_p k$ and the substrate parameter. Results of these calculations are shown in Fig. 6.

To investigate the merits of reducing thermal conductivity by decreasing the foam density (i.e., increasing porosity) the dependence of thermal conductivity on density was taken as:

$$\frac{k}{k_s} = A \left(\frac{\rho}{\rho_s}\right)^n$$

where 　A 　= constant

　　　　ρ_s = density of the solid material

　　　　k_s = thermal conductivity of the solid material

　　　　n 　= constant

The above expression has been used in conjunction with parametric study results to yield the influence of decreasing density (hence, decreasing thermal conductivity). In Fig. 7 an insulation weight parameter ($W''C_p$) is shown as a function of density $\rho_s C_p k_s A (\rho/\rho_s)^{n+1}$. The weight of insulation required decreases with decreasing density -- with the rate of this decrease depending upon the absorbed heat flux. It should be noted that for

the form of conductivity-density variation assumed, the weight requirement is independent of n. An insulation thickness parameter $(L^2 \rho_s C_p / k_s A)$ is shown as a function of density in Fig. 8 for the case n = 1. The thickness of insulation required increases with decreasing density, with the rate of increase again depending upon the absorbed heat flux. Fig. 8 was plotted for n = 1, since this value is a fair approximation of the true variation.

The thermal analysis is useful in understanding effects of various parameters on the performance of an insulator and permits us to achieve property interchanges. By knowing some of the basic properties of the foamed material, it is then possible to determine what other characteristics are of importance for the insulator to perform under a particular heat flux. For instance, from Fig. 1, we know that the emittance does not have any significant effect on the thickness of insulation required. Therefore, in preparing the ceramic foams for our application, it is not necessary to coat the surface with a material of high emittance. The thickness required and the surface temperature at the insulation can also be determined for materials of various densities and thermal conductivities by the use of Figs. 1 and 2.

Several important conclusions can be made from the results of the parameter study:

1. The surface emittance of the insulation has only a slight effect upon the thickness of insulation required; however, surface temperature increases significantly with decreasing emittance. If the higher temperatures can be tolerated, a low emittance material should be employed so that radiant heat exchange within the foam will be lowered.

2. The surface absorptance is by far the most important parameter problem. Efforts should be made to reduce the absorptance as much as possible.

IIT RESEARCH INSTITUTE

3. For a constant density, reductions in thermal conductivity will lead to savings in insulation weight or in the volumetric specific heat requirement. The relative merits of reducing thermal conductivity depends upon the manner in which it is reduced, the range over which it can be altered, and the absorptance.

Results obtained from the parameter study have been used as guidelines in the preparation of composite foams with optimized insulative properties. The experimental program is presented in the subsequent sections.

III. LITERATURE AND TECHNICAL SURVEY

This survey on the preparation and properties of "foamed" ceramic thermal insulation was part of a broader program whose ultimate objective was the development of lightweight foamed ceramics in a modified or tailored form, designed to withstand the thermal radiation and vibrations encountered in the launching of space vehicles. A literature survey was conducted to determine the current state-of-the-art and the performance characteristics of currently available foamed ceramics having a melting point in excess of 2500°F. The primary purpose of this survey was to integrate all available data on foamed ceramics and to critically evaluate this information in light of the program's current and future needs.

This survey includes information gathered from technical journals, reports, and patent literature together with information gathered from prominent manufacturers by way of a technical questionnaire.

The detailed findings of the survey were presented in Summary Report No. 1 (dated June 25, 1965), and therefore will only be summarized in this report.

Although considerable data have been reported on the mechanical and thermal properties of foamed oxides, much of it

is unreliable and very poorly characterized for microstructural variations. This is evident in the wide scatter of reported properties, which makes correlation between physical properties and mechanical and thermal characteristics difficult.

The survey bears out some definite trends about the present state-of-the-art of foamed ceramic insulation materials. First, much of the reported data are for far higher temperature refractory foams than the range required for our application. There are considerable data available for resin-impregnated ablation forms, most of them having a density greater than 60 lb/ft^3. Secondly, there is a lack of useful information on the reflective and emissive properties of ceramic foams. Thirdly, very little attention has been paid to characterizing the properties of these foams as a function of their micropore structure. This is especially important if one is to understand the thermal radiation characteristics of semi-transparent materials such as polycrystalline ceramics, where radiant energy emission is a volume process, and therefore, influenced by the microstructure of the foamed material.

An analysis of the technical questionnaire which was sent to some thirty prominent manufacturers, indicated that silica and alumina foams are the most commonly available materials. A stabilized zirconia foam is also commercially available. One organization reported that they are developing magnesia and thoria foams, most of which are prefired foams.

Compressive strength, flexural strength, and thermal conductivity are the most easily available properties that have been measured by manufacturers. A limited amount of information is available on the emittance values of some of the foams. No data were obtained on the reflectance of any of these foams.

IV. PREPARATION OF CERAMIC FOAMS

A. General Procedure

A number of techniques are available for preparing ceramic foams. However, on the basis of previous work carried out at IITRI, the method of mechanical whipping using an air-entraining agent was selected for preparing zircon, mullite, and calcium aluminate foams. A major part of the experimental effort has been in the preparation of chemically bonded, castable type foams that can be effectively cured at temperatures not exceeding 400°F. Such a curing process is essential for use with large size structural members. Some work was also done on fired foams.

1. Mechanical Whipping Technique

The foaming, on a laboratory scale, has been carried out with a Sunbeam Mixmaster as well as a Hobart mixer for larger batches. When the albumin is dissolved and the binder added to the solution, the mixer is turned to the lowest speed (approximately 270 rpm). With the mixer at this low speed, the solids (previously ball-milled) are added to the mix. This low speed is continued for 1 min after all the solids have been added to assure thorough wetting of the materials. The speed is then increased to the maximum (approximately 920 rpm), and held for 2 to 3 min depending upon the solids used to give the desired foam structure. When "Fiberfrax" is included in the foam composition, this material is added to the water-albumin-binder solution and wetted for 1 min before the addition of the ball-milled solids. The subsequent operations are similar to those described above.

Two types of binders have been investigated: the first is potassium silicate, and the second is monoaluminum phosphate. Depending upon the binder system, various additives have been used. The detailed process for preparation of silicate-bonded

and phosphate-bonded castable zircon foams has been described in Appendix A.

2. Drying and Curing the Foam

Drying was done by infrared lamps. The coated substrate panels and honeycombs were removed from the oven and, while still hot, the foam was cast. The foam was immediately placed in the infrared dryer using the bottom lamps only. Pre-heating the metal substrate at around 115°F decreases the amount of stress that the foam must overcome when they are cured at 240°F. As a consequence, well-bonded foams with minimum cracks were obtained. An alternate modification during the drying process entails the use of a plastic wrapping cover (such as Saran Wrap) in direct contact with the top surface of the foam or held above it during drying.

When a plastic wrapping is not used, a hard surface skin is formed on the foam, especially with silicate-bonded zircon foams, due to the upward migration of the potassium silicate and zircon during drying. Consequently, insolubilization of the binder is reduced and differential shrinkage is significant, giving rise to some surface cracks.

The plastic wrapping minimizes the formation of the hard surface skin by drastically reducing the rate of evaporation of moisture from the foam surface, thus permitting more complete insolubilization of the binder. This not only results in a stronger bonded foam body, but also prevents the formation of surface cracks. However, the top surface is not as hard as that obtained without the use of the plastic wrapper. By using the plastic-wrap cover for only part of the drying procedure, it was possible to prepare zircon foams with a crack-free surface which retained considerable hardness at the surface.

The curing cycle for a Z-88 foam, 9 x 9 x 1/2 in., cast on a honeycomb substrate is shown in Fig. 9. The temperature

at the bottom of the honeycomb substrate was monitored during the curing cycle. A similar curing cycle was also used for preparing 12 x 12 x 1/2 in. specimens on stainless steel plate substrates.

B.   Zircon Foams

1.   Introduction

The major emphasis has been in the preparation of zircon foams because this material has certain properties that make it attractive for rigid heat shield applications. It has good resistance to thermal shock, a low coefficient of thermal expansion, a low thermal conductivity, and a density intermediate to that of alumina and zirconia. Besides, it offers a potential for tailoring the foam with second-phase additives to alter its radiation scattering characteristics.

2.   Silicate-Bonded Foams

a.   Compositional Factors

On the basis of a large number of zircon foams prepared and subsequently evaluated for their insulative and mechanical characteristics (see Sections V and VI), nearly optimized foam compositions were developed. These were cast directly onto honeycomb substrates. The nominal compositions and characteristics of these foams are shown in Table 1.

Zircon powders of various particle sizes have been used for preparing the foams. A detailed characterization of the raw materials used in the experimental foam formulations, indicating the source of these materials, has been presented in Appendix A. The materials designated as "Zircon","Zircon A", and "Superpax" were obtained from Titanium Alloy Manufacturing Corporation. The first has an average particle size less than 44 microns, 1% +200 mesh, and 10% +325 mesh; the second type of powder (Zircon A) has an average particle size less than 44 microns, 0.1% +325 mesh; and the Superpax has an average particle size less than 4 microns, 0.1% +325 mesh.

Table I

CHARACTERISTICS OF CASTABLE SILICATE-BONDED ZIRCON FOAMS
(1/2 IN. THICK) ON HONEYCOMB SUBSTRATES

Foam No.	Nominal Composition										Foam Density (lb/ft^3)	Comments
	Zircon (g)	Zircon A (g)	Superfrax (g)	Water (cc)	Albumin (g)	PS-7 (cc)	Na$_2$SiF$_6$ (g)	Clay (g)	Fiberfrax (g)	Other Additives		
2-69	200	200	100	80	5	100	22.6	8	12	–	52	Specimens prepared with and without plastic wrap. Good foams.
2-70	200	200	155	70	12	198	25.4	12	18	–	48	Plastic wrap covered, no skin, good bonding. Painted with nickel subcoat and zircon surface coat.
2-75	200	200	–	74	4	80	16.9	8	28	Gr. Zircon 12 g	67	Plastic wrap only after 1 hr. drying. Good bonding.
2-76	200	200	–	75	4	80	16.9	8	40	–	51	Plastic wrap only after 1/2 hr. drying. Very little skin formation.
2-77	300	200	155	80	6	198	25.4	12	56	–	42	Plastic wrap only after 1/2 hr. drying. Partial skin formed. No cracks.
2-77	200	200	155	90	6	198	25.4	12	56	Gr. Zircon 12 g	45	Plastic wrap not used; surface skin; faint cracks.
2-78	200	200	100	75	2	132	16.9	8	40	Gr. Zircon 12 g	57	Skin type, faint vertical cracks.
2-82	200	200	100	75	2	132	16.9	8	40	–	48	Plastic wrap after 1/2 hr. drying. Partial skin, no surface cracks.
2-84	200	200	100	75	1.5	132	16.9	8	40	–	56	Plastic wrap after 1 hr. drying. Partial skin, very faint surface cracks.
2-85	200	150	150	75	1.4	132	16.9	8	40	–	60	Several specimens prepared with and without plastic wrap cover. Good foam, well bonded.
2-86	200	200	–	75	1.2	132	16.9	8	40	Gr. Zircon 12 g	57	Foam prepared with and without plastic wrap cover.
2-89	200	200	–	60	1.2	132	16.9	8	40	–	52	Foam prepared with plastic wrap cover. No surface cracks. Well bonded.
2-90	200	200	–	60	1.2	132	16.9	8	40 (fine)	–	59	Foam prepared with partial use and without plastic wrap. No cracks, well bonded.

-13-

Optimized foams are based on a composition which contains Superpax A with no granular zircon (Z-87) and compositions which contain no Superpax with or without granular zircon (Z-88 to Z-90). These foams are approximately 55-60 lb/ft^3 in density, and all contain 10 wt% Fiberfrax (medium diameter) based on the zircon powders with the exception of Z-90, which contains fine diameter Fiberfrax. Figure 10 is a photomicrograph of foam Z-90. In all cases it has been possible to prepare a foam specimen with either a hard surface skin, partial skin, or no surface skin. This is possible by controlling the time during curing when a plastic wrapping cover is used. The least skin effect is obtained when such a wrap is used for the longest time. The insulative and mechanical properties of these nearly optimized foams as a function of their surface properties have been discussed in subsequent sections.

b. Process Control and Characteristics
   of Scaled-Up Foams

In optimizing the castable zircon foams during the first year of this program, foam preparation was carried out in batches containing no more than 400g of the zircon powders. In preparing larger batches, for example, of 3000g of zircon, the final foam density is difficult to control on the basis of the foaming speed and time. To this end, we have devised a simple and straightforward "wet density" evaluation which can be correlated with the final foam density. This has proved to be reproducible for the silicate-bonded zircon foams in batches with zircon content ranging from 300 to 3000g prepared both in the Sunbeam Mixmaster and the Hobart mixer. Minor variations in foam compositions have not been found to affect correlation between the wet and the final densities. Figure 11 shows the relationship between the wet and final densities of some silicate-bonded zircon foams. These foams are essentially modifications of Z-89.

Results obtained on scaled-up foamed structures indicate that migration of the binder is greater in larger dimensioned specimens than in the smaller test specimens. To resolve these problems, modified compositions more suitable to scaled-up foaming and curing processes have been investigated. These modifications are based on the amounts and the ratio of PS-7 (i.e., potassium silicate binder) and sodium silicofluoride (Na_2SiF_6) which is essentially a "placement" material for the PS-7. The experiments are discussed in the subsequent paragraphs.

Due to the problems encountered during scale-up and in order to increase the tensile strength of the silicate-bonded zircon foams, the effects of certain compositional modifications have been studied. The modifications have been carried out on compositions based on Z-89 and Z-90. Table II shows the constituents that have been varied. All foams shown in this Table contain 400g zircon, 8g clay, albumin (1.2-1.4g) and water (50-70cc). The amounts of albumin and water have been varied to control foam density, and these slight variations do not affect the foam strength, since all foams have a similar micropore structure. Variables that have been considered are the amounts and ratio of the PS-7 and Na_2SiF_6, as well as the type (fine or medium diameter) and percentage of Fiberfrax fibers. Tensile strength values of the foams are also shown in Table II. The values were obtained on 2 x 2 in. specimens prepared from a starting mix containing 400g zircon. The quantity of the starting mix seems to significantly affect tensile strength of the foams, as will be discussed in subsequent paragraphs.

The results shown in Table II can only be correlated by taking into consideration the significant effect of density upon the tensile strength. It seems that an increase in the amount of PS-7 is beneficial, especially in the preparation of large batches. It is difficult, due to the preliminary nature of the experimental evidence, to draw any definite conclusions on the effects of the percentage of fibers added. Both Z-110 and Z-111, which contain 15

Table II

COMPOSITIONS AND PROPERTIES OF MODIFIED

SILICATE-BONDED ZIRCON FOAMS

Foam No.	PS-7 (cc.)	Na$_2$SiF$_6$ (g.)	PS-7/Na$_2$SiF$_6$	Fiberfrax (g.)	Foam Density (lb/ft^3)	Tensile Strength (psi)
Z 89 NS	132	16.9	7.8	40 m* (10%)	57	70-45
Z 108 NS	150	19.0	7.9	40 m	44	29
Z 109 NS	150	21.75	6.9	40 m	57	48
Z 110 NS	150	21.75	6.9	60 m (15%)	77	97
Z 111 NS	150	21.75	6.9	80 m (20%)	60	33
Z 112 NS	150	21.75	6.9	20 m (5%)	70	58
Z 90 NS	132	16.9	7.8	40 f* (10%)	64	39
Z 103 NS	132	16.9	7.8	20 f (5%)	60	63
Z 104 NS	150	19.0	7.9	20 f	58	78-45
Z 105 NS	150	17.0	8.8	20 f	65	44

*m - medium long staple fiberfrax

f - fine long staple fiberfrax

and 20 wt% fibers (medium), respectively, as compared to Z-89, Z-108 and Z-109 which contains 10 wt% fibers, failed closer to the interface rather than within the foam. On the other hand, Z-112 which contains only 5 wt% fibers did not break entirely within the foam either. It is conceivable that strengthening within the foam body causes high stresses at the interface, thereby resulting in interfacial failure. However, further experimentation is necessary to establish the quantitative effects of fiber addition.

All silicate-bonded zircon foams shown in Table II were subjected to a maximum curing temperature of ~260°F. The effects of a higher curing temperature on the tensile strength were investigated in the case of Z-112. Foams cured at 260°F had tensile strengths averaging 63 psi, and failure was partly at the interface and partly within the foam. However, when similar foams (identical density) were subjected to a maximum curing temperature of 400°F, average tensile strength was 37 psi and failure was interfacial. This concurs with earlier evidence that in the case of castable zircon foams a higher curing temperature causes high stresses at the interface which weakens the foam-substrate bonds.

Compositional modifications to foam Z-89 for binder stabilization and strength increases were also investigated. The substitution of 25 wt% zirconia or 25 wt% alumina in the starting zircon mix did not improve the tensile strength of the foams. Curing at a higher temperature of 400°F, in fact, gave lower tensile strength values. The additions of 25 wt% zirconia or alumina does not seem to prevent interfacial breaks.

The mixing and foaming processes themselves play a significant role in scale-up and on the tensile strength of the foams. This is shown by the results presented in Table III. Three batches -- the first containing 400g zircon in the mix, the next with 800g zircon, and the third containing 3000g zircon -- were used to prepare foams cast on a 2 x 2 in. substrate. On testing these identically sized foams,

Table III

EFFECT OF SCALE-UP ON TENSILE STRENGTH

OF Z-109 (DENSITY 60 lb/ft^3)

Amt of Zircon in Starting Mix	Tensile Strength* of Foam
(g)	(psi)
400	63
800	39
3000	36

*Measured on 2 x 2 in. specimens

prepared from varying quantities of starting mixes, a definite decrease in tensile strength was recorded as the degree of scale-up increased. The variation in tensile strength within a foam cast on a large size substrate (12 x 12 in.) is itself a critical factor. The results in Table III show that the mixing and foaming processes in scale-up also cause variations in the strength of these foams. It is believed that in preparing larger batches, disproportionation of some of the constituents, especially the binder (PS-7) and the "placement materials" (Na_2SiF_6 and/or clay), may be a factor, and therefore a correspondingly linear increase of the materials may be inadequate. The distribution of the binder and the "placement" materials in a foamed mix may well be a function of the volume and surface area of the mixture. For example, when a chemical precipitation process is scaled-up, the larger volume and lower wall-to-volume ratio will produce larger particle sizes. This is considered normal when attempting to correlate the effects of small-sized equipment to the behavior of larger units where reactions more complicated than a second order are employed.

c.   Discussion

The foams optimized for rigid heat shields are essentially castable zircon foams, chemically-bonded with potassium silicate and containing certain additives. In concept they may be considered "composite" ceramic foams. A typical optimized foam contains the following nominal constituents: zircon, albumin, potassium silicate, clay, Na_2SiF_6, and dispersed Fiberfrax fibers. Although the functional characteristics of the various additives are known, the exact reactions involved are at best speculative.

The foaming action is obtained by mechanical whipping of the mix, using albumin as the foaming agent. The albumin, which is a surface-active protein-based agent, stabilizes the entrained air structure.

The binder system is potassium silicate. The commercial potassium silicate binders usually range in composition from $K_2O \cdot 3.9SiO_2$ to $K_2O \cdot 3SiO_2$. On appropriate drying and curing, the binder is essentially in the form of a highly polymerized potassium silicate. Its adhesion properties are caused by the reactivity of the Si-O-K groups.

For the adhesive to perform its function, it must undergo a large increase in viscosity and maintain its integrity in the form of a thin film across the interconnecting pores of the foamed material. Clay added to the mix acts as an extender and stabilizes the foamed body. It also aids in the retention of the solids in supension, and the clay maintains a suitable viscosity when added to silicate solutions. The addition of clay could also contribute to the integrity of the silicate viscous film across the pores by promoting the easy release of water and preventing the foaming or disruption of the binder film.

The beneficial effect observed on adding the Na_2SiF_6 along with the clay to the mix, was that it prevented the excessive migration of the binder upon curing. Migration of the binder results in a weakened foam. We can speculate on the beneficial roles of the Na_2SiF_6 addition. Sodium silicofluoride (Na_2SiF_6) increases the rate of gelation, thereby preventing excessive migration of the binder. It probably acts as a deflocculant further extending the clay. Deflocculation produces a homogeneous mass with less water, thus facilitating the drying with a minimum of cracks. The Na_2SiF_6 can also be considered as a placement material, i.e., it affects the placement of the silicate bonds, thereby keeping the silicate uniformly distributed. Clay also adds a thixotropic quality which aids in the placement of the silicate binder.

Zinc oxide (ZnO) was also used to insolubilize the binder and prevent migration; however, Na_2SiF_6 was preferred in the optimized foams. With a potassium silicate binder, ZnO may react to form some

zinc silicate leaving an amorphous siliceous precipitate or a hard gel, depending upon the amount of water in the mix. However, no definite evidence exists that this is the primary reaction.

The use of chopped Fiberfrax fibers enhances the mechanical properties of the foam by reinforcing it. Not only is the structural integrity maintained during curing and drying, but also during subsequent vibrational testing. Additions of 3 to 10 wt% Fiberfrax permitted us to increase the binder content without surface cracking during the curing cycle.

Therefore, what is actually happening in the preparation of our chemically-bonded castable foam is that a thixotropic potassium silicate gel is foamed in the presence of a zircon mix which is aerated with the aid of albumin (foaming agent) and further stabilized and reinforced by adding clay (Ajax P), Na_2SiF_6 and Fiberfrax fibers.

3. Phosphate-Bonded Foams

a. Compositional Factors

The development of castable zircon foams, using a phosphate binder, was carried out to obtain foams with higher mechanical strengths.

A 50% solution of monoaluminum phosphate ($Al_2O_3 \cdot 3P_2O_5 \cdot 6H_2O$), as AP in tables, showing foam formulations, was used as the binder. The effects of various additives to stabilize the foam, lower the curing temperature of the binder, and improve the mechanical strength have been studied. The source of the raw materials used in the experiments is shown in Appendix A.

In our earlier experiments with phosphate-bonded zircon foams, it was found that those having a high tensile strength have a striated micropore structure, while foams with the desirable fine micropore structure have lower tensile strengths. A fine micropore structure would tend to be more insulative to the radiant environment than one that was striated. Therefore, emphasis was directed toward

improving the foam micropore structure of stronger foams by compositional adjustment and variations in curing cycles. Table IV shows nominal compositions and microstructural characteristics of the prepared foams. Additives that have been considered include zinc oxide (ZnO), magnesium oxide (MgO), calcium oxide (CaO) and plaster of Paris. The effects of these additives were evaluated by correlating tensile strengths of prepared foams with the observed microstructure.

Although it is difficult to quantitatively define the role of the above additives on the micropore structure and tensile strength of the foams, it is possible to describe certain broad trends. Addition of MgO and CaO by themselves results in very rapid setting of the foam; this can be reduced by the addition of plaster of Paris. The use of ZnO along with CaO has resulted in a strong foam with a striated structure. The degree of striations can be reduced by adding plaster of Paris and by reducing the amount of ZnO. This can result in a slight reduction in tensile strength of the foam. By using a small amount of MgO along with CaO and plaster of Paris, but without any ZnO, it is possible to prepare foams with a fine micropore structure. However, these foams do not have the high strength of ZnO-containing foams. CaO may be responsible for the formation of a strong foam-metal substrate bond.

The effect of curing was also evaluated. Foam compositions ZP-48 to ZP-51 were exposed to a prolonged curing of 64 hours at 140°F instead of the usual 15 to 17 hrs. Poorer structures resulted from this longer curing cycle.

In ZP-53, prepared with a skin, the amount of ZnO was reduced from that used in ZP-37 to prevent laminations in the foam. MgO, which causes rapid setting of the foam, was eliminated. The amount of plaster of Paris was also reduced from that used in ZP-40, but the CaO was held constant. The resulting foam had a fine pore size and was free from laminations. However, cracks appeared, especially near the metal substrate interface, and the foam was very weak. The

formation of a skin, due to the absence of a plastic wrapper during curing, may be responsible for the cracks. In ZP-54, the ZnO and plaster of Paris were nearly identical to the quantities used in ZP-53, but the amount of CaO was reduced by half. Foams were cured without a plastic wrapper (skin type) and with the partial use of the wrapper (partial skin type). The extent of crack formation decreases with increasing time during curing when the plastic wrapper was used (i.e., with reduced skin). Partial skin foams (PS-30, PS-60 and PS-120) did show moderate strengths, while skin type foams had lower strengths. In all cases the failure took place at or around the foam substrate interface. In ZP-55, the amount of CaO was again increased by 40 wt% and the water content decreased to 150cc; otherwise, the foam composition was similar to that of ZP-54. The foams were prepared with various surface textures: no skin, hole, PS-30 and CB type (prepared by using a 1/16 in. thick cardboard instead of the plastic wrapper). The use of the cardboard was initiated to obtain a drying rate in between that obtained with and without a plastic wrapper. However, foams prepared with a cardboard top are very similar to the skin type so the use of cardboard is worthless. Both the no skin and hole types were bloated; the CB type had cracks, although it was free from bloating; while the PS-30 type foam had reduced cracks and was free from bloating. The tensile strength for all these foams was disappointingly low. In order to improve the homogeneity of the foam structure, ZP-56 was prepared with a composition identical to ZP-55, but with the water content further reduced, as shown in Table IV. The foams did not bloat and had a medium size micropore. The PS-45 type had a tensile strength averaging 45 psi.

b. Optimization of Foam Compositions

The nominal compositions of foams that have shown promise are shown in Table V. The two types of compositions that have high tensile strength values and desirable micropore structures are ZP-58 and ZP-62. Compositions ZP-65 and ZP-66 are modifications of ZP-58 with varying Fiberfrax fiber contents. Our results indicate that composition ZP-58

Table IV

CHARACTERISTICS OF CASTABLE PHOSPHATE-BONDED ZIRCON FOAMS

(1/2 IN. THICK) ON HONEYCOMB SUBSTRATES

FOAM NO.	NOMINAL COMPOSITION											FOAM DENSITY lb/cu ft	COMMENTS
	Zircon A (g)	Zircon (g)	Ajax P (g)	Plaster of Paris (g)	MgO (g)	ZnO (g)	CaO (g)	Water (cc)	Albumin (g)	AP (cc)	Fiber-frax (g)		
ZP-47	100	80	2	25	2	–	4	50	0.6	95	10 (f)*	58	No skin type: Good micropore structure but separation from plate.
ZP-48	100	80	2	–	4	–	5	50	0.6	95	10 (f)	75	No skin type: Poor, striated, bloated structure. Foam began stiffening during the foaming process.
ZP-49	100	80	2	25	2.5	–	5	50	0.6	95	10 (f)	63	No skin type: Some bloating in the foam; some fine structure, separation from plate.
ZP-50	100	80	2	15	–	10	5	50	0.6	95	10 (f)	65	No skin type: Bloated, striated, very hard foam.
ZP-51	100	80	2	25	–	8.5	5	50	0.6	95	–	76	No skin type: Poor striated structure.
ZP-53	400	320	8	40	–	28	20	200	2.0	380	40 (m)	58	Skin type foam; fine pore size, no striations. However, foam has cracks near interface.
ZP-54	320	400	8	40	–	32	10	200	2.0	380	40 (m)	54	Partial skin (PS-120, PS-60, PS-30) and skin type foams were prepared. All have fine micropore. Degree of cracks decreases with increasing use of plastic wrapper (i.e., reduced skin)
ZP-55	400	320	8	40	–	32	14	150	2.0	380	20 (m)	50 (PS-30) 57 (CB)	No skin, partial skin (PS-30), hole type paper covered. No skin and hole type showed excessive bloating. C-Board covered has fine pores but some cracks; partial skin has intermediate pores, no cracks. Faint separation at plate.
ZP-56	200	160	4	20	–	16	7	50	1.0	190	20 (m)	50 (PS-45) 59 (CB)	Partial skin, PS-45, and paper covered types, fine pores and crack on one sample, faint separation PS-45 intermediate pore sizes, faint crack near bottom.

*(f) fine fibers

(m) medium fibers

Table V

NOMINAL COMPOSITION OF PHOSPHATE-BONDED
CASTABLE ZIRCON FOAMS (DENSITY 60 lb/ft^3)

Nominal Composition		Foam No.			
		ZP-58	ZP-62	ZP-65	ZP-66
Zircon	(g)	300	300	300	300
Zircon A	(g)	240	240	240	240
Albumin	(g)	1.5	1.5	1.5	1.5
"AP"	(cc)	285	285	285	285
Ajax P	(g)	6	6	6	6
Water	(cc)	150	75	150	150
ZrO	(g)	24	24	24	24
MgO	(g)	6	6	6	6
Plaster of Paris	(g)	45	45	45	45
CaO	(g)	-	7.5	-	-
Fiberfrax [med.]	(g)	30	30	60	120

has greater potential for use in scaled-up rigid heat shields; therefore, major emphasis has been placed on this composition, rather than on ZP-62.

In preparing foams with larger areal dimensions, the rate of drying and curing is critical to the formation of a fine microstructure along with high mechanical strength. If the foam is not subjected to an optimum drying and curing cycle, the resultant microstructure (especially in larger dimension foams) tends to be laminated and contains large cavities.

The curing cycle for a ZP-58 foam 9 x 9 x 1/2 in., cast on a honeycomb substrate is shown in Fig. 12. Curing temperatures were monitored as a function of time by means of thermocouples placed at the foam-substrate interface (T_i) and at the base of the honeycomb substrate (T_b). This was essential to obtain foams with a uniform micropore structure, free from laminations. An extended curing cycle of 63 1/2 hrs was found to be preferred over that of 39 1/2 hrs for ZP-58 type foams. The longer curing time was found to enhance tensile strength of the foam.

Increased fiber content, as in ZP-65 and ZP-66 (compared to ZP-58 in the case of 9 x 9 x 1/2 in. foams), resulted in fewer surface cracks.

A number of techniques for the controlled rates of drying for phosphate-bonded zircon foams have been evaluated. "CCBP" types were prepared by having a plastic wrapper over a cardboard (CB) placed on the foam surface and removing it after 17 hrs at 140°F. Other variations in drying include "PS 30 CH", which implies a surface conditioning similar to the PS 30, except that the plastic wrapper was held 1/8 in. above the foam surface and not on the surface as in PS type foams.

In the case of ZP-58, the CHP or "controlled humidity-partial" types gave the best results with respect to tensile strength

and microstructure. In preparing samples of areal dimensions
(2 x 2 in.), the best results were obtained by holding the plastic
wrapper 1/8 in. above the foam surface, and removing it after 17 hrs
at 140°F. This type has been referred to as CHP (1/8). Results
indicate that, in scaling-up ZP-58, an increased distance between
the wrapper and the foam surface is required to that used for speci-
mens with 2 x 2 in. areal dimensions. A longer curing time is
also necessary for scaled-up foams. In the case of ZP-58 foams
prepared in dimensions of 2 x 2 x 1/2 in., best results have been
obtained by holding the wrapper at a height of 1/8 in. above the
foam surface. In scaling-up, we have attempted to determine the
increased optimum height by taking into consideration the "shape
factor." This is a function of the ratio of the foam surface
area to the foam perimeter. However, further experimentation is
necessary before this relationship can be finalized. By following
this approach, we have been able to prepare 3 x 6 x 1/2 in. and
9 x 9 x 1/2 in. ZP-58 foams, cast on a honeycomb substrate, which
have good micropore structure. In the case of the 3 x 6 x 1/2 in.
foam, the samples were prepared with the wrapper held at 3/8 in. as
well as at 7/8 in., while with the 9 x 9 x 1/2 in. foam, the wrapper
was held at 2 1/4 in.

A prefired zircon foam was prepared by firing a castable
ZP-58 foam composition to a temperature of 1830°F, for 2 hrs.
This foam has been referred to as prefired ZP-58. The firing was
carried out in an electric furnace in ambient atmosphere.

C. Mullite Foams

Mullite powders from two different sources were used in
preparing the foams listed in Table VI.

The mullite powder used in preparing foams M-3 to M-13
was -325 mesh, manufactured by H. R. Porter and Company. It
contains small quantities of a silica phase.

Table VI

CHARACTERISTICS OF MULLITE FOAMS (1/2 IN. THICK) PREPARED BY MECHANICAL WHIPPING

Foam No.	Nominal Composition							Foam Density (lb/ft³)	Comments
	Mullite (g)	Water (cc)	PS-7 (cc)	SW 2336 (cc)	Albumin (g)	Clay (g)	Other Additives		
M-3	200	30	60	20	—	—	Methanol HG 6g	—	Foam collapsed.
M-4	200	70	60	20	—	—	Baymal 20 g	—	Baymal incompatible with PS-7 binder; did not go into suspension.
M-6	200	35	75	20	—	60	Na_2SiF_6 20 cc	45	Large pores. Little shrinkage on drying.
M-7	200	46	75	—	10	60	—	50	Fine pore structure. Good strength and uniformity.
M-8	200	120	—	—	10	60	—	62	Fired to 2330°F. Strong foam body.
M-9	200	70	75	—	25	60	—	37	Very slow air drying needed to prevent rupture.
M-10	200	50	75	10	12	60	—	35	Medium size pores (between M-6 and M-7).
M-11	200	145	—	—	—	60	Gelatin 60 g	—	Fine pores, but larger than those obtained with Albumin.
M-13	95	75	—	—	25	60	—	25	Foam cast on aluminum plate. Well bonded to metal substrate.
M-20	150	70	70	—	6	50	—	37	Excessive shrinkage.
M-21	200	50	45	—	5	5	—	61	Large cracks, some debonding.
M-22	200	60	47	—	6	5	—	44	Fine cracks, well bonded.
M-23	200	60	50	—	6	5	Na_2SiF_6 4.5 g	37	Plastic wrap cover used during drying. Faint surface cracks. Foam well bonded.

NOTE: Foams M-3 through M-13 were prepared with mullite powder supplied by H. E. Porter and Co. and contains excess silica.
Foams M-20 through M-23 were prepared with mullite powder supplied by Norton and Co. and contains slight excess alumina.

Mullite foams M-20 to M-23 were prepared with a mullite powder obtained from the Norton Company and designated as "Mullite B, 325F." This mullite product has no silica phase, but a very slight excess of alumina, and is lighter in color than other mullite materials investigated.

All these foams were prepared by mechanical whipping. The nominal compositions of the starting materials are given for each of these foams. These results indicate that (for mullite foams) albumin is the preferred foaming agent, as it forms foams with a fine uniform micropore structure. All these foams, with the exception of M-8 and M-11, are castable. Foam M-8, which is a mullite foam without a binder, was fired at a high temperature (2330°F). The other foams have been oven dried only and not cured at higher temperatures; however, they indicated good bonding. Foam M-22 was obtained with a minimum of fine surface cracks but was well bonded to the substrate. Further optimization is required to obtain crack-free mullite foam structures. This has been accomplished to a degree with composition M-23, which was covered with plastic wrap while drying.

D. Calcium Aluminate Foams

Preliminary work has been carried out on calcium aluminate foams. The starting material was calcium aluminate cement manufactured by Alcoa Chemicals. Alcoa calcium aluminate designated as "CA-25" is a high-purity, hydraulically setting refractory cement, and is composed of about 79% alumina, 18% lime, and not more than 2% impurities. This composition conforms to the empirical molar formula $2CaO \cdot 5Al_2O_3$.

Table VII shows compositions and densities of the calcium aluminate foams prepared by mechanical whipping. Although further optimization is required, this low thermal expansion material has shown considerable promise on preliminary investigation. Foam specimens were also tested by immersion in boiling water for 3 hrs and showed very little deterioration.

Table VII

CHARACTERISTICS OF CALCIUM ALUMINATE CEMENT FOAMS (1/2 IN. THICK) PREPARED BY MECHANICAL WHIPPING ON STEEL PANELS

Foam No.	Nominal Composition					Foam Density (lb/ft^3)	Comments
	Cal. Alum. (g)	Al$_2$O$_3$ (g)	Water (cc)	Albumin (g)	Clay (g)		
CA-1	300	—	100	9	—	60	Crack free foam.
CA-2	400	—	130	13	8	67	Fine cracks, poor bond.
CA-3	300	—	110	10	6	60	Fine pore structure; pore size 0.002-0.005". Crack free, some debonding.
CA-4	300	—	110	10.5	7	55	Double base coat of CA + 30 WT % H$_2$O applied to substrate. Foam intact, well bonded.
CA-5	500	125	210	21.3	—	72	Density as cured. On firing to 2900°F density 82 lb/ft^3.
CA-6	400	100	195	20	20	42	Faint vertical cracks, foam intact.
CA-7	550	—	225	22	27.5	45	Faint vertical cracks, foam intact.
CA-8	500	125	245	25	—	53	Fine pores. 0.002-0.004". No cracks.

In the case of the calcium aluminate foam, an undercoat of calcium aluminate cement in 30 wt% water was found to give better adhesion to steel substrates than the previously used aluminum oxide bonded with PS-7.

Composition CA-5 was prepared in two specimens, one cast on a steel plate and cured, and the other fired to 2900°F. CA-6 and CA-7 were cast on bare panels. Due to the weakness of cast foams bonded to steel panels, no further work was conducted with cast calcium aluminate compositions. Composition CA-8 showed a density of approximately 60 lb/ft^3 when this foam was fired to a temperature of 2900°F. This sample was cemented onto a steel panel with a silicate-bonded Al_2O_3 base coat.

V. EFFECTS OF HEAT FLUX WITH SIMULTANEOUS VIBRATION AND ACCELERATION ON CERAMIC FOAMS

A. Final Test Program

1. Introduction

In the final test program, the effects of 40 Btu/ft^2-sec heat flux (primarily radiant) with a simultaneous vibration of 60 cps, a double amplitude displacement of 1/2 in., and an acceleration level of 90 g's were evaluated on the nearly optimized castable, composite zircon foams.

Test evaluations were carried out for 1/2 in. thick foams cast on a 1 in. thick honeycomb substrate of areal dimensions 3 x 6 in. and 9 x 9 in. with open face metal reinforcements of the design developed for the Saturn-V heat shield. This honeycomb sandwich construction consists of 10 mil thick face sheets and a 1 in. thick honeycomb core having 1/4 in. square cell openings and a wall thickness of 2 mils. The components were fabricated from a high-strength stainless steel and joined with a silver-brazing alloy. A 190 mil thick honeycomb reinforcement core, having 1/2 in. square cell openings and a wall thickness of 2 mils, is brazed to one face

of the basic honeycomb structure. About 45 mils of the upper portion of the core walls were crimped over by crushing or bending using a hydraulic press. The foam is cast onto this core panel. A set of thermocouples were placed at the foam substrate interface and at the bottom of the honeycomb to monitor the interface (T_i) and backface temperature (T_b) during testing.

2. Test Equipment

The chemically bonded foam on a honeycomb substrate was bolted to a rigid frame, which in turn was directly bolted onto the vibrational pad. A set of two thermocouples welded on the top face at the foam-substrate interface and on the bottom stainless steel sheet for a 3 x 6 x 1 in. honeycomb was monitored during the test. The entire fixture with the foam is shown in Fig. 13.

A radiant heating facility was used to provide the radiant heat fluxes called for in the final tests. The equipment consisted of a water-cooled aluminum reflector (Research, Inc. No. WC 14-12), equipped with air-cooled ceramic lamp holders (Hi Shear Lux-Therm Dual Lamp Holders No. LT 1200), and twenty-four 3600-watt quartz lamps (General Electric No. 3600/T3/ICL/HT).

Test sample temperatures are monitored on a 12-channel Brown Recorder. The magnitude of the incident heat flux is measured by a slug calorimeter whose millivolt output is recorded on a Varian Type G 22 Continuous Recorder.

The present equipment is capable of providing an incident heat flux to the sample in excess of 40 Btu/ft^2-sec while operating the lamps slightly below rated voltage. A survey of the incident heat flux indicated negligible variation over a surface dimension of 12 x 12 in.

The vibration facility includes a fully integrated random vibration system, consisting of a 6 kva electronic driver console and an MB C10E 1200 lb sinusoidal vector, 2250 lb peak random force electromagnetic exciter. The frequency spectrum can be manually

shaped as desired or to compensate for mechanical resonances. A frequency spectrum display is provided for visually monitoring the response of the driver system is 5 to 2000 cps, 70 g's acceleration or 1 in. total excursion. A second unit capable of 90 g's acceleration with 1/2 in. peak-to-peak displacement is also available and was used later in the optimization testing program.

3. Experimental Results

a. Silicate-Bonded Zircon Foams

Results of the final testing are shown in Table VIII. The backface and interface temperatures of some of the optimized foams after 2 1/2 and 5 min exposure to the final test conditions have been indicated in Table IX.

These results indicate that castable type, chemically bonded zircon foams have been developed with densities not exceeding 60 lb/ft^3, which in 1/2 in. thicknesses have the ability to limit the backface temperature (T_b) of the specimen to far less than the 400°F requirement after 2 1/2 min exposure to the final test conditions. In fact, these optimized foams, 1/2 in. thick, are capable of limiting the backface temperature to no more than 400°F even after 5 min exposure to the final heat flux and vibrational conditions.

The surface texture of the foam significantly affects its insulative characteristics. As discussed in the preceding sections, we can control the surface texture of the foam by the disuse, partial use, or full use of a plastic wrapping, such as Saran Wrap, during the drying cycle; thus forming a hard skin, partial skin, or no skin, respectively, on the surface. Foams without a hard skin have a lower backface (T_b) and interface (T_i) temperatures than those with a hard skin; partial skin foams are intermediate in insulative properties, as shown in Table IX. This difference is especially significant for test exposure of 5 min instead of 2 1/2 min., and is shown in Fig. 14 for a zircon foam of composition Z-87. There is a backface (T_b) difference of about 115°F and an interface (T_i) difference of 280°F, between two foams of identical densities and nominal compositions, but differing in surface textures.

Table VIII

FINAL TEST RESULTS ON ZIRCON FOAMS (1/2 IN. THICK)

ON 1 IN. THICK HONEYCOMB SUBSTRATES

Foam No.	Foam Type(a)	Foam Density lb/ft³	Test Cycle No.	t, sec	Temperatures, °F T_b	T_i	Comments
Z-67	NS	52	1	60 120 150 180	100 168 190 235	110 225 310 400	Foam interface intact. Very faint cracks developed on cooling.
Z-67	S	52	1	60 120 150 180 240	122 215 260 308 392	142 345 455 555 665	Vertical cracks. (Uncrimped open face honeycomb substrate.)
Z-73	PS	67	1	60 120 150 180	88 130 175 215	88 230 318 400	No cracks.
			2	60 120 150 180 240	125 157 185 218 290	105 250 340 420 545	First recycle. Sample remained intact, with hairline cracks.

Table VIII (Cont'd)

Foam No.	Foam Type(a)	Foam Density lb/ft³	Test Cycle No.	t, sec	Temperatures, °F T_b	T_i	Comments
Z-73 (Cont'd)	F?	67	3	60	98	98	Second rerun. Jigsaw type vertical cracks, but specimen intact
				120	140	225	
				150	168	305	
				180	193	387	
				240	250	510	
				300	300	600	
Z-75	PS	42	1	60	110		No cracks after testing; specimen intact.
				120	155		
				150	180		
				180	210		
				240	270		
				330	340	685	
Z-79	S	57	1	60	125	175	Faint vertical cracks on surface.
				120	200	400	
				150	250	510	
				180	290	605	
				240	375	710	
				300	420	800	
Z-79 (1/4 in. thick)	S	57	1	60	190	550	Faint vertical cracks.
				120	450	920	
				150	530	1080	

Table VIII (Cont'd)

Foam No.	Foam Type(a)	Foam Density lb/ft³	Test Cycle No.	t, sec	Temperatures, °F T_b	T_i	Comments
Z-79 (1 in. thick)	S	57	1	60	90	90	Completely intact.
				120	120	120	
				150	140	145	
				180	150	165	
				240	168	192	
				300	175	210	
Z-83	PS	49	1	60	120	120	No cracks appeared after 5 min testing.
				120	160	198	
				150	175	260	
				180	193	328	
				240	228	445	
				300	270	535	
			2	60	130	105	No vibration and acceleration during this cycle. Very faint hairline cracks developed on surface of foam.
				120	175	188	
				150	200	260	
				180	230	330	
				240	300	465	
				300	358	570	
			3	60	120	100	Some cracks developed on surface of foam. Foam and interface bond absolutely intact.
				120	155	208	
				150	180	275	
				180	200	340	
				240	243	450	
				300	280	535	

Table VIII (Cont'd)

Foam No.	Foam Type(a)	Foam Density lb/ft³	Test Cycle No.	t, sec	Temperatures, °F T_b	T_i	Comments
Z-85 (9/16-5/8 in. thick)	PS	56	1	60	120	122	Very faint hairline cracks slightly enlarged on testing.
				120	160	205	
				150	180	270	
				180	208	330	
				240	265	448	
				300	310	550	
Z-86	S	66	1	60	130	148	Faint cracks at surface.
				120	190	335	
				150	225	435	
				180	260	525	
				240	330	675	
				300	385	770	
Z-87	S	60	1	60	125	140	Some vertical cracks.
				120	195	320	
				150	225	415	
				180	280	520	
				240	358	668	
				300	395	750	
Z-87	PS	60	1	60	120	120	No cracks after 5 min testing.
				120	170	240	
				150	200	310	
				180	225	390	
				240	270	500	
				300	315	590	

Table VIII (Cont'd)

Foam No.	Foam Type[a]	Foam Density lb/ft^3	Test Cycle No.	t, sec	Temperatures, °F T_b	T_i	Comments
Z-87	NS	60	1	60 120 150 180 240 300	120 155 175 198 235 280	105 180 235 290 390 470	No cracks after 5 min testing.
			2	60 120 150 180 240 300	140 180 205 225 260 298	100 190 243 300 400 468	Faint hairline cracks developed.
Z-88	S	57	1	60 120 150 180 240 300	115 170 205 240 305 355	150 300 390 475 615 715	Faint cracks
Z-88	NS	57	1	60 120 150 180 240 300	115 170 195 220 275 320	130 230 295 375 505 595	No cracks after 5 min testing.

Table VIII (Cont'd)

Foam No.	Foam Type[a]	Foam Density lb/ft^3	Test Cycle No.	t, sec	Temperatures, °F T_b	T_i	Comments
Z-88 (Cont'd)	NS	57	2	60	115	138	Foam intact
				120	180	190	
				150	215	248	
				180	240	310	
				240	300	430	
				300	345	520	
Z-89	NS	52	1	60	138	120	Foam intact
				120	190	215	
				150	220	300	
				180	253	375	
				240	310	515	
				300	350	610	
			2	60	145	115	Foam intact after recycling test.
				120	190	215	
				150	225	300	
				180	253	375	
				240	310	515	
				300	358	610	
				360	385	685	
Z-90	S	59	1	60	120	150	Faint hairline cracks on heating.
				120	185	313	
				150	225	405	
				180	265	498	
				240	340	650	
				300	385	730	

Table VIII (Cont'd)

Foam No.	Foam Type(a)	Density lb/ft^3	Test Cycle No.	t, sec	Temperatures, °F T$_b$	T$_i$	Comments
Z-90	PS	59	1	60	90	100	Foam intact. No surface cracks. However, foam broke on recycling in less than 1 min.
				120	180	215	
				150	200	285	
				180	230	355	
				240	290	470	
				300	330	560	
Z-90	NS	59	1	60	125	125	Foam intact. No surface cracks. However, foam broke on recycling "in less than 1 min.
				120	163	220	
				150	200	300	
				180	230	370	
				240	295	485	
				300	345	585	
Z-90 (Foam was soaked in water for 97 hr prior to testing)	PS	59	1	60	85	85	Foam intact.
				120	163	200	
				150	185	218	
				180	190	220	
				240	200	220	
				300	200	220	

Table VIII (Cont'd)

Foam No.	Foam Type(a)	Foam Density lb/ft^3	Test Cycle No.	t, sec	Temperatures, °F T_b	T_i	Comments
Z-90 (Cont'd)	PS	59	2	60	100	120	Foam intact
				120	160	185	
				150	185	235	
				180	215	298	
				240	270	430	
				300	320	540	

The tests were carried out at a heat flux of 40 Btu/ft^2-sec and simultaneous vibration of 60 cps with a double amplitude displacement of ½ in. and an acceleration level of 90 g's.

(a)The type denotes the foam surface: S indicates that foam has a hard surface skin, PS a partial skin, and NS no hard surface skin.

Table IX

BACKFACE TEMPERATURES OF SOME NEARLY OPTIMIZED

ZIRCON FOAMS (½ IN. THICK)

ON 1 IN. HONEYCOMB SUBSTRATES ON FINAL TESTING

Foam No.	Foam Type	Foam Density lb/ft^3	Backface Temperatures °F			
			2½ min exposure		5 min exposure	
			T_b	T_i	T_b	T_i
Z-79	S	57	250	510	420	800
Z-87	S	60	225	415	395	750
	PS	60	200	310	315	590
	NS	60	175	235	280	470
Z-88	S	57	205	390	355	715
	NS	57	195	295	320	595
Z-89	NS	52	220	300	350	610
Z-90	S	59	225	405	385	730
	PS	59	200	285	330	560

All specimens were subjected to a heat flux of 40 Btu/ft^3-sec with simultaneous vibration of 60 cps, acceleration of 90 g's, and ½ in. double amplitude displacement.

This effect is probably due to the fact that the hard surface skin predominatly consists of albumin, which is yellowish, and would therefore have a lower reflectivity than that of a skin-free surface, which is whiter. A high reflectivity (i.e., low absorptivity) has been shown in our thermal analysis (see Section II) to be a critical parameter in limiting the backface temperature.

Further, foams without a skin or with only a partial skin form fewer or no surface cracks when subjected to recycling of final test conditions.

The most insulative zircon foam developed in the density range of 57 to 60 lb/ft^3 (1/2 in. thick) is Z-87 without a skin and which contains Superpax A as well as Fiberfrax. This foam gave backface temperatures (T_b) as low as 175° and 280°F after 2 1/2 and 5 min exposure, respectively, to final test conditions. Further, it was able to withstand recycling under the final flux and simultaneous vibrational and acceleration test conditions while maintaining its insulative properties and mechanical integrity. Addition of Fiberfrax to zircon foams is essential, and improves the structural integrity of the foam, especially during drying and curing and probably contributes to some amount of radiant scattering.

Recycling characteristics of these foams have also been evaluated. The foams were subjected to a full 5 min exposure under the final test conditions, allowed to cool down to room temperature and then exposed to the final test conditions once again. The backface and interface temperatures of some of the optimized foams on recycling have also been shown in Table VIII. Zircon foams, both with and without Superpax, showed good recycling characteristics. However, foam Z-90 which contains 10 wt% fine diameter Fiberfrax (instead of 10 wt% medium diameter Fiberfrax, as the other optimized foams contained) failed upon recycling. This foam also has the highest flat-wise tensile strength of all the prepared foams, and its failure to maintain its structural integrity on recycling may be due to its inability to strain relieve

itself because of higher rigidity of foam structure, compared to the other foams. Subjecting foam Z-90 to a 97 hr water soak did not impair its insulative or mechanical characteristics. The values of T_b and T_i obtained on subjecting a soaked foam to the final test conditions are shown in Table VIII. In fact, the soaked Z-90 specimen withstood the recycling test without rupture.

The effect of foam thickness on insulative properties has been investigated. The T_b and T_i values of three identical foams of 1/4, 1/2, and 1 in. thicknesses on a 1 in. thick honeycomb, as a function of time (under heat flux and vibrational conditions corresponding to the final test) are shown in Fig. 15 for a nearly optimized composition (Z-79-2). The backface (T_b) temperature of the 1/4 in. thick foam was 530°F after 2 1/2 min exposure. The performance of 1/4 in. thick Z-88 and Z-89 foams have also been evaluated under the final test conditions. The T_b and T_i values obtained for these 1/4 in. thick foams have been compared with those obtained for similar 1/2 in. thick foams, in Table X. In addition, both the Z-88 and Z-89, 1/4 in. thick foams successfully withstood four test cycles, without thermal or mechanical degradation.

These results indicate that 1/4 in. thick silicate-bonded zircon foams not only show good insulative properties, but can also withstand recycling without failure.

The performance of silicate-bonded zircon foams, reported in the preceding paragraphs was evaluated on specimens with 3 x 6 in. areal dimensions. In order to determine whether the excellent insulative properties of these foams were also inherent to foams cast in larger dimension, tests were carried out with Z-88, 9 x 9 x 1/2 in. specimens. The positioning of thermocouples is shown in Fig. 16. In the first cycle, values for T_b and T_i were 140 and 350°F, respectively, after 2 1/2 min, and 375° and 750°F, respectively, after 5 min exposure to a 40 Btu/ft^2-sec heat flux

Table X

INSULATIVE PERFORMANCE* OF Z-88 AND Z-89

FOAMS (ON 1 in. THICK HONEYCOMB) AS A FUNCTION OF

FOAM THICKNESS

Foam No.	Foam Thickness (in.)	Back Face Temperature,°F			
		2½ Min Exposure		5 Min Exposure	
		T_b	T_i	T_b	T_i
Z-88 NS	¼	365	700	478	848
	½	195	295	320	595
Z-89 NS	¼	325	700	435	840
	½	220	300	350	610

* All specimens were subjected to a heat flux of 40 Btu/ft^2-sec with simultaneous vibration of 60 cps, ½ in. double amplitude displacement and 90 g acceleration.

with simultaneous vibration. On the second cycle, the foam broke after about 30 sec of exposure.

b. Phosphate-Bonded Zircon Foams

The results obtained on subjecting the optimized phosphate-bonded zircon foams to a heat flux of 40 Btu/ft^2-sec, with 60 cps simultaneous vibration, 1/2 in. double displacement, and an acceleration level of 90 g's, have been shown in Table XI.

The backface (T_b) and interface temperature (T_i) have been obtained for 1/2 in. thick foams, during 5 min exposure to the final test conditions. In all cases, the foams were able to withstand test conditions without spalling or interfacial separation from the substrate; however, they failed, close to the foam-substrate interface, on recycling.

The failure of castable, phosphate-bonded zircon foams on recycling can be due to a number of factors. It should be pointed out that these foams do have greater rigidity than the corresponding silicate-bonded foam; which have been able to withstand recycling (with the exception of Z-90 which was a silicate-bonded zircon form with increased rigidity). Therefore, it is conceivable that the thermal and vibrational stresses, set-up at the end of the first cycle, cannot be sufficiently relieved in rigid foams which accounts for their failure on recycling.

The second point that must be remembered, is that castable phosphate-bonded zircon foams, go through a color change between 400° to 1200°F which is probably associated with chemical changes within the foam. (This has been discussed in detail in Section Vc.) In a typical castable, phosphate-bonded, 1/2 in. thick foam (subjected to a heat flux of 40 Btu/ft^2-sec for about 5 min), the surface of the foam (which is normally light beige to white in color turns white to a depth of approximately 1/8 in., while the rest of the foam turns dark gray. So, it is possible that the chemical-structural gradient in the foam, due to these color changes, results in failure on recycling.

-46-

Table XI

FINAL TEST RESULTS ON PHOSPHATE-BONDED ZIRCON FOAMS

(1/2 in. THICK) ON HONEYCOMB SUBSTRATES

Foam No.	Density (lb/ft^3)	Areal Dimensions (in.)	Type	Test Cycle No.	Time Sec	Temperature, °F T_b	T_i
ZP-58	60	3 x 6	CHP(7/8)	1	60	110	185
					120	165	350
					150	200	445
					180	240	538
					240	310	670
					300	360	770
	60	3 x 6	CHP(3/8)	1	60	110	125
					120	170	315
					150	208	400
					180	243	480
					240	312	600
					300	363	690
	60	9 x 9	CHP(2 1/4)	1	60	95	225
					120	180	450
					150	240	570
					180	300	680
					240	425	850
					300	525	965
	47	9 x 9	CHP(2 1/4)	1	60	100	190
					120	170	395
					150	220	500
					180	275	590
					240	380	745
					300	480	860

-47-

Table XI (Cont'd)

Foam No.	Density (lb/ft^3)	Areal Dimensions (in.)	Type	Test Cycle No.	Time Sec	Temperature, °F	
						T_b	T_i
ZP-65	59	9 x 9	CHP(2 1/4)	1	60	115	220
					120	185	408
					150	240	520
					180	310	625
					240	440	780
					300	550	905
ZP-66	63	9 x 9	CHP(2 1/4)	1	60	115	225
					120	205	470
					150	280	600
					180	350	720
					240	480	885
					300	580	985
ZP-58 (Foam was soaked in water for 24 hrs before testing)	60	3 x 6	CHP(3/8)	1	60	125	125
					120	160	210
					150	175	220
					180	180	225
					240	190	225
					300	205	233
				2	60	145	185
					120	220	375
					150	250	460
					180	285	545
					240	345	675
					300	385	770
ZP-58	51	3 x 6	Prefired	1	60	115	155
					120	190	320
					150	235	395
					180	285	465
					240	355	575
					300	410	650

Table XI (Cont'd)

Foam No.	Density (lb/ft^3)	Areal Dimensions (in.)	Type	Test Cycle No.	Time Sec	Temperature, °F T_b	T_i
ZP-58 (Cont'd)		3 x 6	Prefired	2	60	120	160
					120	210	360
					150	270	455
					180	315	525
					240	395	630
ZP-58*	53	3 x 6	"as-cured"	1	60	115	180
					120	165	300
					150	190	375
					180	225	450
					240	285	560
					300	345	675
				2	60	125	145
					120	190	350
					150	228	460

*The prefired and "as-cured" foams were bonded to the honeycomb substrate with an RTV silicone (Dow Corning's Aerospace sealant).

In order to determine the contributing factor(s) for failure on recycling, tests were carried out on a pre-fired ZP-58 foam and an "as-cured" ZP-58 foam (cast on a plastic wrapper base), which were bonded to a honeycomb substrate 3 x 6 x 1 in. with RTV-30-121 Dow Corning silicone sealant. Both these foams were subjected to a heat flux of 40 Btu/ft^2-sec with simultaneous vibration of 60 cps, 1/2 in. double displacement and 90 g's acceleration level. The objective in these experiments was to better understand failure that occurs in phosphate-bonded castable foams on thermal recycling. These results are shown in Table XI.

The prefired foam developed faint cracks on the surface after the second cycle but remained intact. The as-cured sample spalled off at one edge after recycling, although the rest of the foam was intact. This failure at the edge of the foam may have been caused by poor contact with the honeycomb. The interfacial failure was different from that observed in the case of ZP-58 foams, directly cast and cured on a honeycomb substrate.

The ability of a prefired ZP-58 type foam to withstand recycling under the final test conditions indicate that the failure in the corresponding castable foams is not due to its rigidity, but rather to factors intrinsic to the chemical nature of the castable foam. The fact that the RTV silicone-bonded, as-cured ZP-58 type foam withstood some recycling and had only a partial failure that was distinctly different from the castable foam, indicates that the change in color within the foam on exposure to the heat flux is not primarily responsible for the failure upon recycling. These results tend to indicate that the failure in the foams directly cast on honeycomb substrates is probably due to interfacial stresses, inherent in the foam from curing and drying. The fact that similar silicate-bonded castable zircon foams can successfully withstand recycling may be attributed to the comparative ease with which these foams can be cured.

The reasons behind the slight increase in the T_b and T_i

values for the 9 x 9 x 1/2 in. foam, as compared with the values obtained for the 3 x 6 x 1/2 in. foams under identical test conditions, are not clear. Cross-sectioning the 9 x 9 x 1/2 in. foam after testing did not indicate the presence of large air pockets or any other microstructural defects which may have resulted in a decrease in insulative properties. This difference in the temperatures could be due to the fact that the larger heat shield is not able to dissipate heat at the same rate as the smaller one. However, it should be pointed out that in testing silicate-bonded zircon foams at 40 Btu/ft^3-sec heat flux, no significant differences in T_b and T_i were observed between the smaller and larger heat shields. The fact that the silicate-bonded castable zircon foams are more insulative, due to their higher reflectance at the surface, could make them less volume or size dependent to insulativeness than the phosphate-bonded foams, which have a lower reflectance.

The effect of water on ZP-58, subjected to a heat flux of 40 Btu/ft^2-sec with simultaneous vibration of 60 cps, 1/2 in. double amplitude displacement, and an acceleration level up to 90 g's, was determined on a 1/2 in. thick sample, cast on a 3 x 6 x 1 in. honeycomb substrate. The foam was soaked in water for 24 hrs and then exposed to the test conditions within 1 hr after removal from the water. Results are shown in Table XI. The foam withstood 2 cycles each of 5 min duration. After the second cycle, faint surface cracks were observed, but the specimen was still intact. The backface temperature (T_b) after 5 min was 205°F in the first cycle and 385°F upon recycling.

c.   Thermal-Optical Interactions of Phosphate-
     Bonded Zircon Foams

Color changes have been observed to occur in phosphate-bonded zircon foam on exposure to the final heat flux. When these 1/2 in. thick foams are exposed to a 40 Btu/ft^2-sec heat flux for

about 5 min, the surface of the foam (which is normally beige in color) turns white to a depth of approximately 1/8 in., while the rest of the foam turns gray to dark brown.

In order to understand these color changes, a series of experiments were carried out. A ZP type foam was exposed to temperatures of 260°, 500°, 1400°, 1700° and 2000°F for 2 hrs at each temperature. It was observed that the foam (originally light beige) changed in color at increased temperature as follows:

1. Dark beige at ~ 260°F
2. Dark brown at ~ 500°F
3. Grayish-black at ~ 800°F
4. Black at ~ 1100°F
5. Lighter at ~ 1400°F
6. White at ~ 1700°F
7. Slight yellowish tinge at ~ 2000°F

These color changes are in agreement with those actually obtained under a final heat flux of 40 Btu/ft^2-sec where the non-equilibrium temperature at the foam surface is around 1700°F, while the interface temperature at the end of 5 min exposure is about 1000°F.

A second series of experiments were done where various compositional mixes in the form of small patties were exposed to various temperatures which were similar to those to which the composite phosphate-bonded zircon foam was exposed. However, in the second series of experiments, the small patties consisted of various combinations of the composite mix rather than the mix in its entirety. The object of the experiments was to pin-point those components of the composite mix that might be responsible for these color effects. The results are shown in Table XII. They may be summarized as follows:

1. The phosphate binder, by itself, is not responsible for the darkening color effect.

Table XII

COLOR EFFECTS DUE TO VARIOUS COMPONENTS

OF A PHOSPHATE-BONDED ZIRCON MIX

Test Specimen	Components					Color at Various Temperatures			
	Zircon	ZnO	Albumen	Fiberfrax	AP	250°F	500°F	1100°F	1700°F
A	X				X	w	w	w	w
B	X	X			X	w	w	w	w
C	X		X		X	w	b	b-g	w
D	X	X	X		X	b	b	g	w
E	X	X		X	X	w	w	w	w
F	X	X	X	X	X	b	b	g	w
G				X	X	w	w	w	w
H	X		X			w	b	w	-

x = components used in test specimens

w = white

b = beige

g = grey

-53-

2. Any possible reaction of zinc oxide and the phosphate binder, leading to the formation of zinc phosphates, does not cause coloring.

3. A dark gray color is obtained in the temperature range 500°-1100°F due to a reaction between albumin and the phosphate binder.

4. The addition of ZnO to a mix containing albumin and the phosphate binder increases the degree of coloration.

5. Fiberfrax fibers do not appear to be responsible for causing color changes.

B. Sinusoidal Sweep-Random Vibration Test Program

1. Introduction

In addition to the vibrational and acceleration levels specified under the Final Test Program (Section V,A), foams developed for use in rigid heat shields should also be able to withstand certain sinusoidal vibration and random vibration profiles.

The test evaluations were carried out in two stages, for 1/2 in. thick foams cast and/or bonded to a steel plate substrate 12 x 12 x 0.093 in. In the first stage the panels were subjected to a sinusoidal sweep test without a heat flux. On completion of the sweep test, the foam-substrate panel was subjected to 5 min of random test levels with a simultaneous radiant heat flux of 40 Btu/ft^2-sec.

The detailed test conditions are as follows:

(1) Sinusoidal Sweep Test Levels (without heat flux):
   5 -   18 cps   0.5 in. double amplitude displacement
  18 - 2000 cps   8.5 g's peak

(2)   Random Test Levels (with 40 Btu/ft^2-sec, heat flux):

20	-	600 cps	0.1 g^2 per cps
600	-	1200 cps	6.0 db per octave
1200	-	1600 cps	0.4 g^2 per cps
1600	-	2000 cps	-9.0 db per octave

Figure 17 shows the sinusoidal vibration profile and Figure 18, the random vibration spectrum.

2.   Test Equipment

The vibration test setup is shown in the block diagram of Fig. 19. The specimen is mounted in the test fixture on the electromagnetic shaker. An accelerometer mounted on the flange of the test fixture senses the input vibrational level and its signal is used to automatically maintain a preset level throughout the tests. Strain gages on the panel are monitored on a direct writing oscillograph using strain gage amplifiers and a calibration system.

During the testing, the vibration at the test fixture is monitored by an accelerometer located such that it experiences a representation of the true vibration input to the sample. This accelerometer is used both for monitoring and recording the levels as well as for controlling the acceleration in the case of the sinusoidal sweep tests.

Instrumentation of the response of the panels to determine mode shapes and maximum transmissibility can be accomplished by several means. In the sinusoidal vibration tests where the panel is at room temperature at all times, it is a relatively easy matter to monitor the nodal points by a movable non-contacting displacement transducer or by strain gages located on the underside of the plate. During the heat flux testing, it is necessary to carefully shield the sensors from incidence from the high radiant heat field to both prevent permanent damage to the sensors and to insure valid response measurements on the sample.

Data from the response sensor systems are recorded on a direct recording oscillograph. A CEC Model 5-114 is used for the sinusoidal vibration tests, and an instrumentation magnetic tape recorder for the random vibration tests. In addition, timing and any other auxiliary signals from the experiments can also be recorded. A representative data recording system is diagrammed in Fig. 20 showing sensors, signal conditioning circuits, auxiliary event signal inputs, and timing signals. In addition, a log-frequency converter can be used to provide a dc voltage proportional to excitation frequency so that the frequency at any point of time on the oscillographic traces can be determined. For the random vibration tests, vibration levels are recorded as a g^2/cps analog signal rather than the "raw" vibration data. Similarly, for the sinusoidal vibration tests, vibration levels (acceleration, or displacement) are recorded.

During these vibration tests, the foam panel is simply supported on all four edges. It is to be expected that any form of support will change the vibrational modes and frequencies of the foam panel. However, the design shown schematically in Fig. 21 provides maximum constraint in all other directions.

The 12 x 12 in. foams are cast on a stainless steel plate 13 x 13 x 0.093 in. to leave a 1/2 in. wide strip of bare plate around the edge. This strip is gripped between ball bearings in the top and bottom sections of a supporting frame which is attached to the vibration exciter. Thus the panel is free to flex and bow at the edges and to expand and contract, since the frames are clamped no tighter than necessary to constrain the panel to follow the motion of the vibration exciter. This design is inherently very stiff and no difficulty is anticipated with resonances within the frequency range of interest.

Response measurements on the wide-band random excitation of the panels is accomplished as follows: A preliminary investigation is conducted with a sample panel mounted in the vibration test

IIT RESEARCH INSTITUTE

fixture, which is subjected to the prescribed random excitation. The mode shape or shapes are noted visually with the aid of a fine powder to determine where strain gages should be placed to obtain the transmissibility factors at the anti-nodes. It is anticipated that these mode shapes will not change significantly during the incident of radiant heat flux.

The foam-panel structures to be subjected to radiant heat are instrumented with high-temperature strain gages on the bottom side of the metal panel (away from the incident radiation) at the anti-node positions determined in the preliminary investigation. The output of these strain gages is monitored during the tests both on a direct writing oscillograph for immediate viewing and on an instrumentation type tape recorder (Ampex type AR200) for possible future analysis.

The strain gages to be used on the panel are of a high-temperature type (usable to 600°F) and are compensated for temperature changes for the greater part of the temperature range. The temperature of the back side of the panel is recorded at a number of gage positions from which final corrections to the data are made. A typical strain gage applicable to this service is the Budd Metal-film type S-610 applied with a ceramic cement.

3. Experimental Results

Tests were performed to check out the vibratory testing equipment to be used for sinusoidal sweep and random testing experiments. These tests also provided the information for placing the response instrumentation. A stainless steel panel 13 x 13 x 0.093 in. was installed in the support position of the vibration test fixture used for sweep and random testing with a quantity of sand placed on the plate. The panel was swept through the sinusoidal frequency range (5 to 2000 cps) to determine the modes at which it would vibrate. The mode shapes obtained with the metal panel alone show fairly distinct patterns over as high as the fifteenth mode. Eight

distinct mode patterns were noted, and one or two transitional patterns appeared. The transitional patterns are probably due to a change in clamping conditions at these specific frequencies. This change in clamping (at the edge of the panel) probably accounts for the mode frequencies deviating from the integral multiple relationship.

The experimental results obtained on Z-88, Z-89 and "prefired ZP-58" foams under sinusoidal test conditions have been shown in Tables XIII to XV. The mode frequencies are tabulated with the mode number. The product of the mode number and fundamental frequency are also tabulated for comparison. The mode shapes for the bare panel, Z-88, and the prefired ZP-58 were sketched from the pattern evolved by the fine sand while it was excited. Lines in the square represent the anti-nodes and are masked by the accumulation of sand particles which are not moving.

Excitation of the panels, with a random excitation of the approximate profile specified for the tests, showed no detectable mode shapes other than the first.

The results with Z-88 indicate that the foam on a stainless steel plate substrate exhibits somewhat more clamping than the bare substrate.

The foam was then successfully subjected to the heat flux simultaneous with random vibration for 5 min, at the end of which it was intact, except for some slight interfacial separation at one edge. Table XVI shows the average backface temperatures obtained from a set of six thermocouples. The positions of these thermocouples relative to the panel are shown in Fig. 22. Results indicate that the average back plate temperature after 5 min exposure was 477°F. It should be noted that in this experiment the heat flux at the center of the 12 x 12 in. foam surface was determined to be 46 Btu/ft^2-sec instead of the required 40 Btu/ft^2-sec.

Table XIII

MODE PATTERNS OBTAINED IN SINUSOIDAL SWEEP TEST FOR BARE SUBSTRATE PANEL
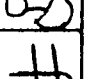
Frequency f_n cps	Mode Number N	Nf_1 cps	Mode Shape
130	1	130	
270	2	260	
310	-	-	
315	-	-	
385	3	390	
470	-	-	
520	4	520	
585	-	-	
660	5	650	
740	-	-	
760	6	780	
810	-	-	
990	8	1040	
1400	11	1430	
1900	15	1950	

Table XIV

MODE PATTERNS OBTAINED IN SINUSOIDAL SWEEP TEST

FOR Z-88 FOAM
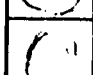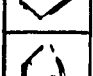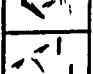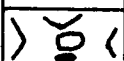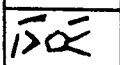
Frequency f_n cps	Mode Number N	Nf_1 cps	Mode Shape
110	-	-	
220	2	220	
330	3	330	
500	4	440	
560	5	550	
820	7-8	$\frac{770}{880}$	
1650	15	1650	
1990	18	1980	

Table XV

MODE PATTERNS OBTAINED IN SINUSOIDAL SWEEP TEST
FOR "PREFIRED ZP-58" FOAM

Frequency fn (cps)		Mode Number N		Nf_1 (cps)		Mode Shapes	
(a)*	(b)*	(a)	(b)	(a)	(b)	(a)	(b)
160		1		160			
	190		1		190		
360	~360	2	2	360	380		
475		3					
	550		3		570		
925		6					
	1650		9		1710		

*(a) for one 12 x 12 x 1/2 in. foam.

(b) for four 6 x 6 x 1/2 in. pieces cemented together to form a 12 x 12 x 1/2 in. foam.

Table XVI

TEST RESULTS ON FOAMS Z-88 AND Z-89 SUBJECTED

TO SIMULTANEOUS HEAT FLUX* WITH RANDOM VIBRATION

Foam No.	Foam Density (lb/ft^3)	Time (Secs.)	Av. Back-Plate Temp. (°F)
Z-88	60	60	75
		120	150
		150	190
		180	247
		240	247
		300	477
Z-89	68	60	90
		120	130
		150	155
		180	190
		240	255
		300	315

* The heat fluxes on Z-88 and Z-89 were 46 Btu/ft^2-sec. and 40 Btu/ft^2-sec., respectively.

In the case of prefired ZP-58 foam, results have been obtained for both a single foam specimen 12 x 12 x 1/2 in., as well as for foams 6 x 6 x 1/2 in. pieces, cemented together with an RTV silicone to form a 12 x 12 x 1/2 in. heat shield. The prefired foam was cemented onto the steel plate substrate with RTV silicone as well.

Both the prefired ZP-58 foams were subjected to the random vibration, without heat flux, and successfully withstood the test.

Foam Z-89 was evaluated by placing strain gages on the underside of the substrate panel, in order to attempt to identify the modes. The positioning of the strain gages on a typical panel is shown in Fig. 23.

Prior to the test run, strain gages were calibrated by introducing an electrical signal into the circuit equivalent to a known strain level. This calibration signal was recorded on the oscillograph as two channels which were used to determine actual strain levels from the oscillograms taken during the test.

During the test run the following peak sinusoidal vibration levels were maintained:

Frequency	Vibration Level
5 to 18 Hz	0.5 in. double amplitude displacement
18 to 2000 Hz	8.5g peak

One sweep through the frequency range was made at the rate of 1 octave per min. During this time the strain gage response signals were recorded on the oscillograph. At frequent intervals the excitation frequency was marked directly on the oscillogram.

Strain recordings at an excitation frequency of 180 cps indicated a resonance by peaks in the strain response signals. These response levels at resonant peaks are plotted in Fig. 24, and

superimposed on the specimen profile. The levels at the highest response peaks are fairly low (160 x 10^{-6} in./in. peak for gage position 8). The results plotted in Fig. 24 show that vibrational response was essentially zero at gage 3. In order to verify these results using the sand technique, the sinusoidal sweep was repeated and photographs were taken of the resultant sand patterns at various vibration frequencies. The inner sand ring occurred very close to gage position 3 for the 180 cps mode pattern. Two other distinct patterns showed on the repeat sweep at 140 cps and 650 cps. Either the sample sufficiently changed its vibrational characteristics as a result of the two tests, or the response at the substrate (as determined by strain gages) is not always similar to that on the foam surface, as shown by the sand patterns.

Z-89 was then subjected directly to the specified vibrational test levels, simultaneous with a heat flux of 40 Btu/ft^2-sec. It successfully withstood the entire test cycle. The average backface temperatures at various test times are shown in Table XVI. The average backface temperature after 2 1/2 and 5 min were 155° and 315°F, respectively.

These results indicate that castable foams, such as those developed on this program, may be used along with and even instead of prefired foams for the strap-on type rigid heat shields where the substrate is a flat plate instead of a honeycomb panel.

VI. CHARACTERISTICS OF OPTIMIZED ZIRCON FOAMS

A. Introduction

To optimize ceramic foams for rigid heat shields, they must not only exhibit superior thermal efficiency and maintain mechanical integrity under the final test conditions (see Section V) but they must also possess certain other characteristics. These include desirable mechanical properties (especially a flat-wise tensile strength) and an ability to resist water erosion. To achieve these objectives with the minimum acceptable foam thickness and density, a castable

type, chemically bonded, composite zircon foam was developed and evaluated.

Zircon foam compositions considered for optimization, on the basis of the final testing program, are the silicate-bonded foams Z-87, Z-88, Z-89 and Z-90, and the phosphate bonded foams ZP-58, prefired ZP-58 and ZP-65.

The nominal composition of these foams has been shown in the preceding sections. All foams have a density not exceeding 60 lb/ft^3.

B. Tensile Strength

Flat-wise tensile strength values have been obtained for the nearly optimized silicate-bonded and phosphate-bonded zircon foams.

The zircon foams were cast onto 2 x 2 x 1/4 in. 304 stainless steel plates in order to obtain flat-wise tensile strength data. The cured foam, slightly more than 1/2 in. in height, was ground parallel to a height of 1/2 in. and the fixtures were attached to the foam and substrate with epoxy resin. The foams were then tested on an Instron machine.

. Table XVII shows the results obtained for the silicate-bonded zircon foams. Results indicate that in all cases skin type foams are the weakest. Observation of the fractured specimens indicated that the partial skin and no skin-type foams fractured in the middle of the foam specimen or close to the upper surface, while the skin type failed at the interface (on which the foam was cast) or very close to the interface. This is concurrent with the fact that the formation of a hard surface skin is due to the rapid migration of albumin along with the potassium silicate binder material to the surface during curing, thus causing a depletion of the binder within the foam body and at the interface. The Superpax-containing foams were found to have a lower flat-wise tensile strength than those

Table XVII
FLAT-WISE TENSILE STRENGTH
OF ZIRCON FOAMS AT ROOM TEMPERATURE

Foam No.	Foam Type	Density, lb/ft^3	Average Tensile Strength, psi
Z-87	S	60	33
	PS	60	40
	NS	60	42
Z-88	S	57	49
	PS	57	54
	NS	57	65
Z-89	NS	52	70
Z-90	S	58	55
	PS	58	60
	NS	58	78

without. The highest tensile strength was obtained with foam Z-90, no skin-type. This foam contains fine diameter Fiberfrax instead of the medium diameter Fiberfrax used in other foams.

Tensile strength of phosphate-bonded castable zircon foams are strongly dependent on the surface conditioning during drying and curing of the foam, since this influences the microstructure. Table XVIII indicates the tensile strength and micropore structure of the nearly optimized foams, as a function of their surface conditioning during drying (referred to as "type"). Values have been obtained on 2 x 2 x 1/2 in. specimens cast on plates and/or honeycomb substrates as indicated. The nomenclature used in Table XVIII has been discussed earlier in Section IV. The highest tensile strength values were obtained for ZP-58, with surface conditioning referred to as CHP (1/8) or "controlled humidity partial."

The average tensile strength of the prefired ZP-58 type foam (density, 50 lb/ft^3) is 114 psi. In nearly all cases, failure took place at the base-coated, foam-metal interface. Therefore, the true tensile strength of the prefired foam may be considerably higher.

C. Water Effect

The effect of water on the properties of optimized zircon foams was evaluated by a water boiling and a cold water soak test. Specimens were weighed and then immersed in boiling distilled water for 3 hrs. The specimens were placed in wire baskets and suspended in the container. After boiling, the specimens were dried in an electric oven and weighed again. Specimens were also subjected to a 24 hr cold water soak test. The percentage of weight loss are shown in Table XIX. All castable foams lose about 5 wt% when subjected to a water environment. However, when a 1/2 in. thick foam, ZP-58, was cast onto a 2 x 2 x 1/4 in. metal plate and then tested, its loss was considerably reduced. The prefired ZP-58 foam showed

Table XVIII

FLAT-WISE TENSILE STRENGTH OF PHOSPHATE-BONDED ZIRCON FOAMS

Foam No.	Type	Density (lb/ft^3)	Average Tensile Strength (psi)	Comments
ZP-58	CHP(1/8)	56	92	Medium size pores. Uniform micropore structure; broke at interface.
	CHP(1/8)*	58	124	Uniform, fine pore structure throughout; broke mostly through foam instead of interface.
	CHP(1/8)* (Honeycomb Substrate)	54	120	Uniform, med-fine pore structure; broke mostly at open-face structure of honeycomb substrate.
	CH(1/8)	56	64	Bloated, large pores at center; broke at interface.
	CH(3/8)	56	70	Large pores at center; considerable binder migration; interfacial break.
	S	58	73	Uniform pore structure; interfacial break.
	CCBP	55	26	Powdery in center, high degree of migration, finer pores.
	NS	46	25	Large pores, bloating at center of foam.
	PS45	50	32	Intermediate pores; striated near substrate, soft in center.

-68-

Table XVIII (Cont'd)

Foam No.	Type	Density (lb/ft^3)	Average Tensile Strength (psi)	Comments
ZP-62	PS90	58	82	All types of foams had fine pores at edges; pores in center increase from PS90 to CH.
	PS60	63	80	
	PS30	60	95	
	NS	53	76	
	PS30CH	55	55	
	CHP	55	80	
	CH	58	60	
ZP-65	CHP(1/8)*	65	108	Uniform, fine pore structure; broke both at interface and through foam.
ZP-66	CHP(1/8)*	69	155	Uniform, fine pore structure; specimens broke both at interface and through foam.

* Longer curing time.

Table XIX
WATER SOLUBILITY
OF CASTABLE ZIRCON FOAMS

Foam No.	Type	Percent Weight Loss	
		3 hr Boil	24 hr Soak
Z-87	PS	5.5	5.3
Z-88	PS	4.7	6.0
	NS	3.9	5.7
Z-89	NS	4.3	5.9
Z-90	PS	6.0	4.7
	NS	4.6	6.2
ZP-58	CHP	10	-
ZP-58 (cast on plate before testing)	CHP	2.2	4.8
"Prefired ZP-58"		0.6	0.4

negligible loss on testing. The loss in the castable foams is largely due to the presence of water soluble binders which were added to these foams.

The effect of water on the flat-wise tensile strength of Z-89 was determined after a 24 hr soak test. There was a reduction in the tensile strength from 70 psi to 40 psi.

The tensile strength of ZP-58 is also effected by exposure to water. Samples exposed to water were air-dried for 48 hrs before testing. The specimens soaked in water for 24 hrs showed a strength loss of about 50%, while those boiled in water indicated a slightly higher loss in strength.

However, soaking these foams for as long as 97 hrs did not affect their mechanical integrity when subjected to the final test conditions of 60 cps vibration and 90 g's acceleration, as shown for Z-90 and ZP-58 in Tables VIII and XI. In fact, both foams were successfully subjected to a second 5 min recycle under final test conditions.

D. Thermal Conductivity

The thermal conductivities of silicate-bonded foams, Z-67 and Z-90 (having densities of 52 lb/ft^3 and 60 lb/ft^3, respectively), and of the phosphate-bonded foam, ZP-58 (density 60 lb/ft^3), were determined by the radial heat flow technique over a temperature range.

Results for Z-67, Z-90 and ZP-58 have been tabulated in Tables XX, XXI and XXII, respectively. The phosphate-bonded zircon foam (ZP-58) has a higher thermal conductivity than the corresponding silicate-bonded foams (Z-67 and Z-90).

Figure 25 compares the thermal conductivity of the IITRI-developed, silicate-bonded castable zircon foams with a fired zirconia foam of similar density. Foam Z-67 was prepared from fine grained zircon powder (Superpax) and has a lower thermal conductivity than

Table XX

THERMAL CONDUCTIVITY OF ZIRCON FOAM Z-67

Temperature °F	Thermal Conductivity, Btu/hr-ft-°F
240	.094
460	.084
655	.076
900	.076
1085	.080
1305	.097
1560	.124
1835	.166
2130	.236
2300	.290

Table XXI

THERMAL CONDUCTIVITY OF ZIRCON FOAM Z-90

Temperature °F	Thermal Conductivity, Btu/hr-ft-°F
298	0.125
651	0.136
984	0.157
1293	0.185
1602	0.240
1839	0.285
2048	0.336
2295	0.397

Table XXII

THERMAL CONDUCTIVITY OF FOAM ZP-58

Temperature, °F	Thermal Conductivity Btu/hr ft °F
185	0.22
353	0.27
591	0.38
776	0.47
982	0.55
1203	0.60
1450	0.62
1618	0.63
1823	0.66

Z-90, which was prepared from a coarser particle sized starting material. The effect of radiation transparency is evidenced by the marked increase in conductivity above 1100°F.

E.   Specific Heat

The specific heats of the two optimized zircon foams, silicate-bonded Z-90 and phosphate-bonded ZP-58, have been determined.

The enthalpy of foam Z-90 was measured from room temperature to 2300°F by the drop calorimeter technique. In this method, a sample of the material is heated to a desired temperature in a furnace and then dropped in a modified Parr calorimeter. The enthalpy of the material is calculated from the weight and temperature rise of the water in the calorimeter. The process is repeated at a series of temperatures at approximately 200°F intervals. An equation is fitted to the enthalpy curve, and specific heat is obtained by differentiation of the enthalpy equation with respect to temperature at constant pressure.

The specific heat of zircon foam Z-90 as function of temperature is presented in Table XXIII and shown in Fig. 26. The sudden change in specific heat around 1800°F, as seen in this figure, is probably due to the melting of some unreacted binder, potassium silicate.

The enthalpy of foam ZP-58 was similarly measured, at 200°F, and its specific heat calculated to be 0.162 Btu/lb -°F. Results indicate that both the silicate-bonded and phosphate-bonded castable zircon foams, Z-90 and ZP-58, respectively, have similar specific heat values at 200°F.

F.   Reflectance

Reflectance measurements were made at room temperature on Z-67, Z-88, Z-89, Z-90, ZP-58 and prefired ZP-58 in the range of 0.7 to 2.7 microns. The results are shown in Figs. 27 and 28.

Table XXIII

SPECIFIC HEAT OF ZIRCON FOAM Z-90

Temperature °F	C_p, Btu/lb-°F
200	0.167
400	0.172
600	0.185
800	0.205
1000	0.224
1200	0.239
1400	0.264
1600	0.283
1700	0.291
1950	0.146
2200	0.146

Reflectance measurements were made employing a Beckman DK2-A spectroreflectometer. This instrument measures hemispherical reflectance with normal illumination in the wavelength range 0.20 to 2.7 microns.

The reflectance of silicate-bonded foams prepared without a surface skin (NS type) is very high -- above 90% in the important region of 0.75 to 1.85 microns. Considerable loss of reflectance occurs at higher wavelengths. The presence of a surface skin on this foam reduces the reflectance considerably as indicated by Z-90 with partial skin (PS type). This reduction in reflectance is probably due to the presence of yellowish albumin in the skin layers. On the other hand, the prefired ZP-58 foam has an exceedingly high reflectance, in the entire range and upto 2.7 microns.

The results also indicate that the castable, phosphate-bonded zircon foams, as exemplified by ZP-58, have a lower reflectance than castable silicate-bonded zircon foams (Z-89 NS). The reflectance of ZP-58 is comparable to silicate-bonded zircon foams prepared with partial skin (PS type). The lower reflectance of the phosphate-bonded foams also manifests itself in the higher backface temperatures obtained during exposure to heat fluxes of 40 Btu/ft^2-sec, as compared to silicate-bonded foams of identical density.

VII. SUMMARY

The major emphasis in this investigation has been in the development of chemically bonded, fiber reinforced, castable type, zircon foams for use in rigid heat shields. Work was also done in preparing and evaluating castable mullite and calcium aluminate foams; however, the optimization and final evaluations were confined to the zircon foams, using silicate and phosphate binder systems.

To develop castable zircon foams, which exhibit good insulative properties and maintain structural integrity when subjected simultaneously to high heat fluxes and severe vibrational

and acceleration levels, the concept of composite foams was studied. Fiber reinforced foams, dispersed multi-phase ceramic foams, and layered or sandwich foams are examples of composite foams.

The surface texture of the foams was also found to be of major significance. By the use, partial use, or disuse of a plastic wrapping on the foam surface during the drying cycle, it was possible to control the migration of the binder as well as the albumin to the surface. The change in surface texture significantly affects the reflectance especially in silicate-bonded castable zircon foams, and the microstructure and tensile strength in phosphate-bonded foams.

Generally speaking, silicate-bonded zircon foams were more insulative than the corresponding phosphate-bonded foams, although the latter exhibited higher tensile strengths. In both cases, the optimized compositions were able to successfully withstand severe vibrational and acceleration levels, simultaneous with the specified heat flux.

The use of fibers and stabilizing second-phase materials, along with close control of microstructure and, in particular, surface texture have enabled us to develop castable type, chemically bonded composite zircon foams which can be cured at low temperatures (not exceeding 260°F), and still possess excellent insulative structural properties for use in rigid heat shields. Further, since these foams also exhibit good bonding not only on honeycomb substrates but also on flat stainless steel plates, they can be used in "strap-on" heat shields, thus precluding the use of prefired foams and the development of special high temperature resistant adhesives.

VIII. LOGBOOK RECORDS

All data pertaining to work done in this period are
recorded in IITRI logbooks:

C 14965	C 15130	C 15676	C 15127	C 15135
C 15677	C 15129	C 15675	C 15681	C 15993
C 15994	C 15997	C 16002	C 16009	C 16485
C 16490	C 16494	C 16798	C 16801	C 16810
C 16818	C 16820	C 16978		

IX. PERSONNEL

Major contributions to this report were made by
S. L. Blum, A. J. Mountvala, H. Nakamura, H. L. Rechter,
E. Scharres, and L. Wolf, Jr.
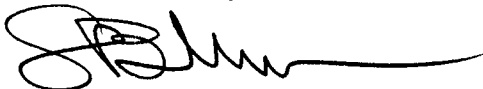
Respectfully submitted,

IIT RESEARCH INSTITUTE

A. J. Mountvala.

A. J. Mountvala
Senior Scientist
Ceramics Research

APPROVED BY:

S. L. Blum

S. L. Blum
Director
Ceramics Research
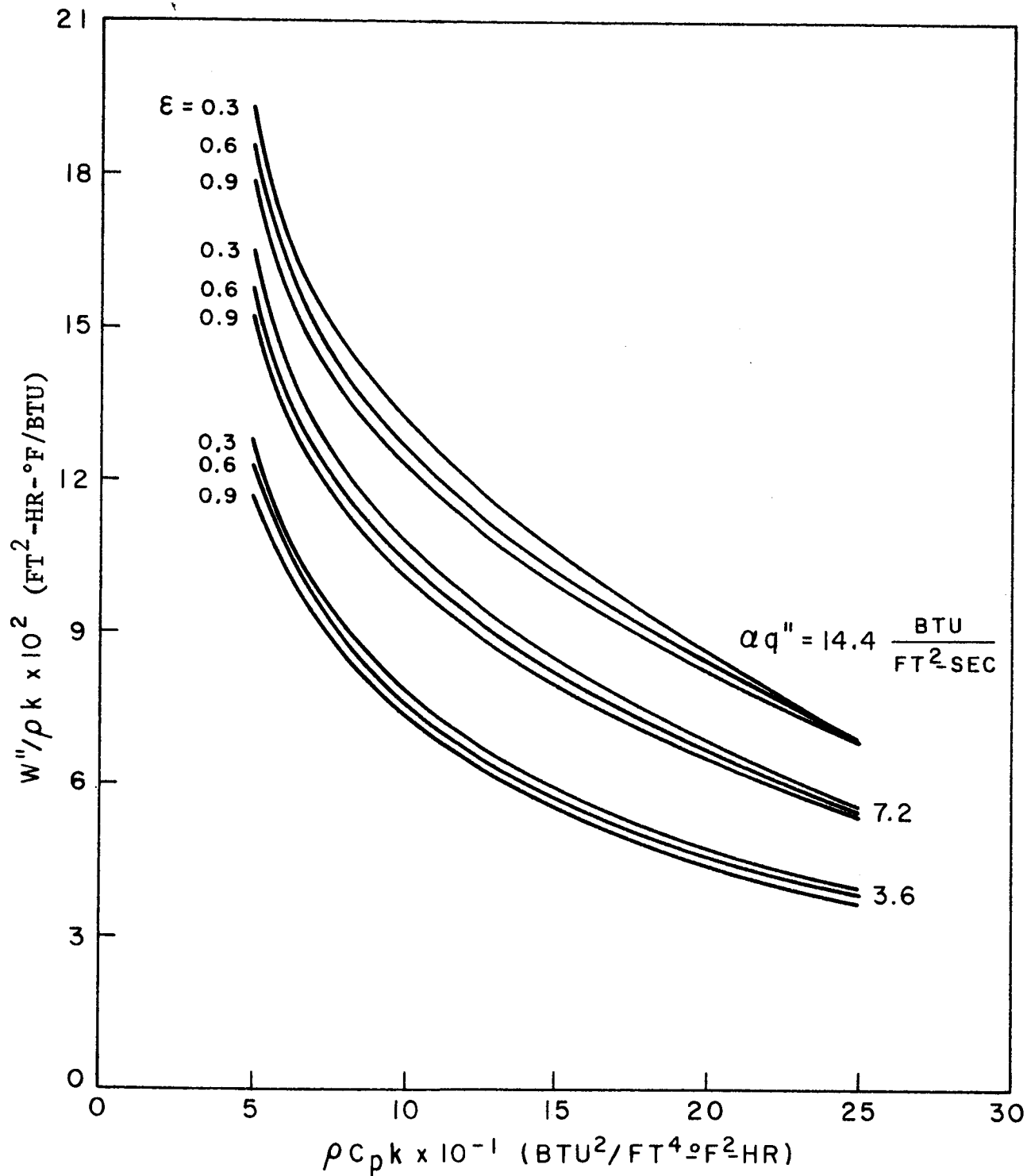
Fig. 1 - INSULATION WEIGHT REQUIREMENT AS A FUNCTION
OF THERMAL PROPERTIES
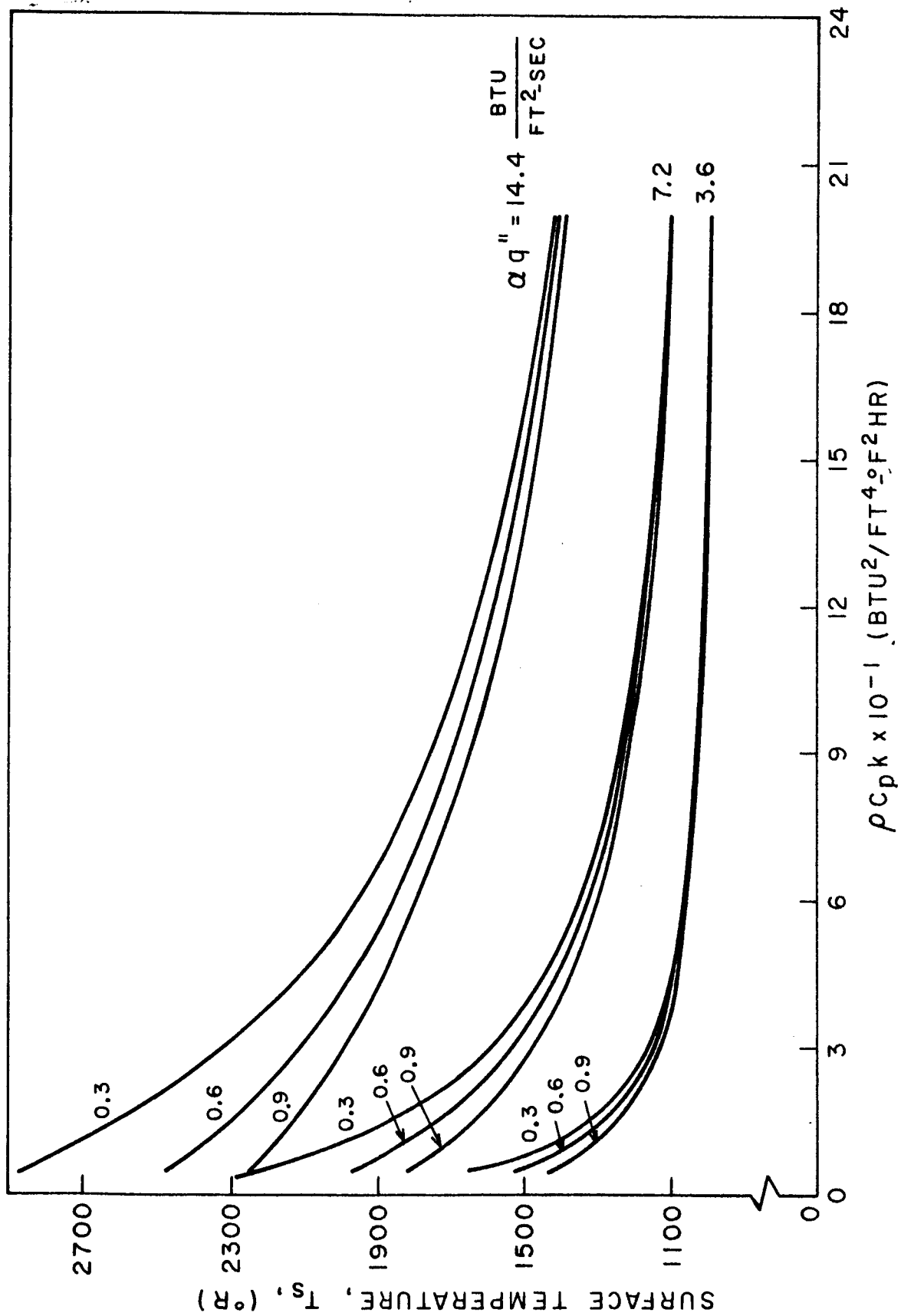
Fig. 2 — SURFACE TEMPERATURE AS A FUNCTION OF THERMAL PROPERTIES
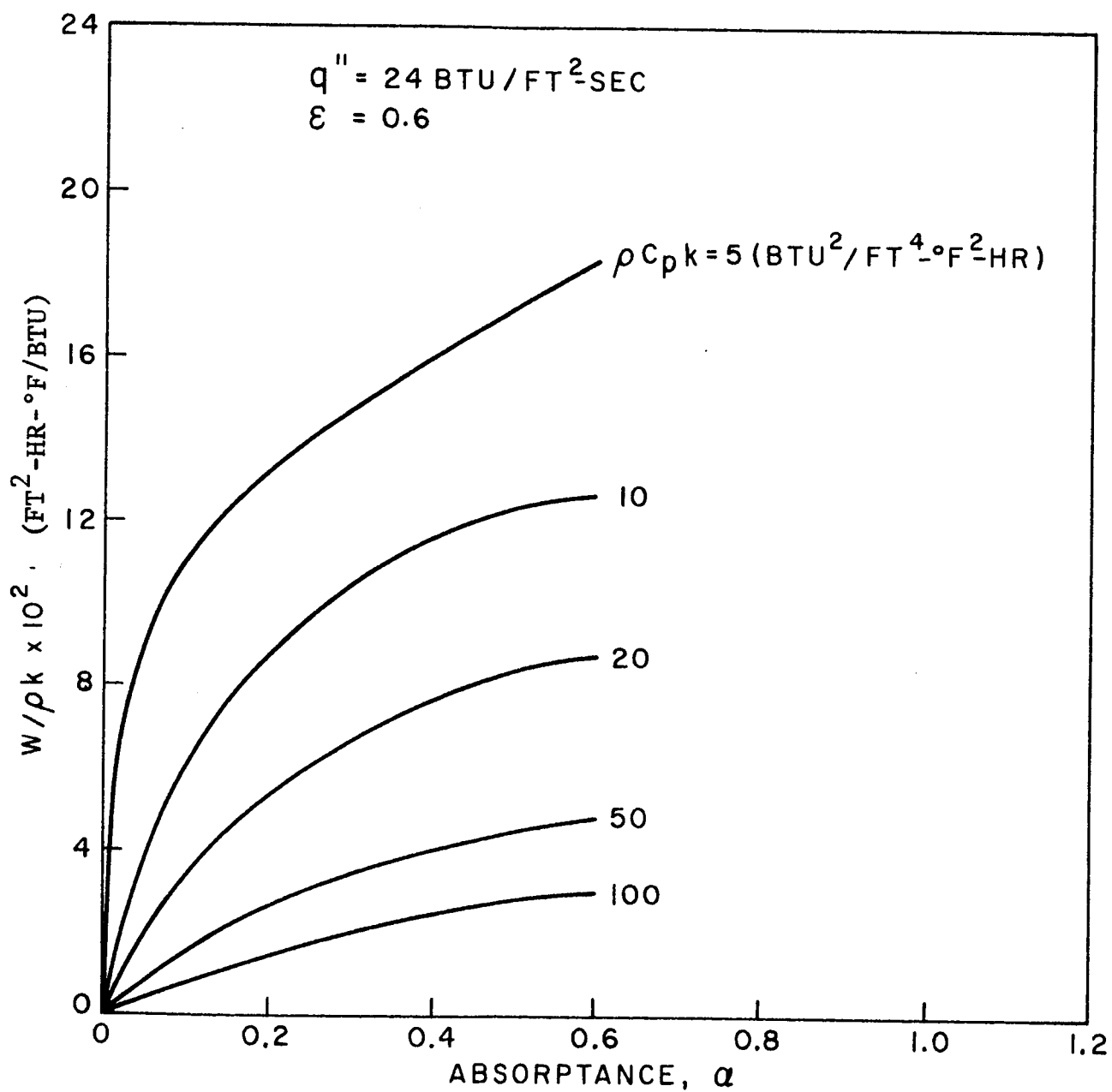
Fig. 3a - DEPENDENCE OF INSULATION WEIGHT REQUIREMENT
UPON ABSORPTANCE
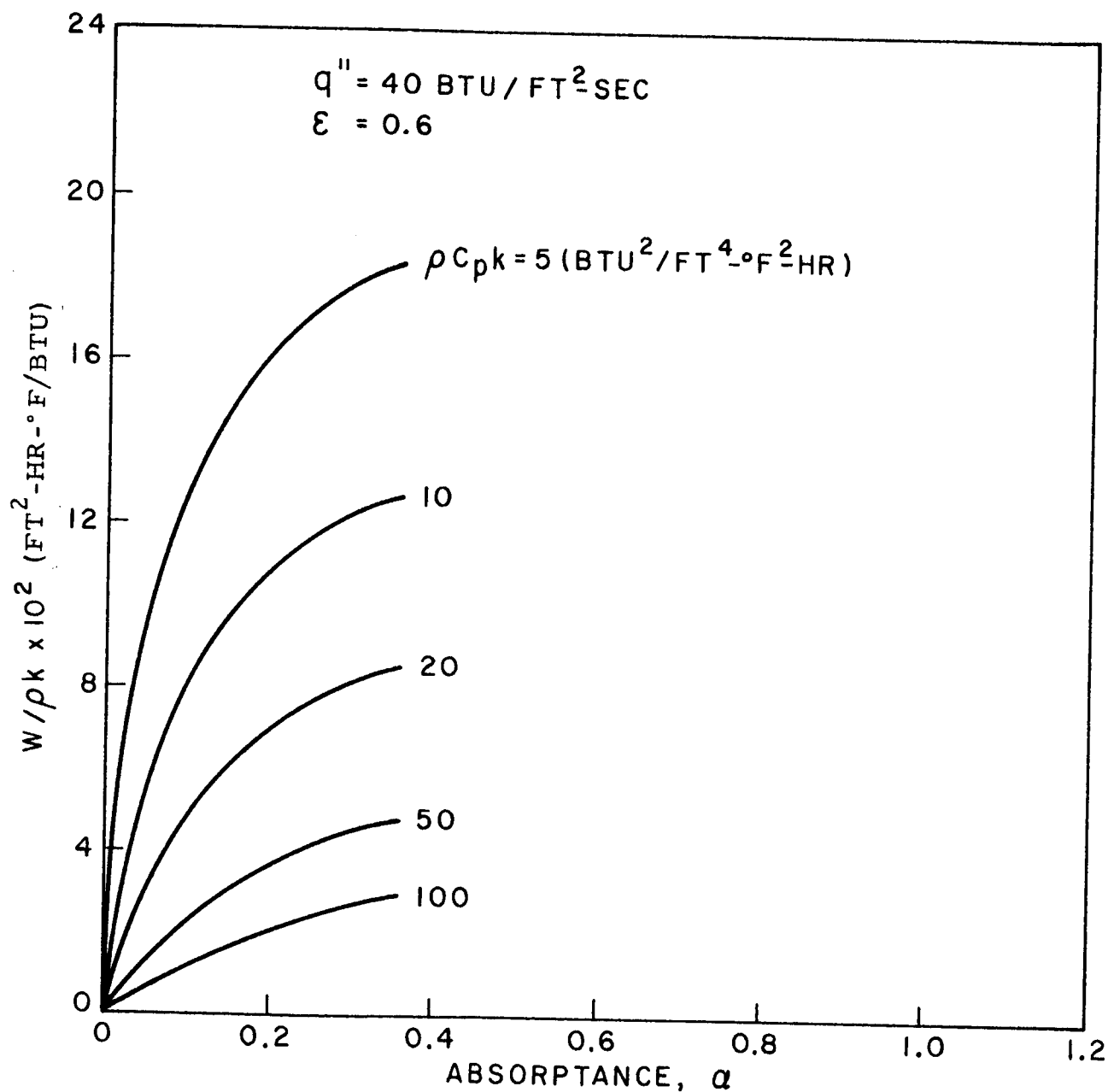
Fig. 3b – DEPENDENCE OF INSULATION WEIGHT REQUIREMENT
UPON ABSORPTANCE
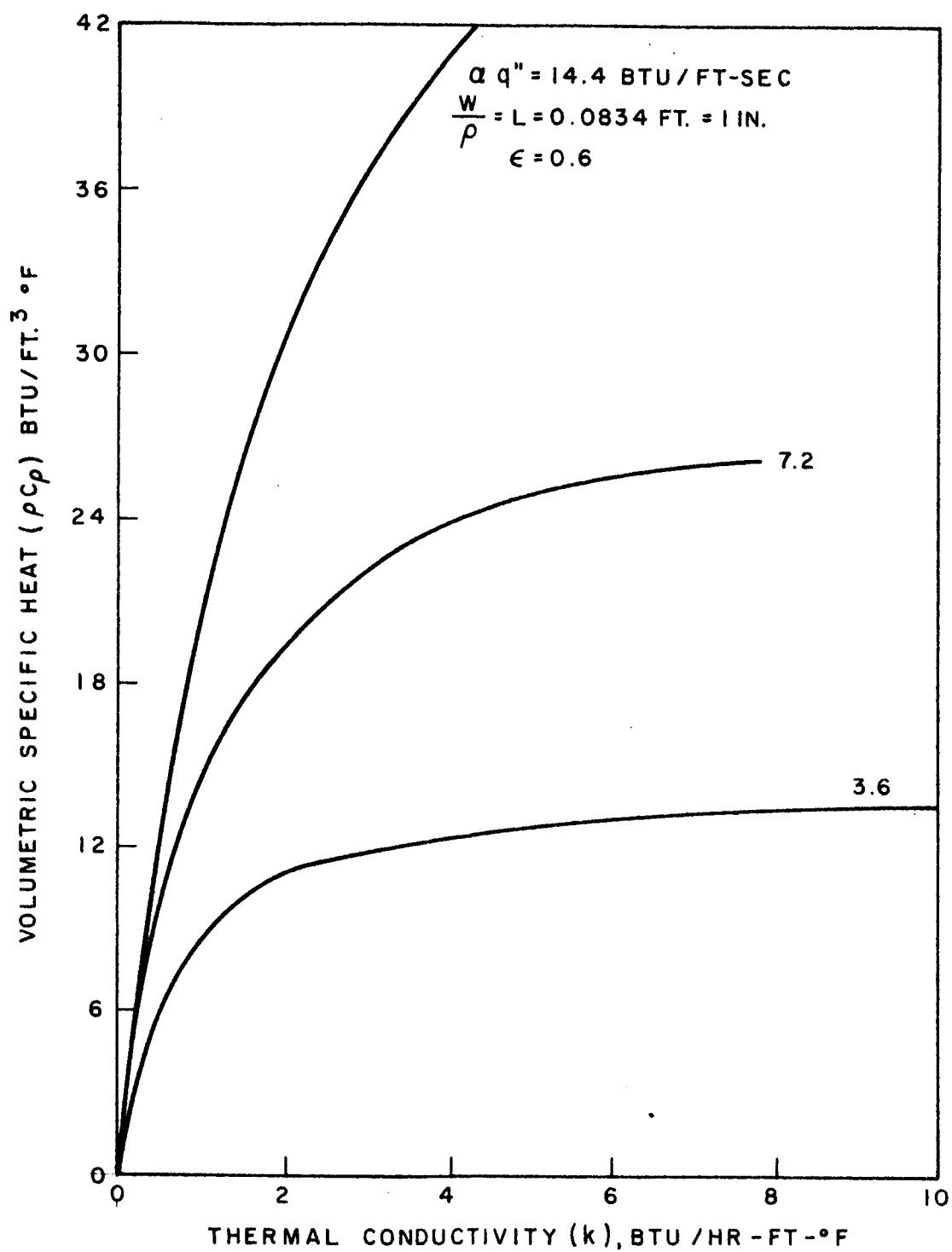
Fig. 4 - MINIMUM VOLUMETRIC SPECIFIC HEAT REQUIREMENT
AS A FUNCTION OF THERMAL CONDUCTIVITY
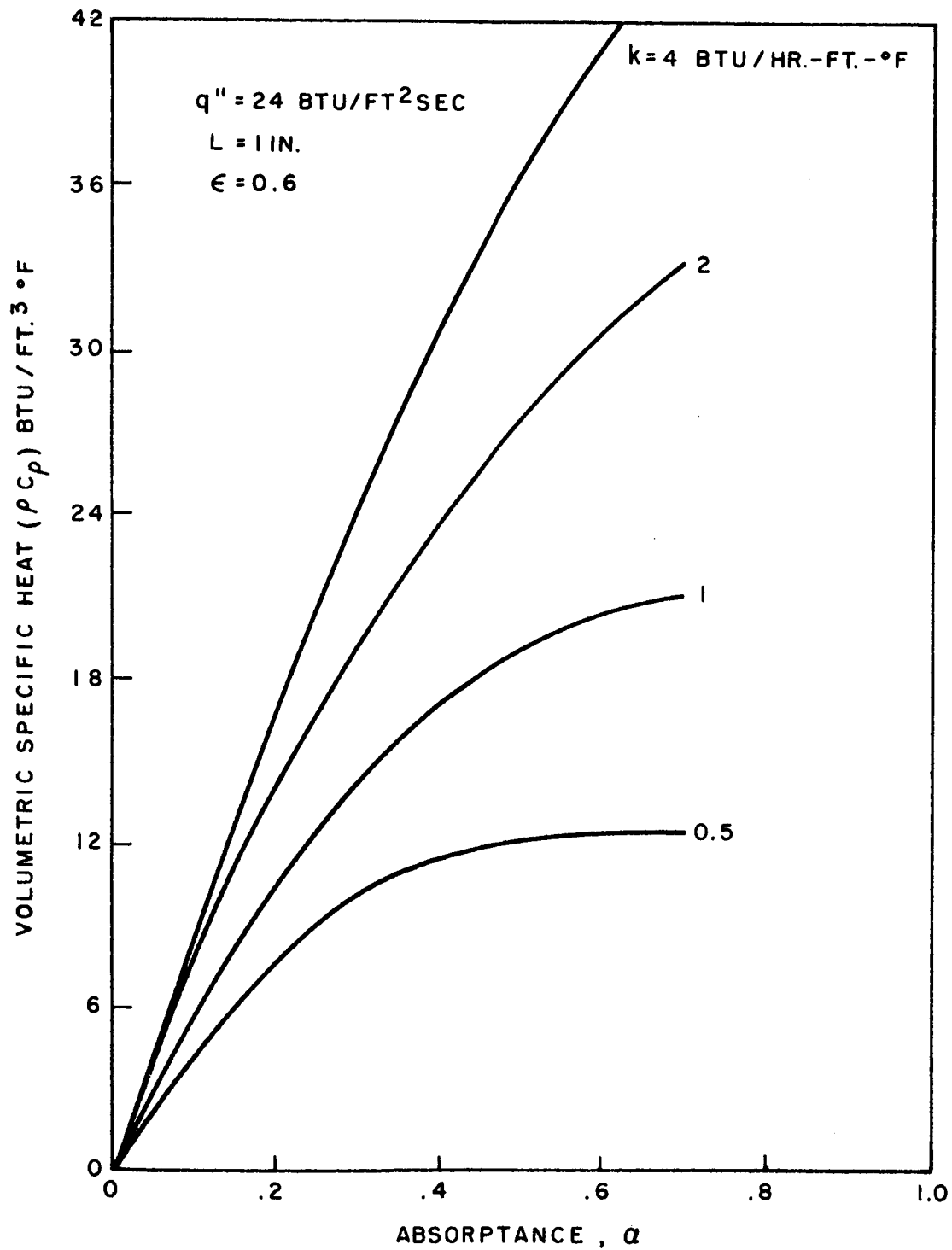
Fig. 5a - MINIMUM VOLUMETRIC SPECIFIC HEAT REQUIREMENT
AS A FUNCTION OF ABSORPTANCE
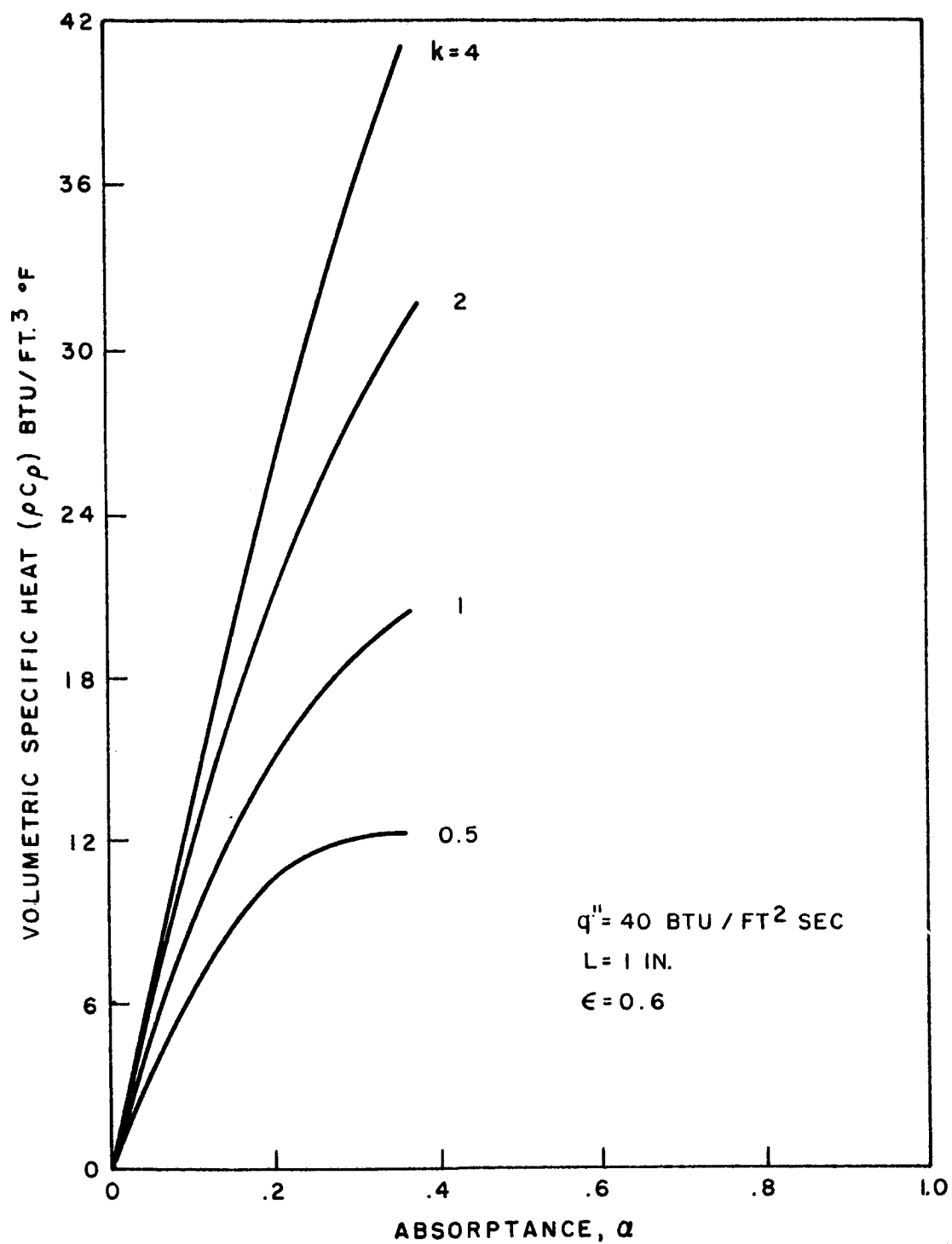
Fig. 5b – MINIMUM VOLUMETRIC SPECIFIC HEAT REQUIREMENT
AS A FUNCTION OF ABSORPTANCE
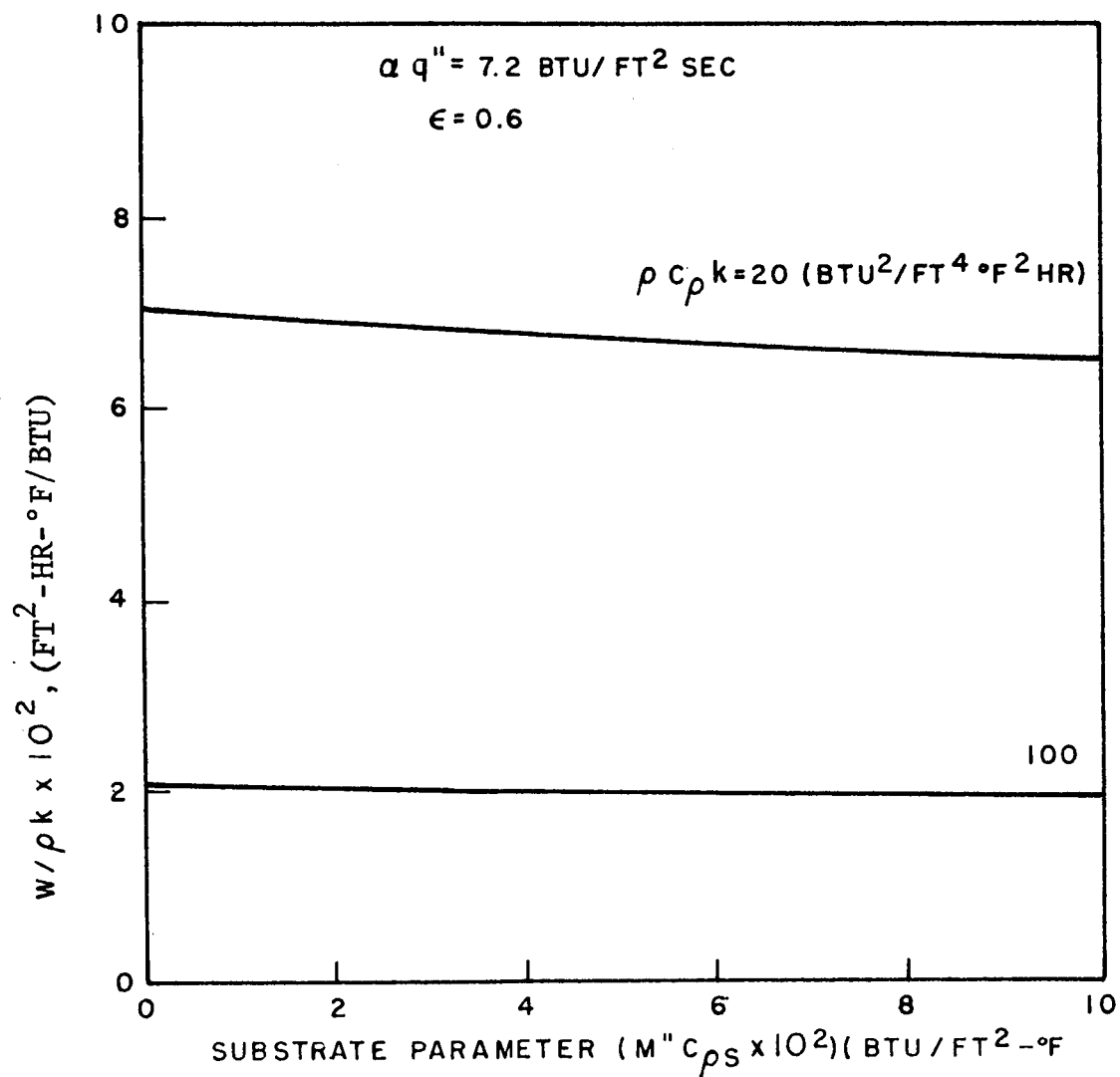
Fig. 6 - INFLUENCE OF SUBSTRATE UPON INSULATION
PERFORMANCE
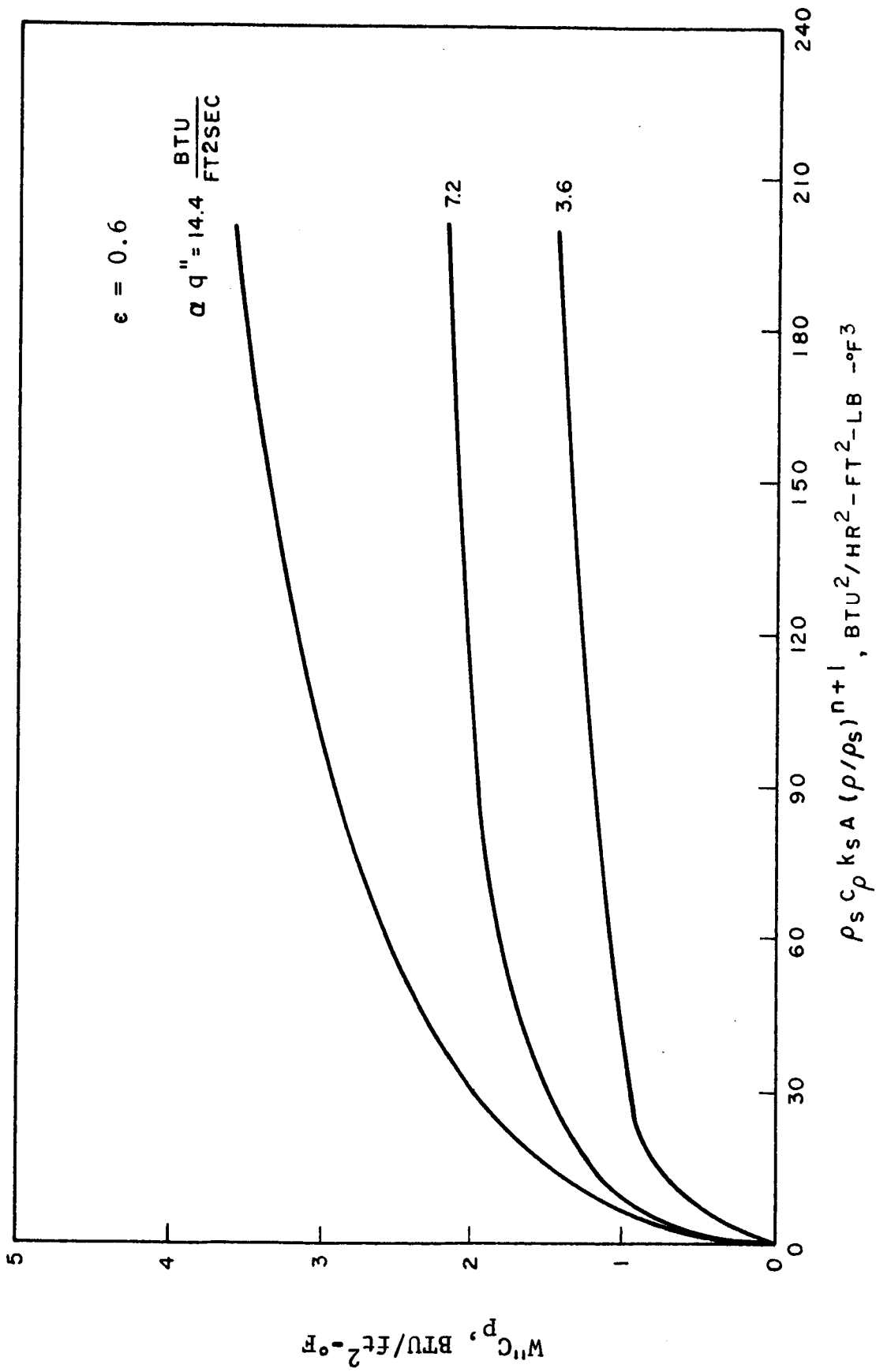
Fig. 7 - INSULATION WEIGHT REQUIREMENT WITH CONDUCTIVITY AS A FUNCTION OF DENSITY
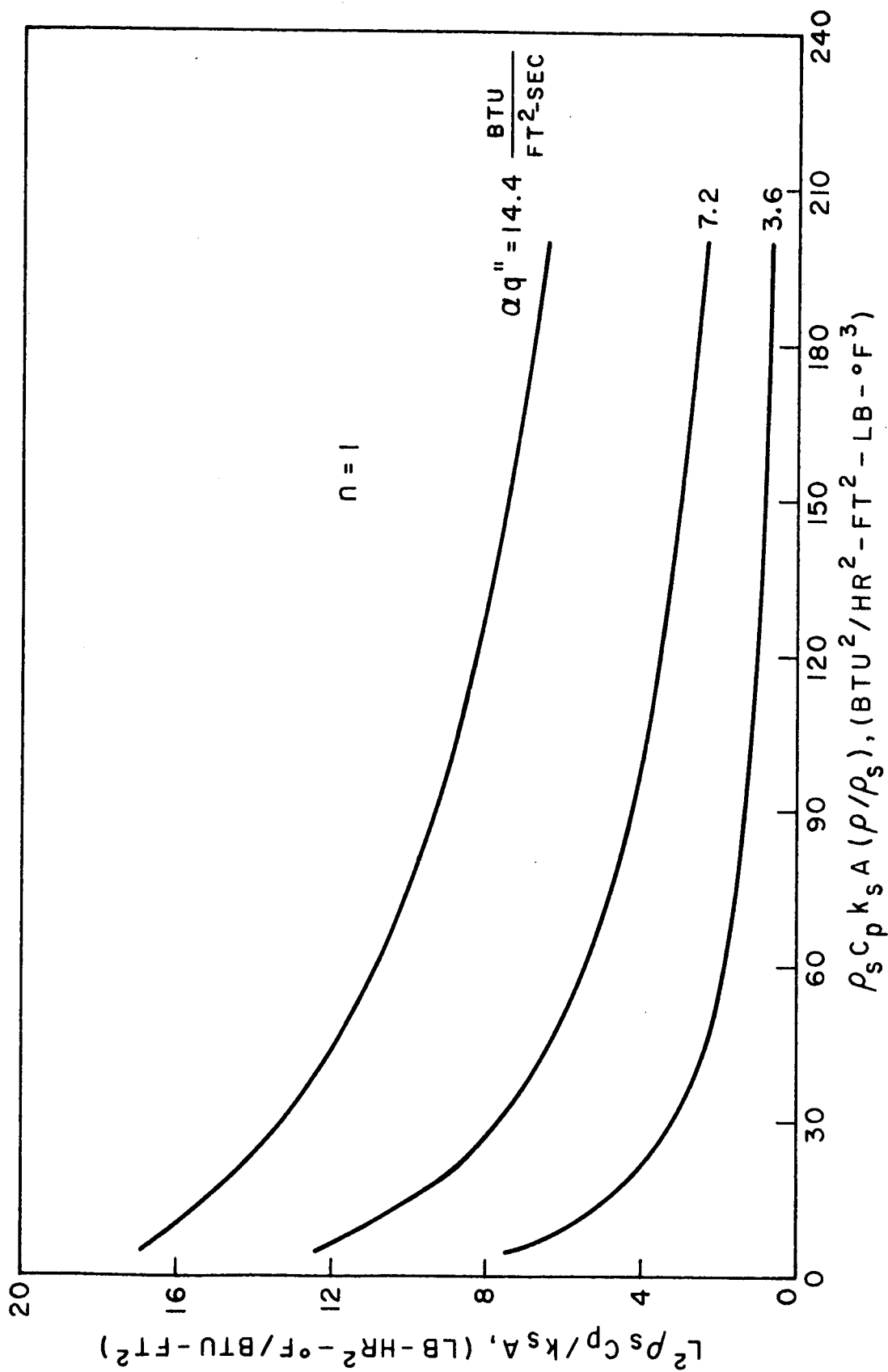
Fig. 8 - INSULATION THICKNESS REQUIREMENT WITH CONDUCTIVITY AS A FUNCTION OF DENSITY

$\rho_s C_p k_s A (\rho/\rho_s)$, $(\text{BTU}^2/\text{HR}^2 - \text{FT}^2 - \text{LB} - {}^\circ\text{F}^3)$

$L^2 \rho_s C_p / k_s A$, $(\text{LB-HR}^2 - {}^\circ\text{F}/\text{BTU} - \text{FT}^2)$

$n = 1$

$\alpha q'' = 14.4 \dfrac{\text{BTU}}{\text{FT}^2 \text{-SEC}}$

7.2

3.6
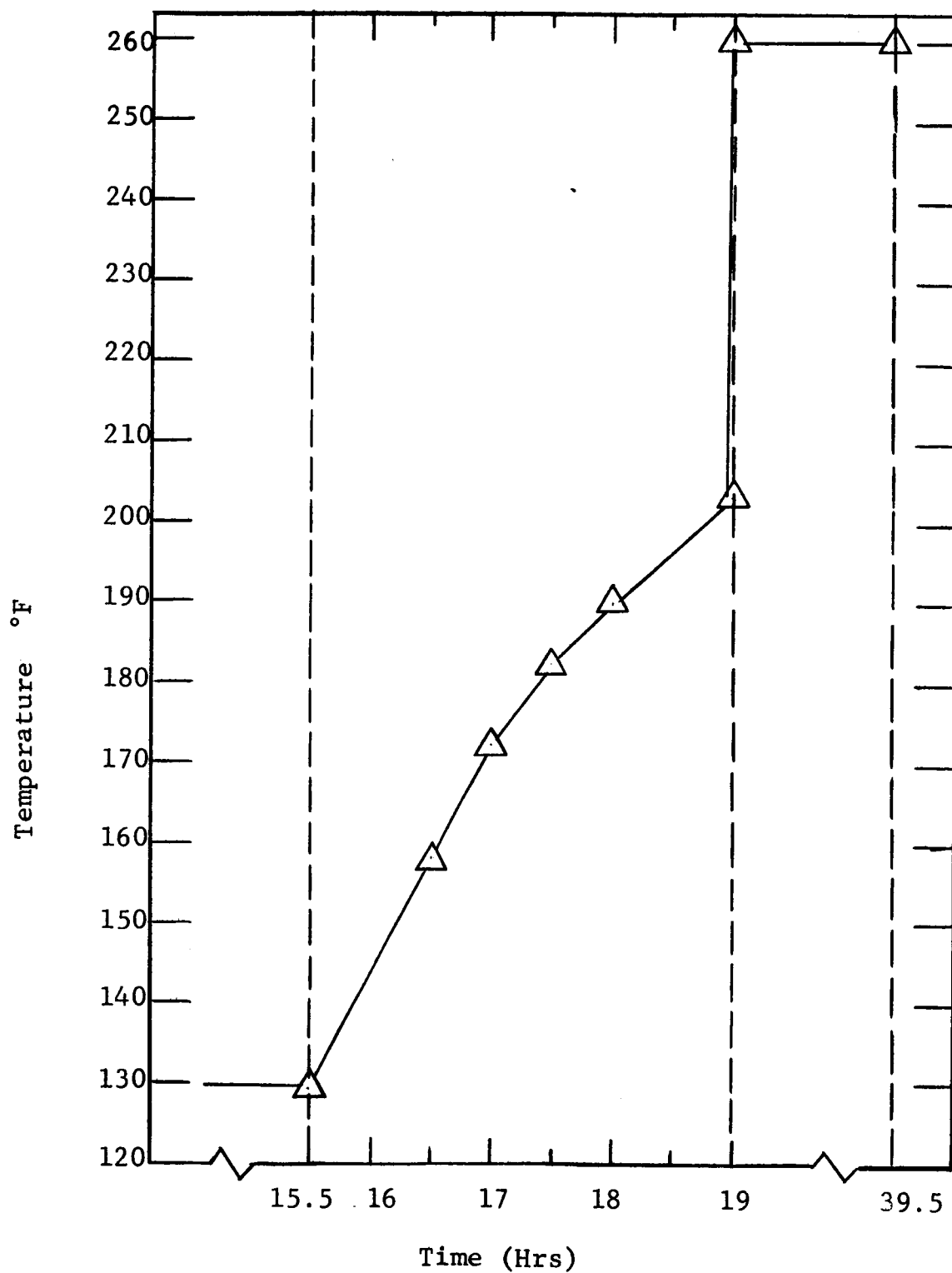
Fig. 9 - CURING CYCLE FOR FOAM Z-88
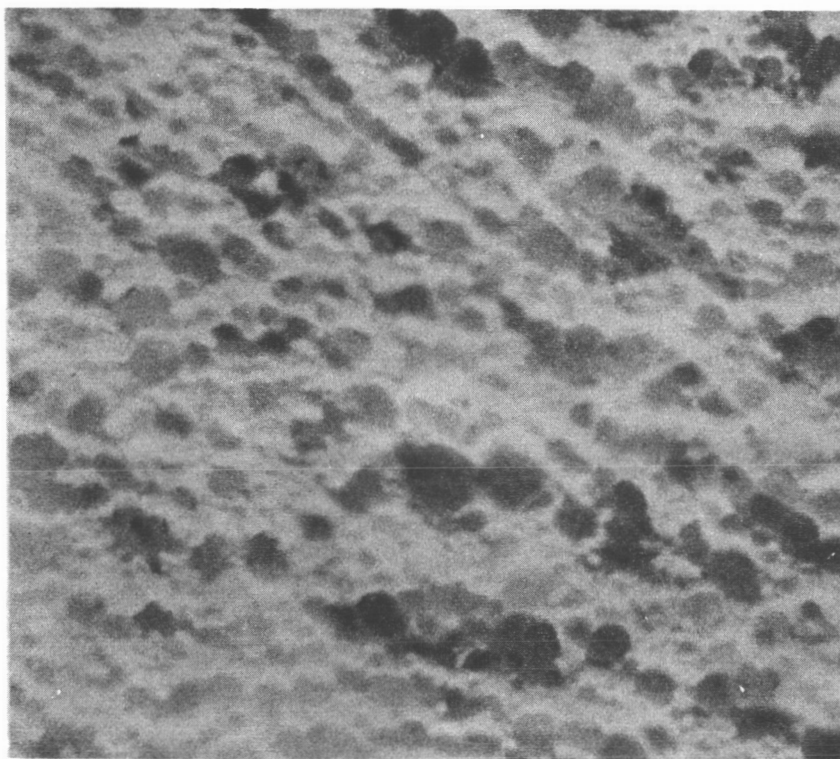
Fig. 10 - PHOTOMICROGRAPH OF OPTIMIZED
ZIRCON FOAM, Z-90 (24x)
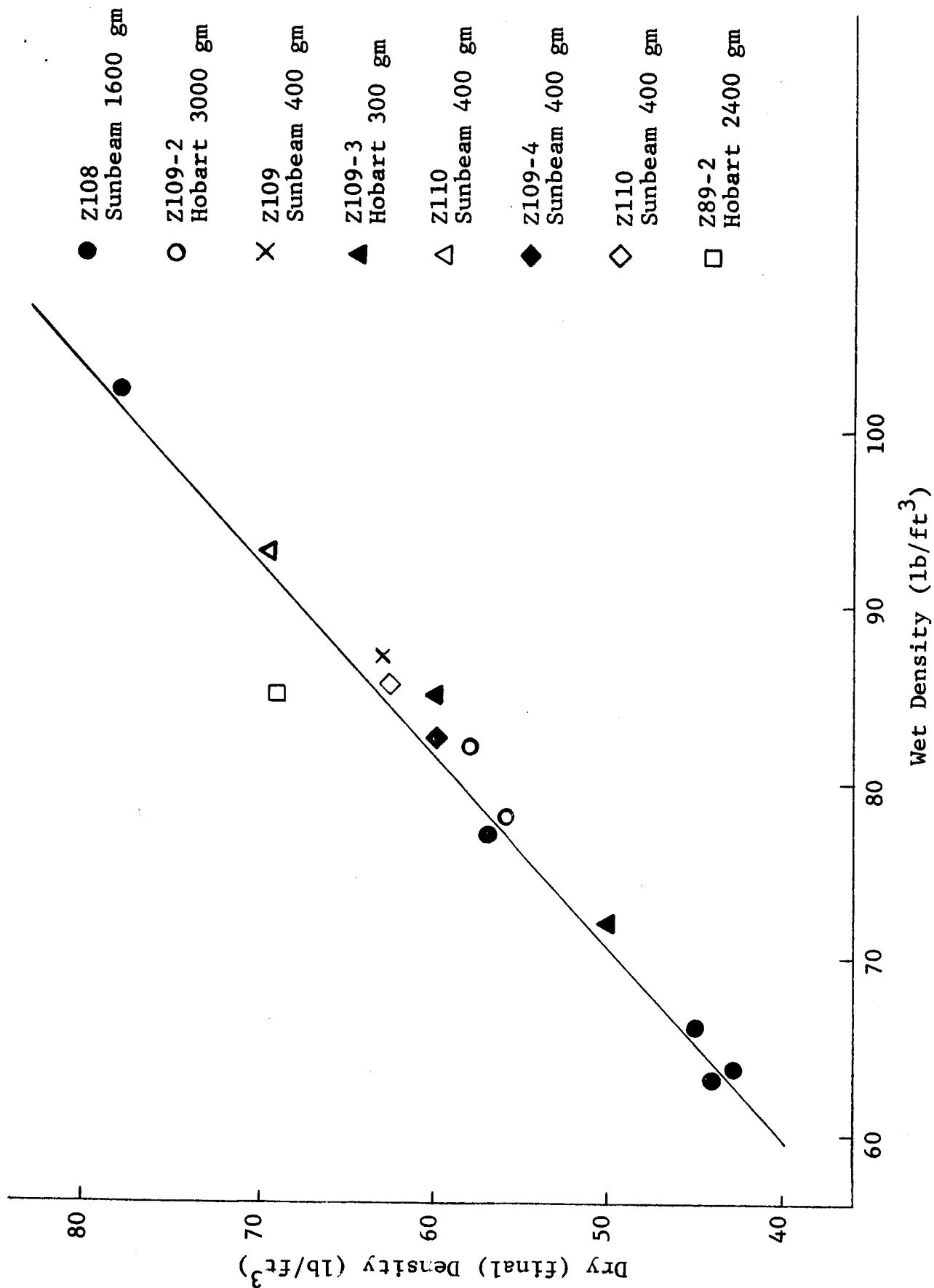
Fig. 11 - CORRELATION BETWEEN DRY (FINAL) AND WET DENSITIES
OF MECHANICALLY WHIPPED SILICATE-BONDED ZIRCON FOAMS
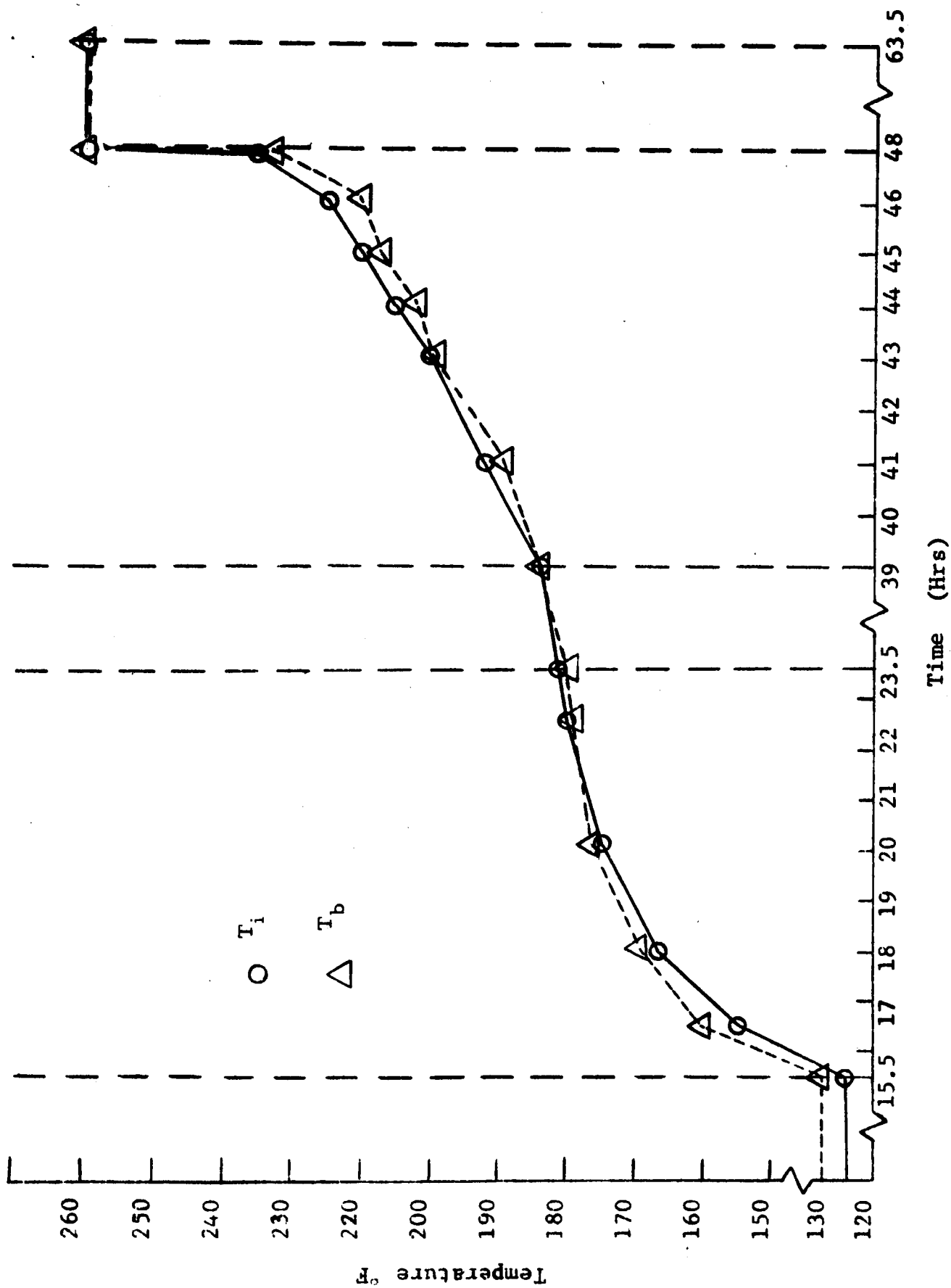
Fig. 12 - CURING CYCLE FOR FOAM ZP-58
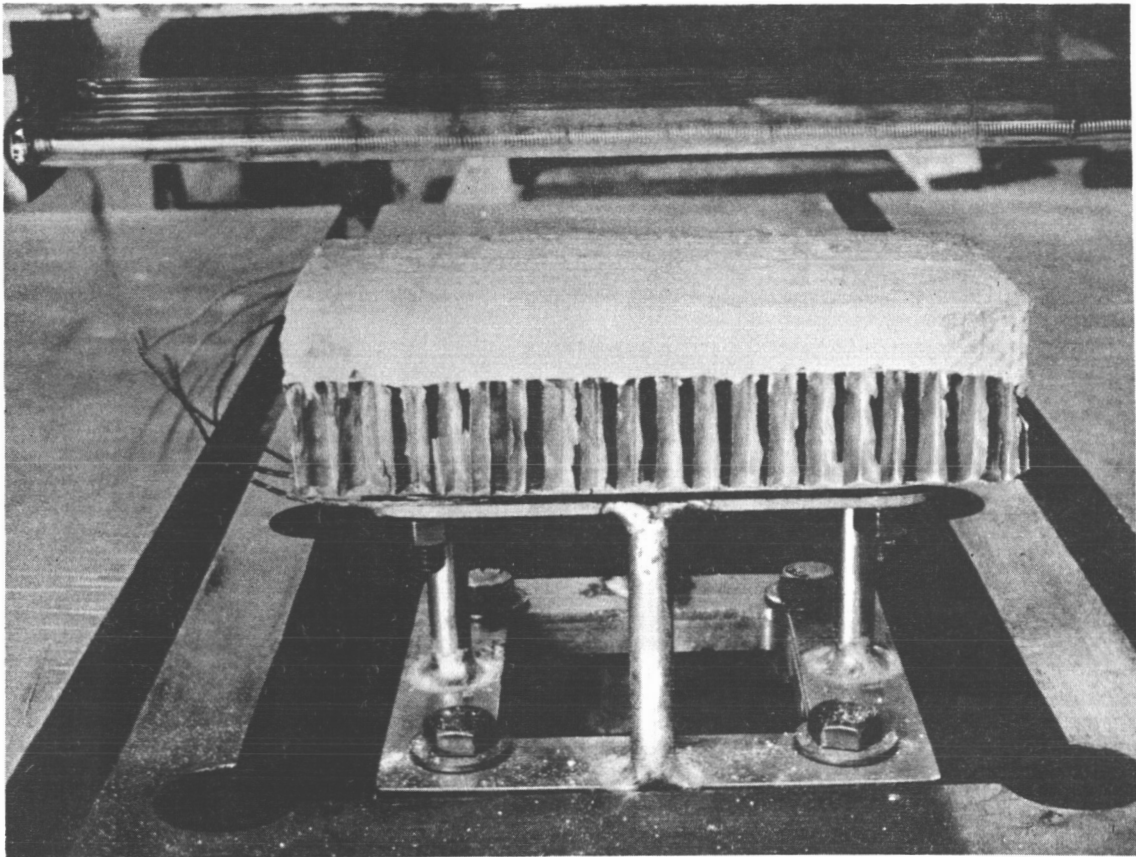
Fig. 13-TEST SETUP FOR SUBJECTING FOAMS TO
HEAT FLUX WITH SIMULTANEOUS
VIBRATION AND ACCELERATION
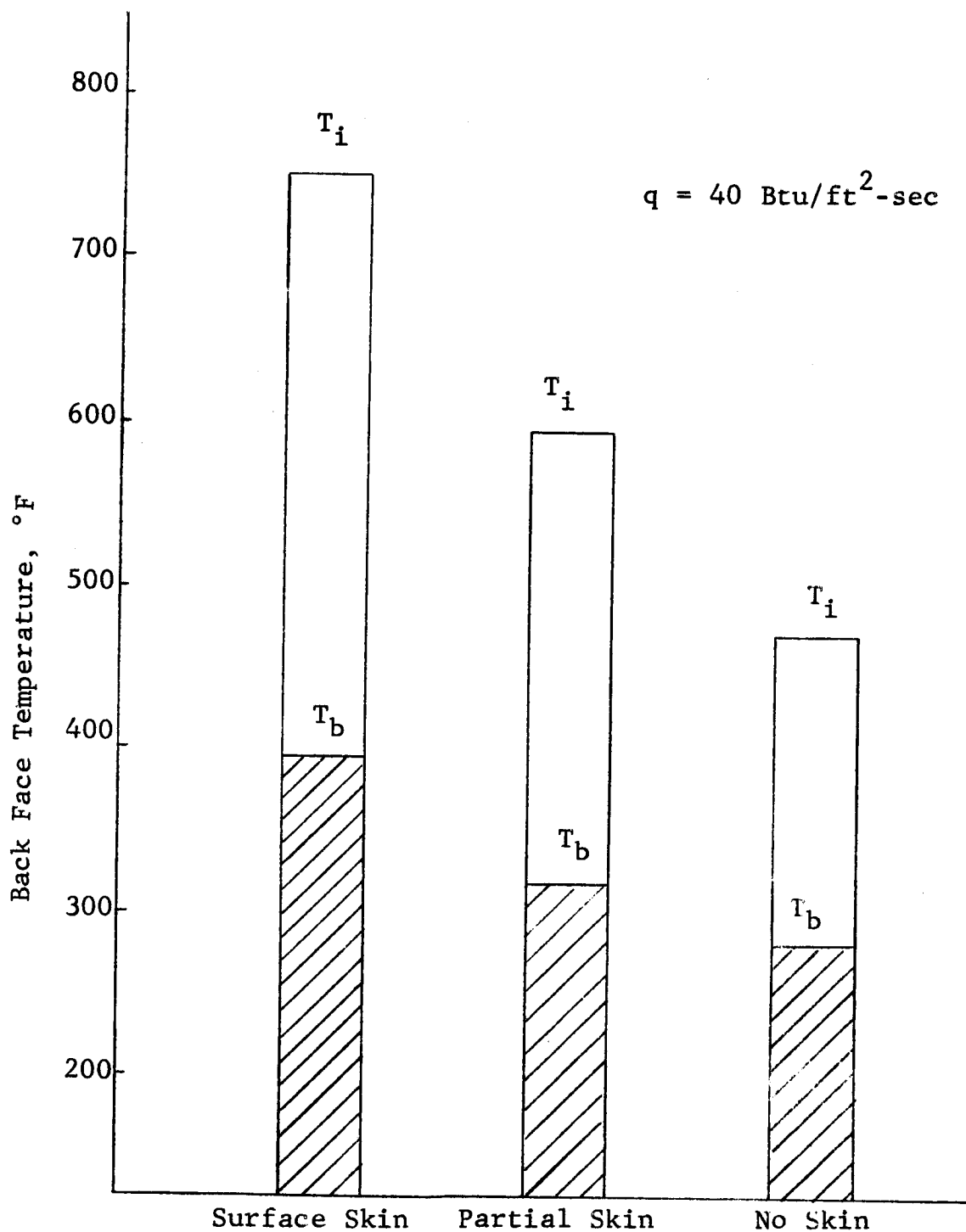
Fig. 14 - THE EFFECT OF SURFACE CONDITIONING ON THE
BACKFACE TEMPERATURE OF ZIRCON FOAM
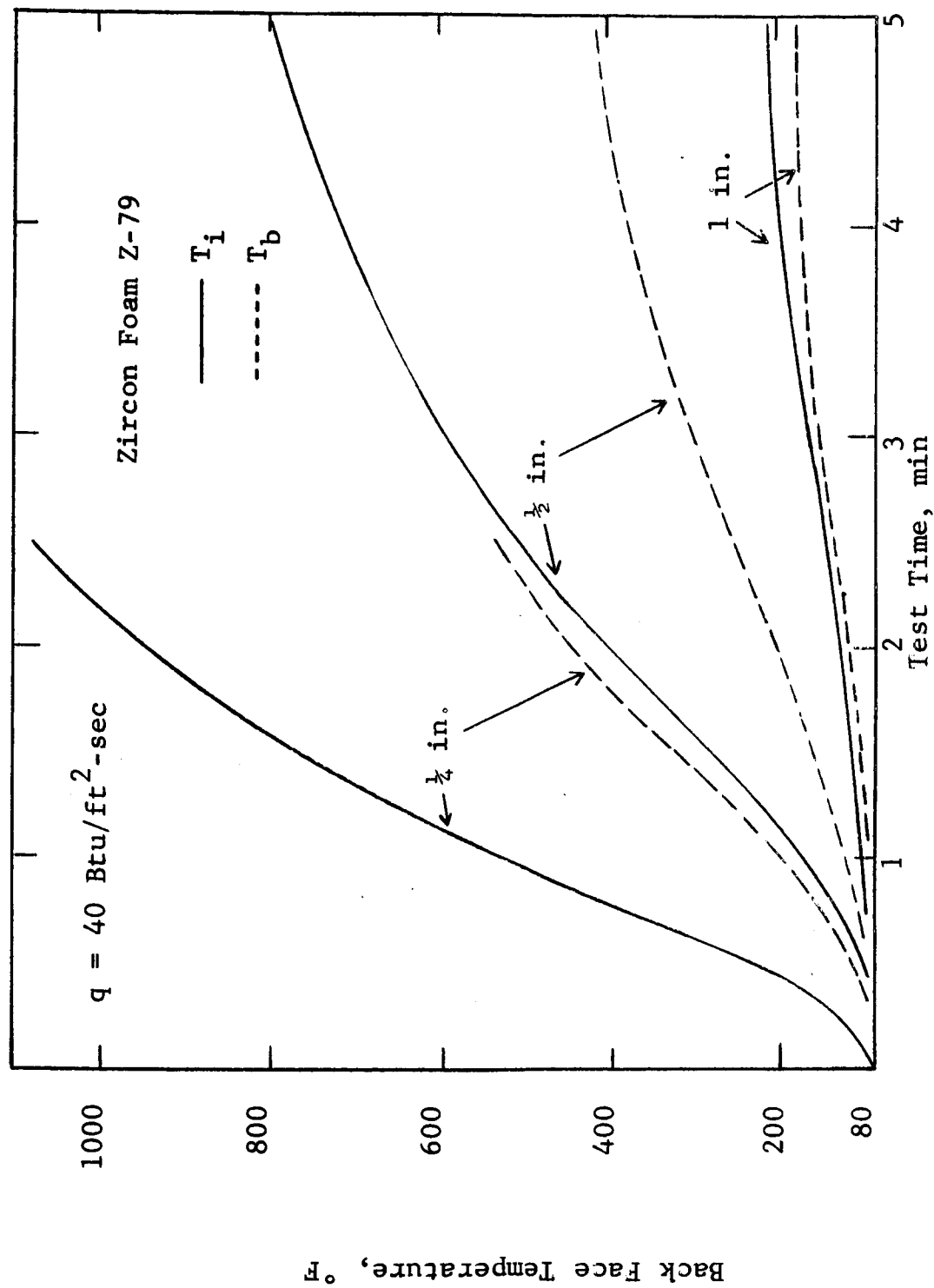Z-87 ($\frac{1}{2}$ IN. THICK), AFTER 5 MINUTES.

Fig. 15 - EFFECT OF FOAM THICKNESS OF INSULATIVE
CHARACTERISTICS OF RIGID HEAT SHIELDS
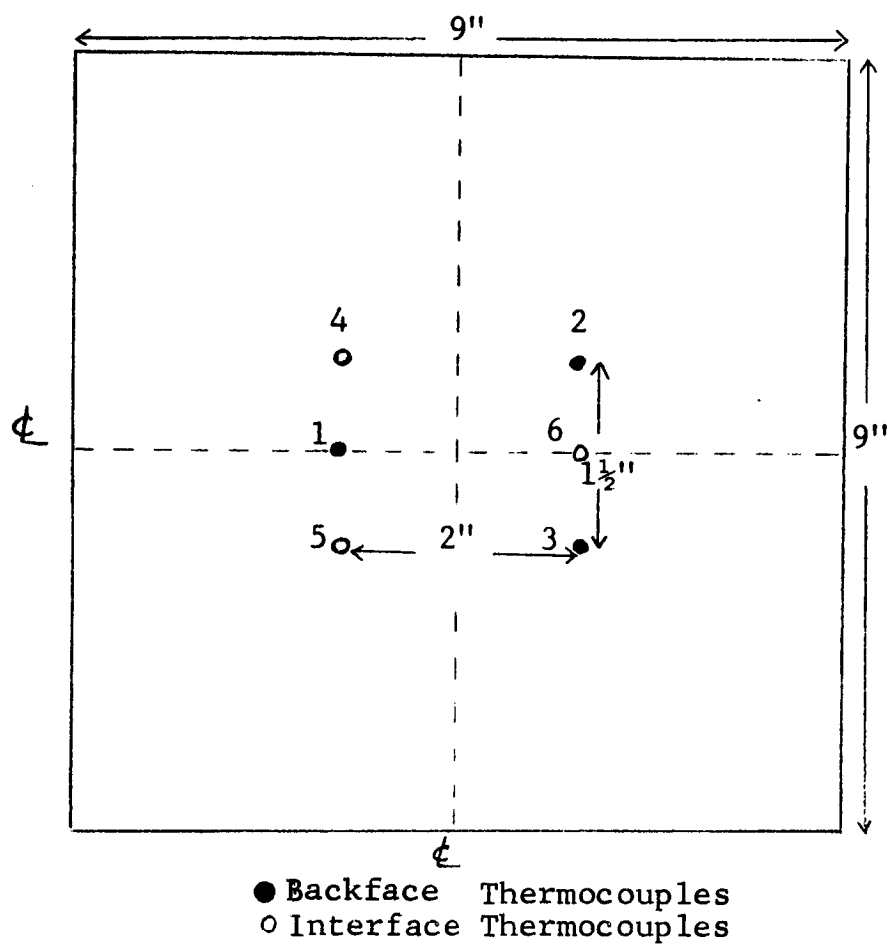
Fig. 16 - LOCATION OF THERMOCOUPLES
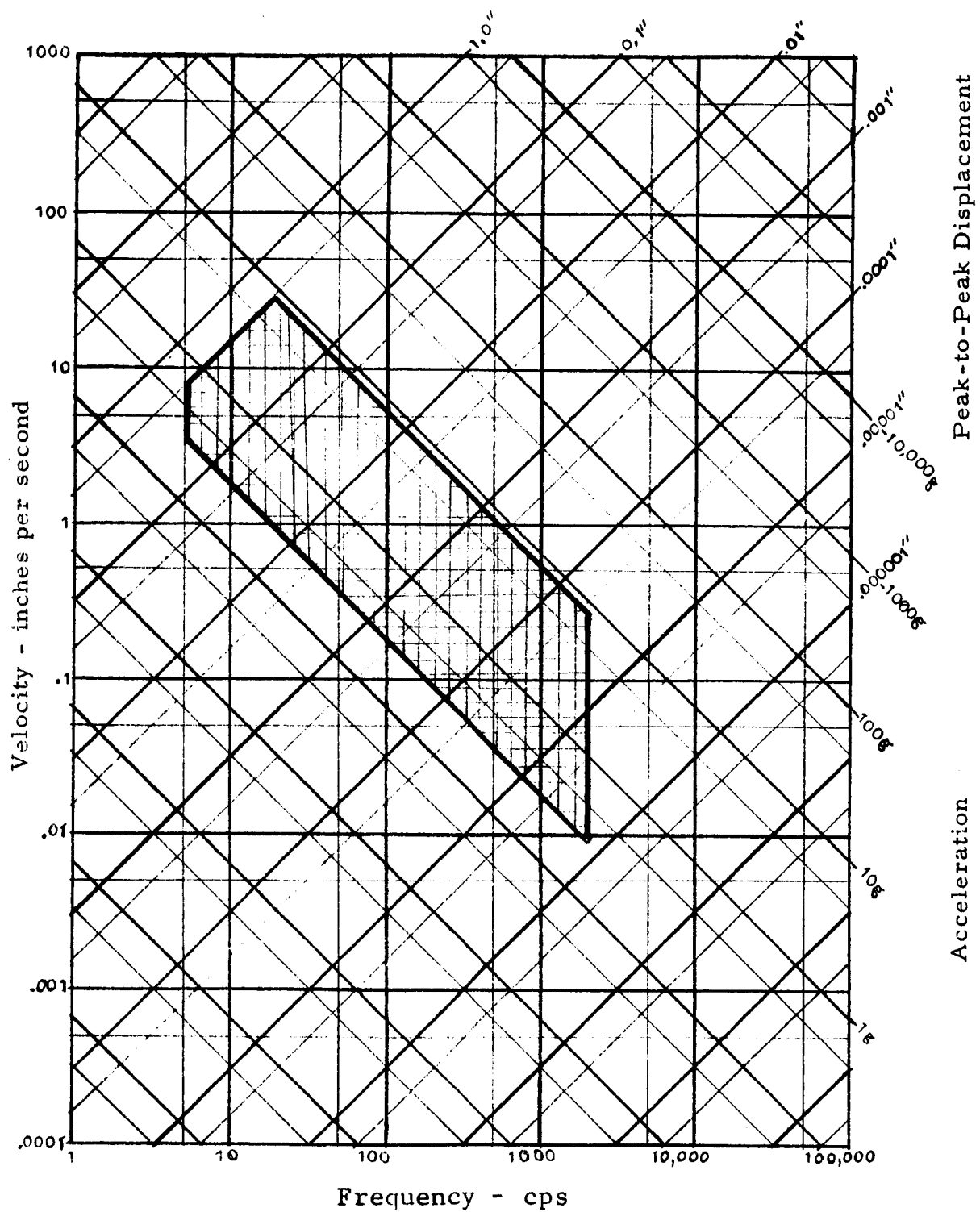ON 9 x 9 in. HONEYCOMB PANEL

Fig. 17- SINUSOIDAL SWEEP TEST PROFILE
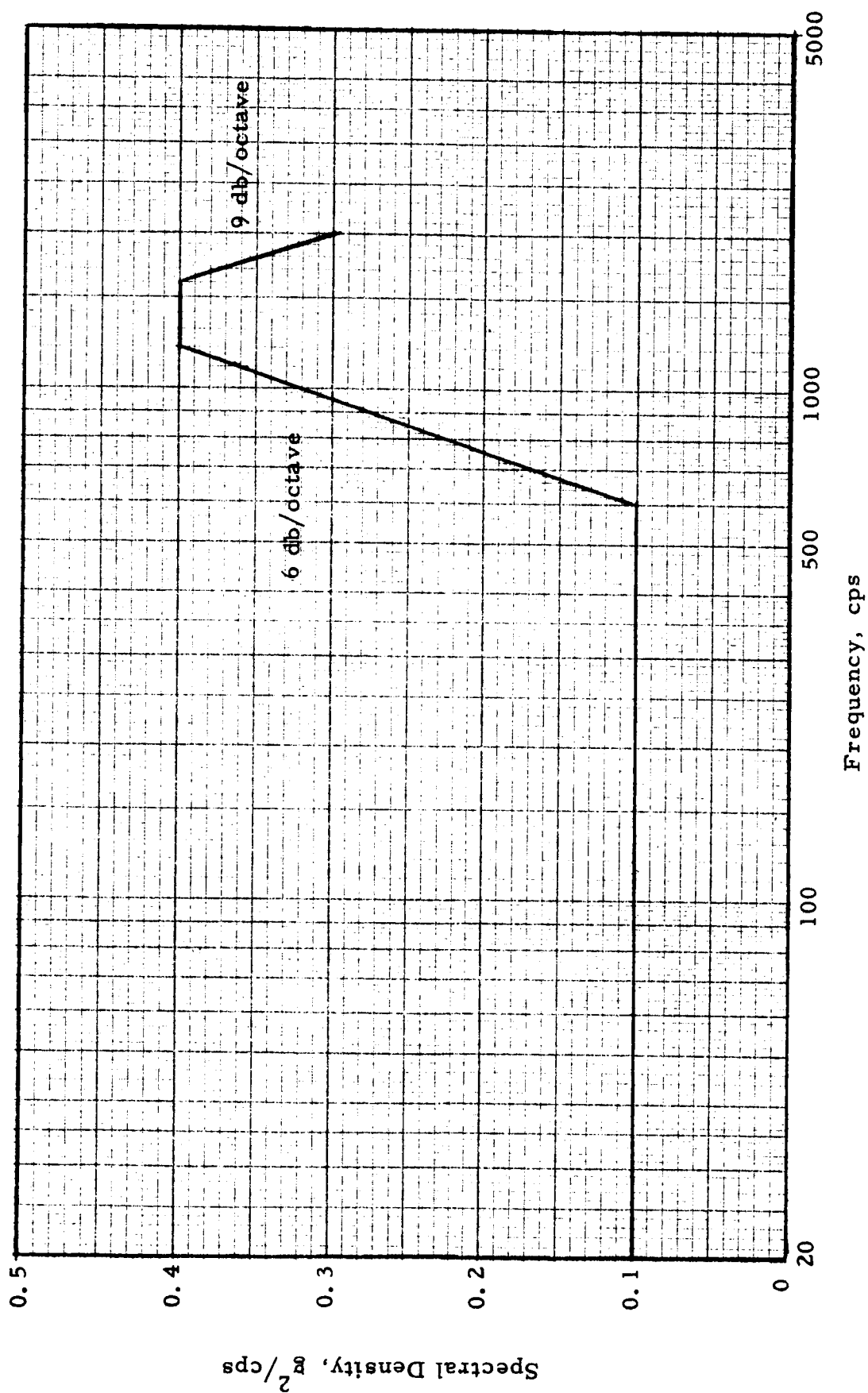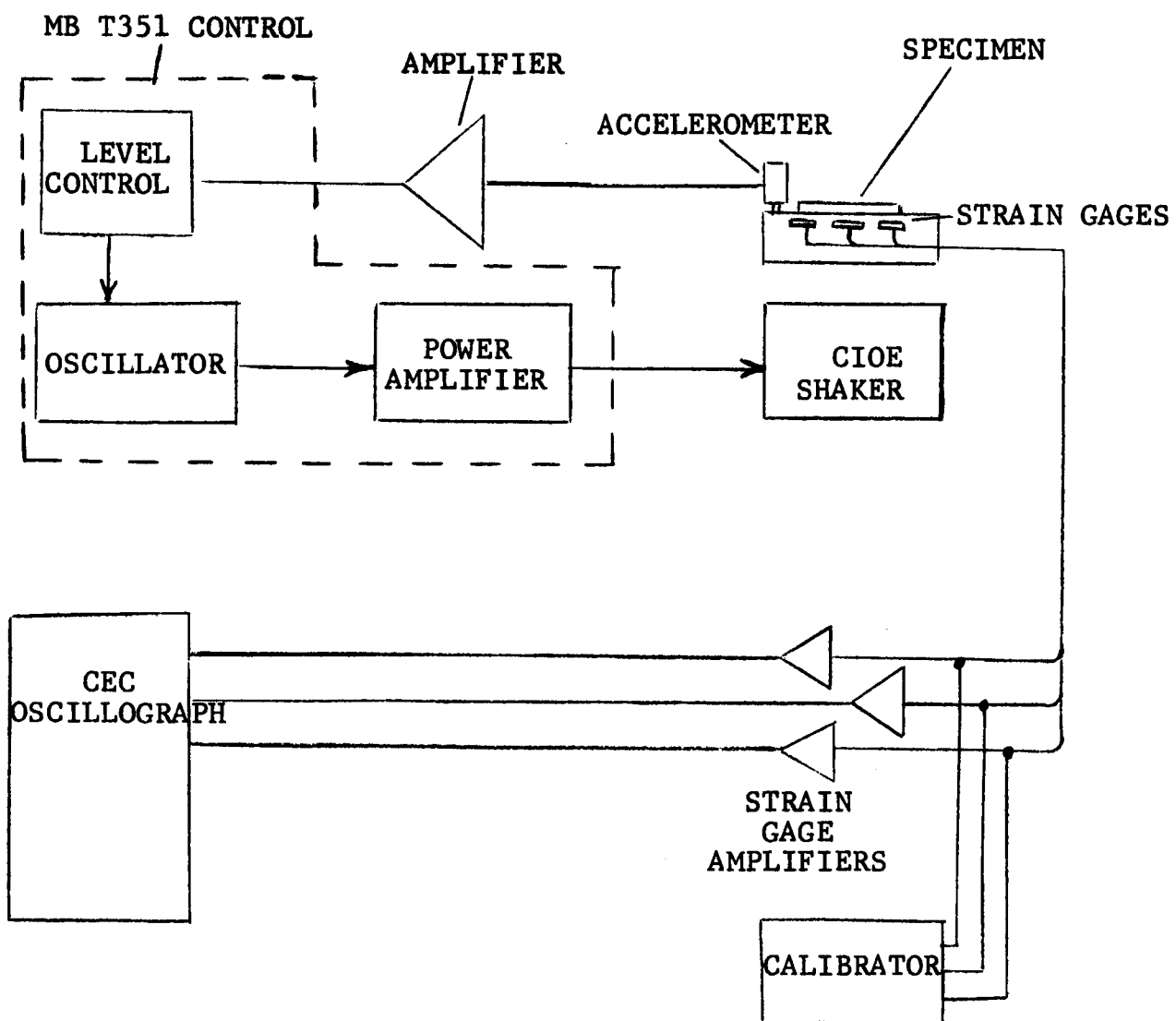(Shaded Area)

Fig. 18 - WIDE BAND RANDOM TEST SPECTRUM.
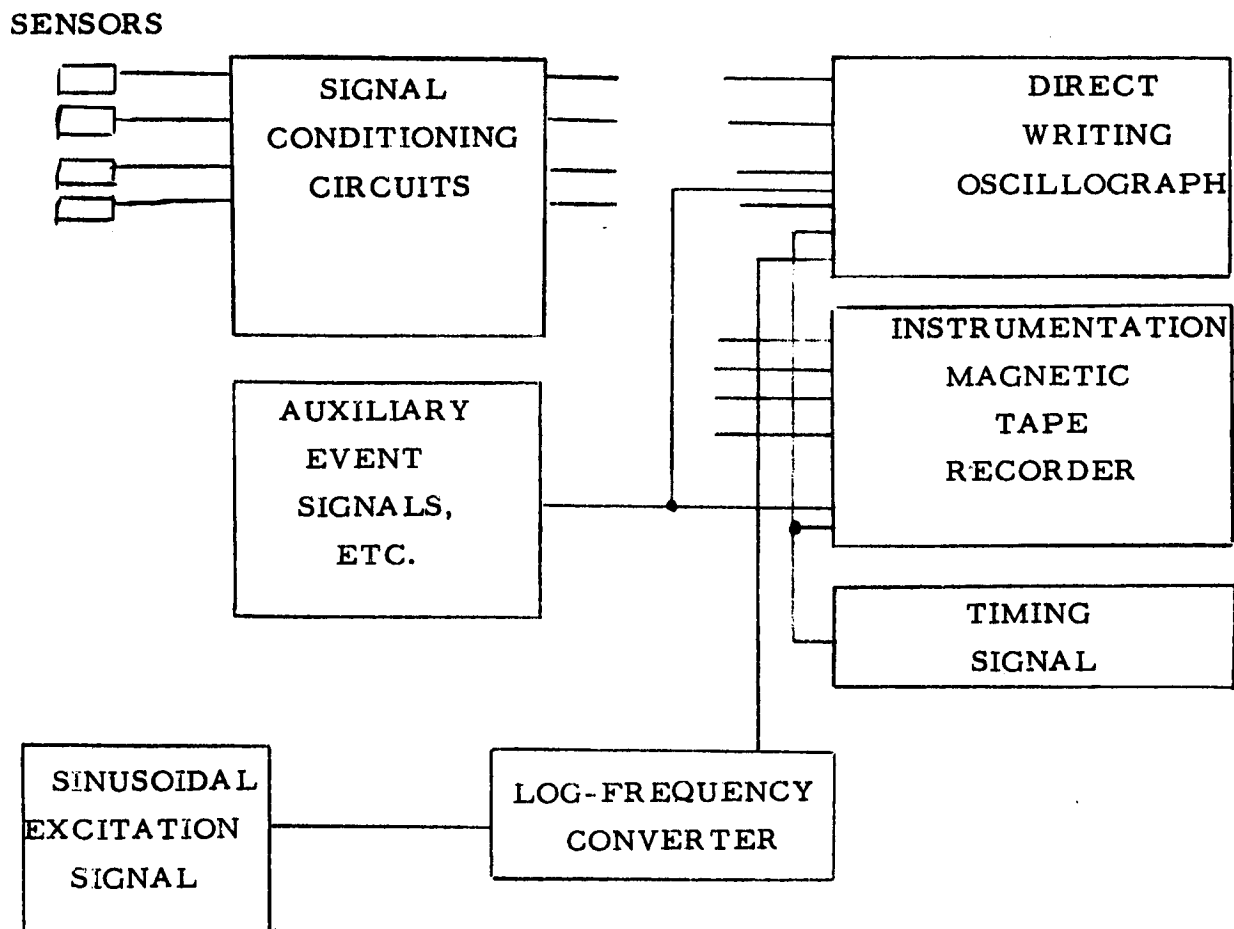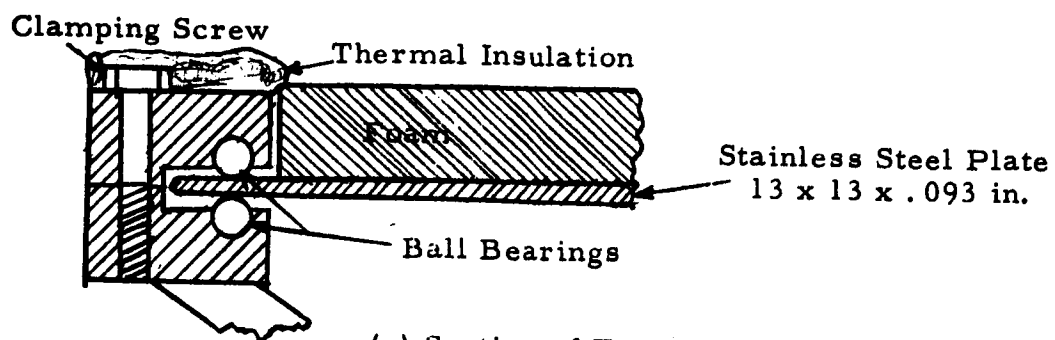
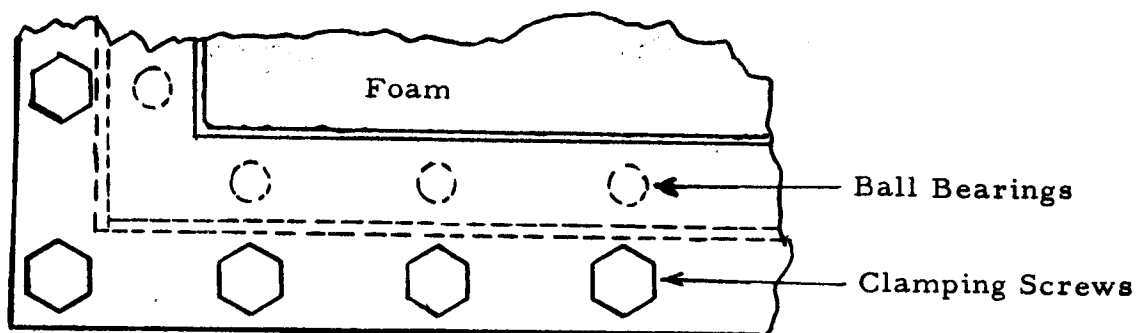-86-

Fig. 19 - BLOCK DIAGRAM OF THE SINUSOIDAL TEST
SET-UP

SENSORS

SIGNAL CONDITIONING CIRCUITS		DIRECT WRITING OSCILLOGRAPH
		INSTRUMENTATION MAGNETIC TAPE RECORDER
AUXILIARY EVENT SIGNALS, ETC.		TIMING SIGNAL
SINUSOIDAL EXCITATION SIGNAL	LOG-FREQUENCY CONVERTER	

Fig. 20 - SCHEMATIC DIAGRAM OF DATA RECORDING SYSTEM

Clamping Screw

Thermal Insulation

Foam

Stainless Steel Plate
13 x 13 x .093 in.

Ball Bearings

(a) Section of Foam Panel Mounting Frame

Foam

Ball Bearings

Clamping Screws

(b) Top View of Corner

Specimen Clamping
Fixture

Support Rods

Stiffening Rods

Vibration Diaphragm
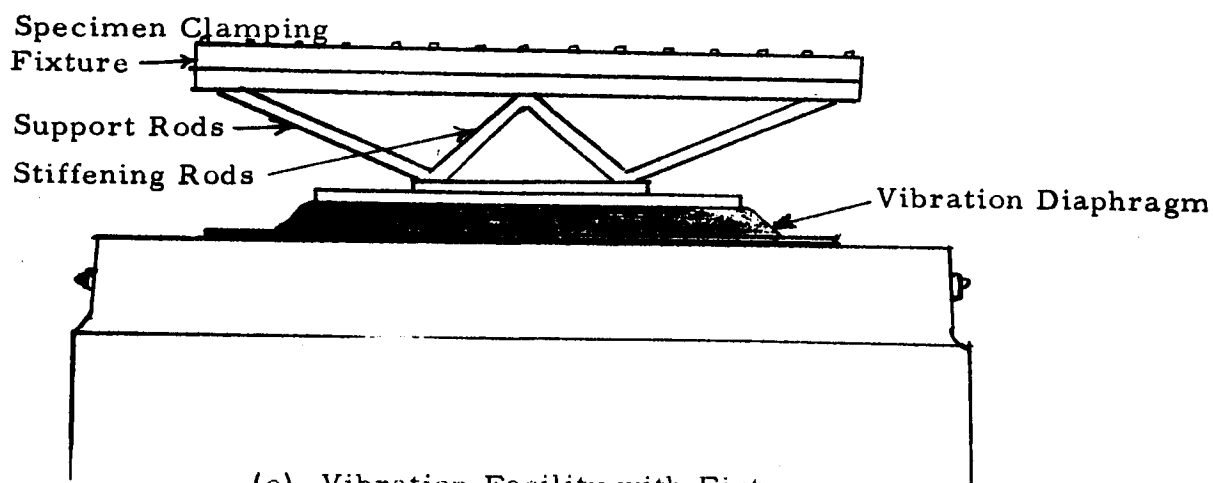
(c) Vibration Facility with Fixture
in Place

Fig. 21 - SCHEMATIC DIAGRAM OF FOAM-PANEL MOUNTING
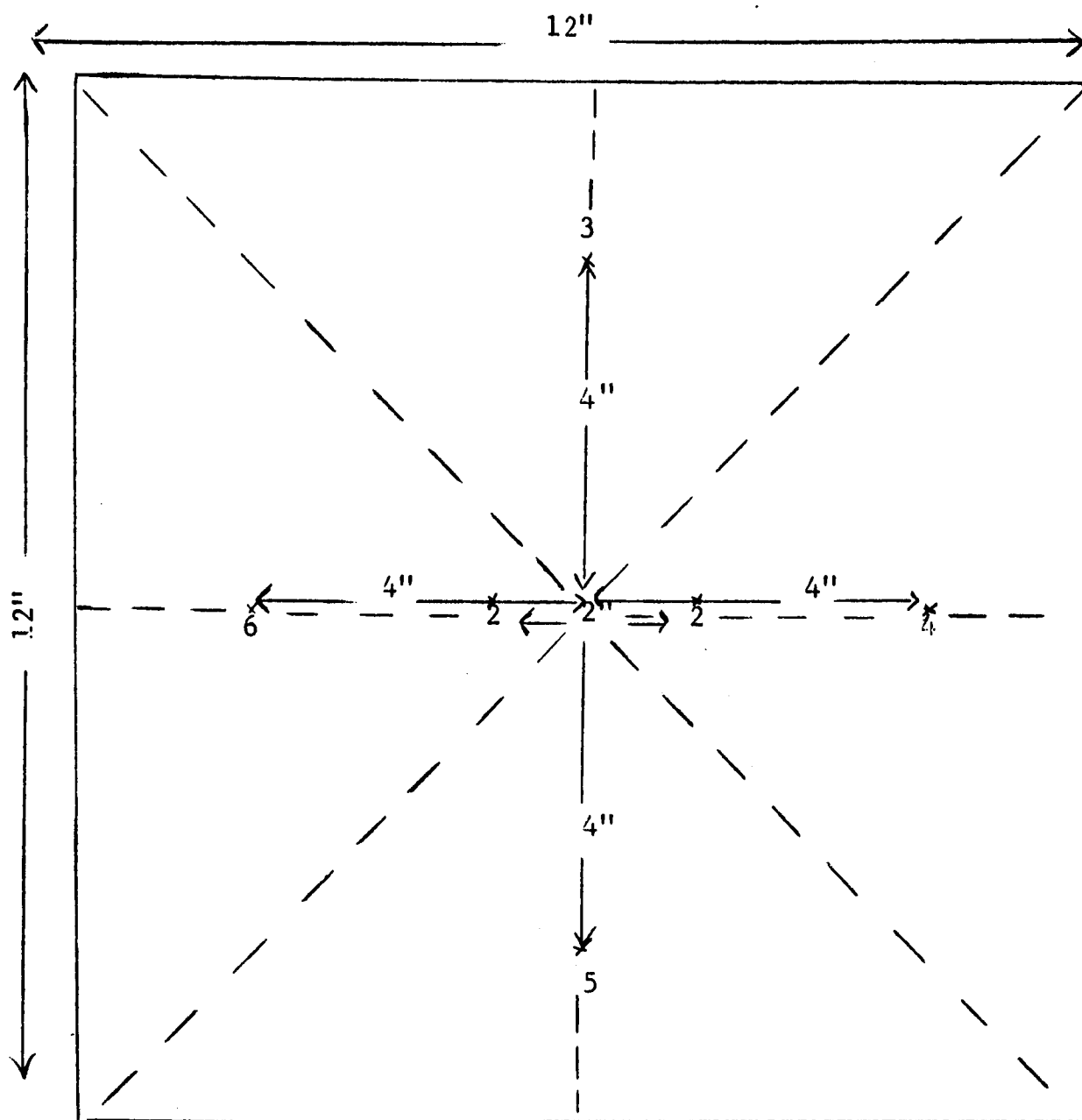UNIT FOR VIBRATION TESTING

Fig. 22 - THERMOCOUPLE POSITIONS ON SCALED-UP SUBSTRATE
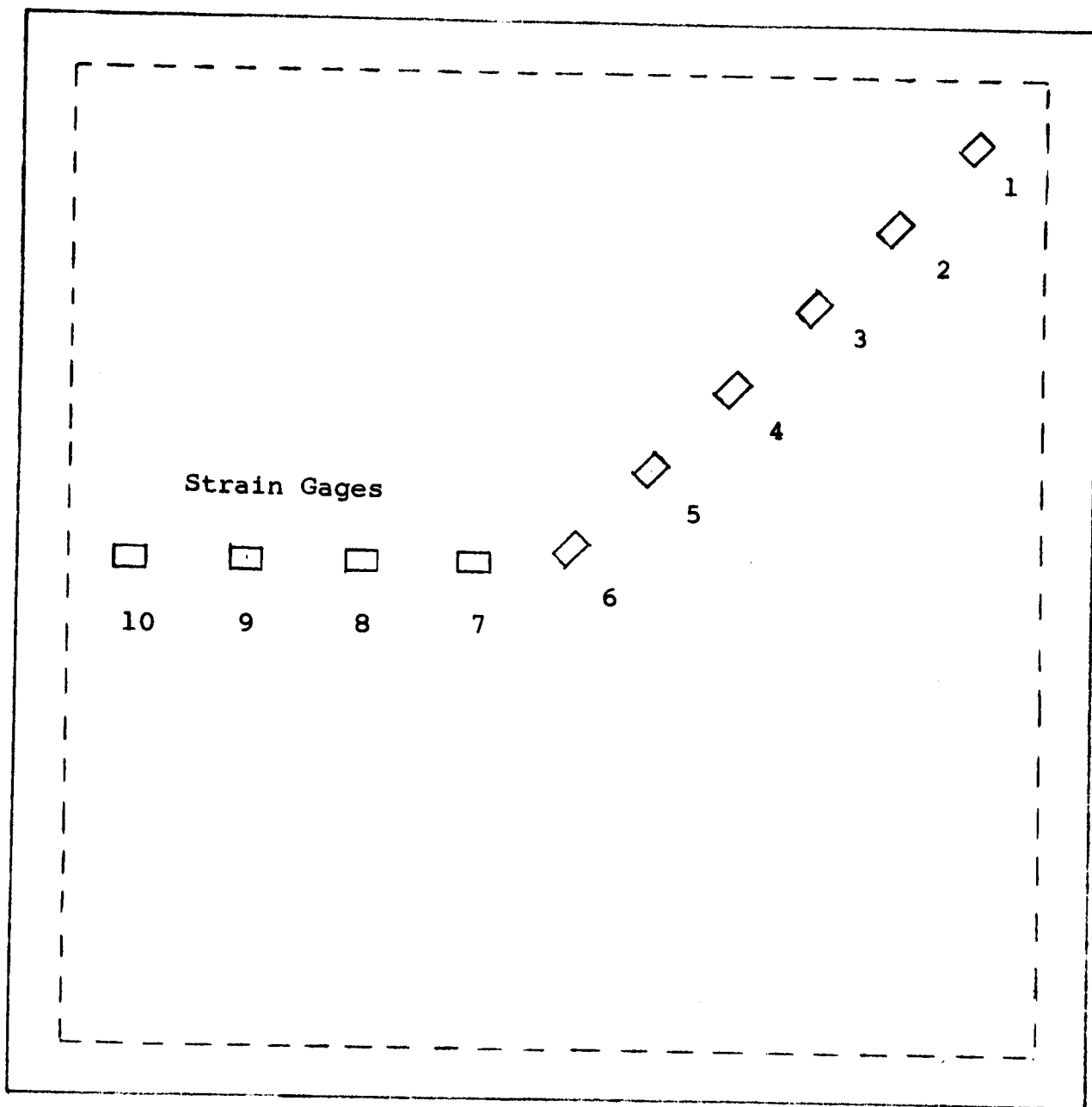
Fig. 23 - DRAWING OF SPECIMEN SHOWING PLACEMENT
OF STRAIN GAGES

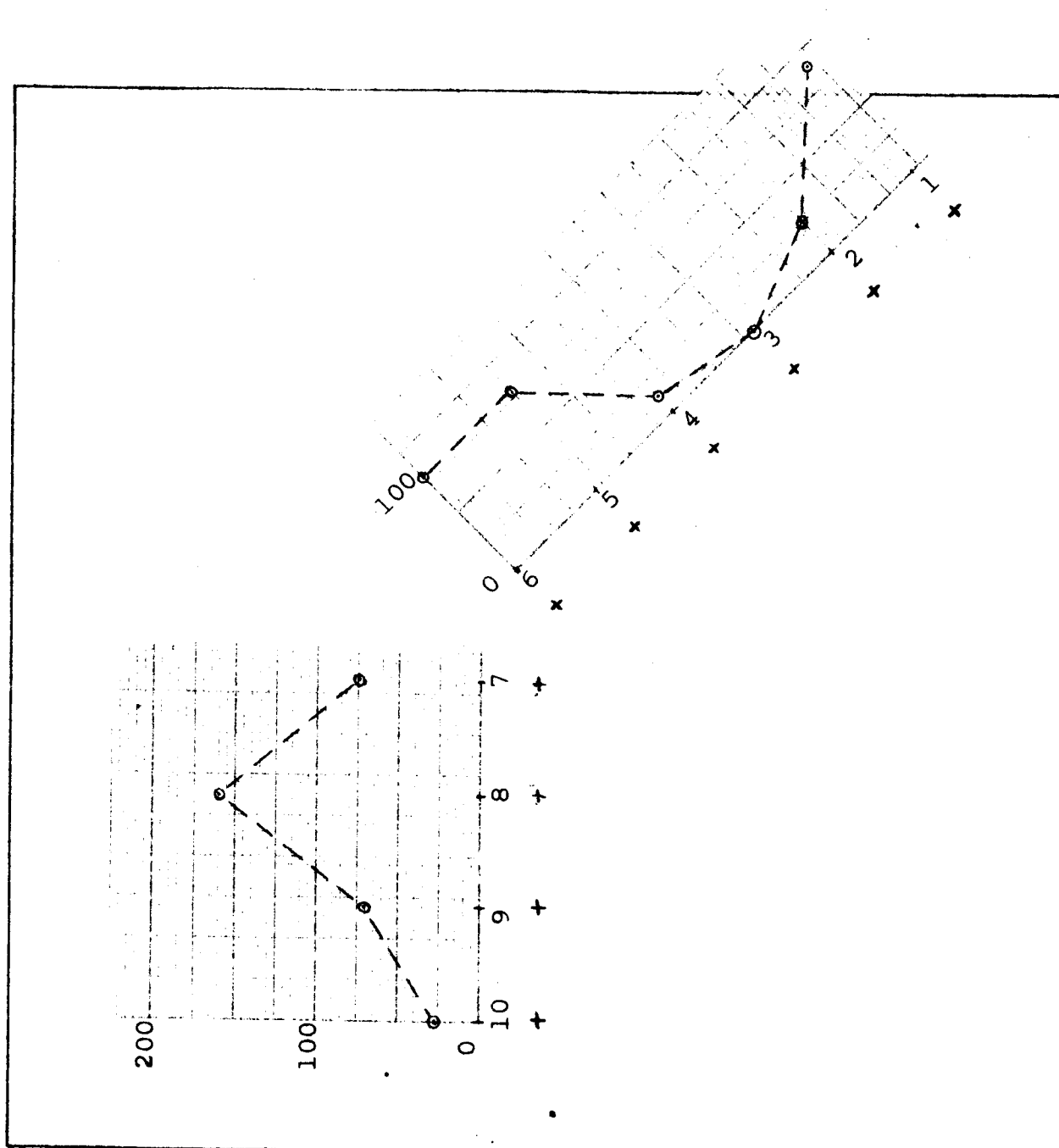Fig. 24 - RESPONSE LEVELS (10^{-6} in./in.) AT 180 cps EXCITATION
FREQUENCY PLOTTED AS A FUNCTION OF GAGE POSITION
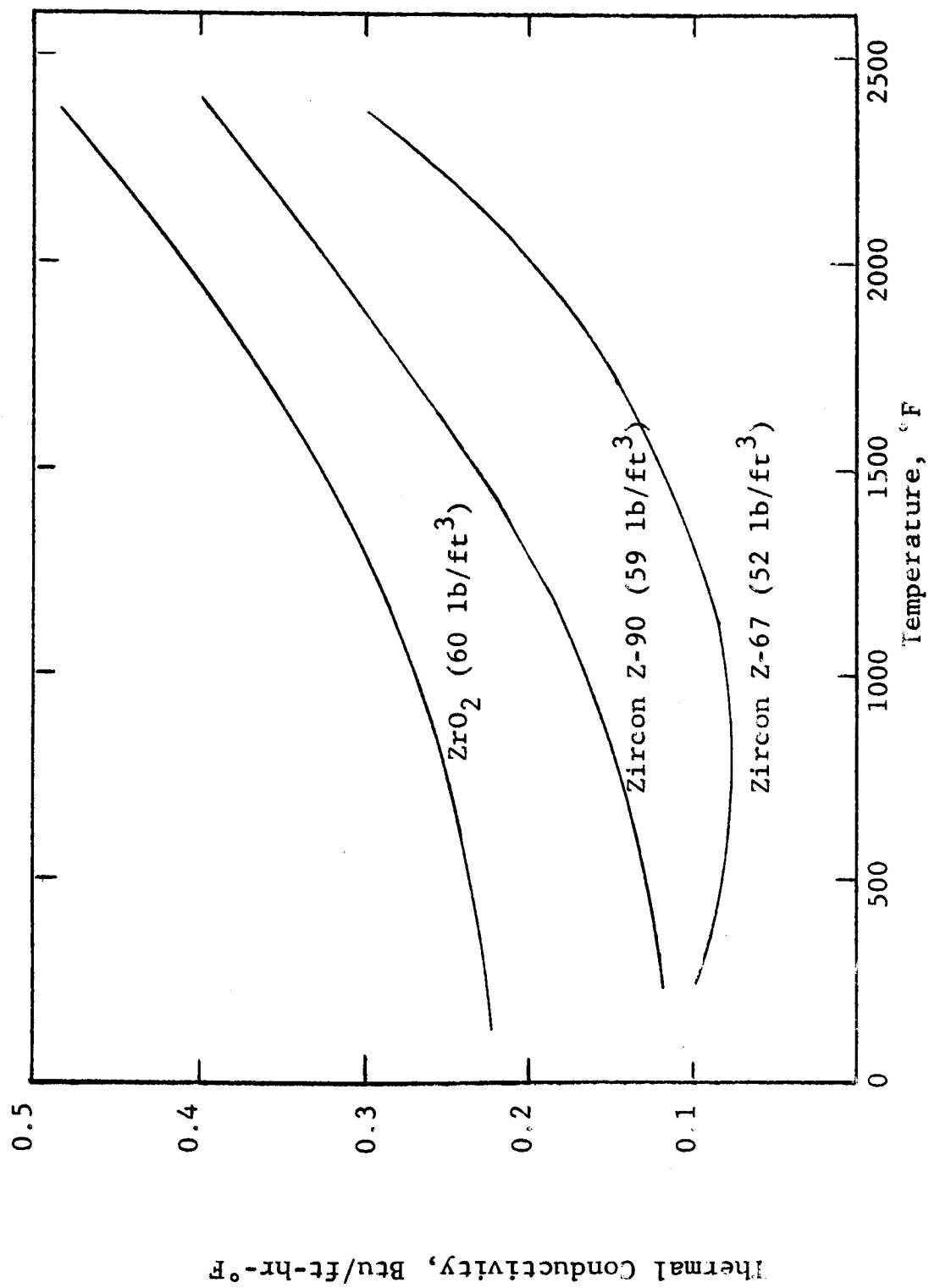SUPERIMPOSED ON THE Z-89 SPECIMEN OUTLINE

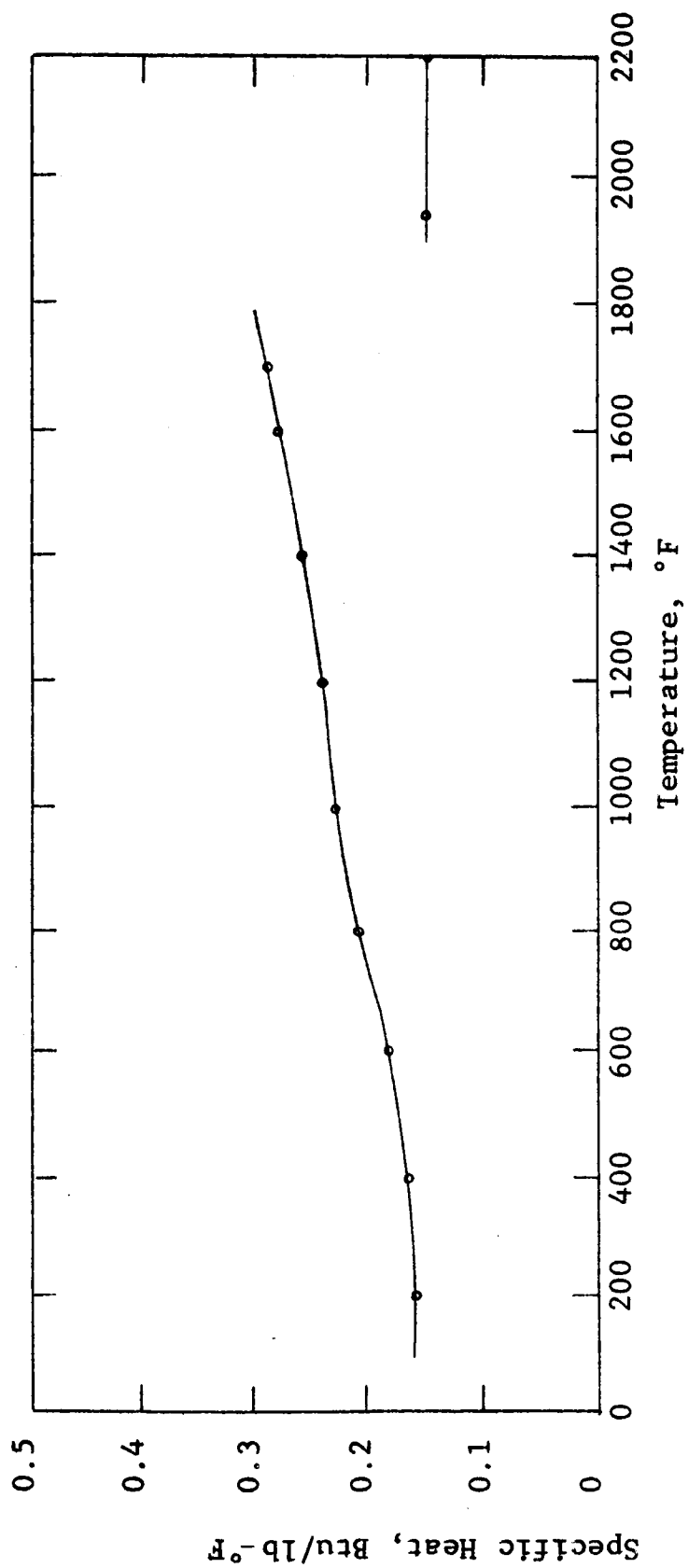Fig. 25 – THERMAL CONDUCTIVITY OF CERAMIC FOAMS

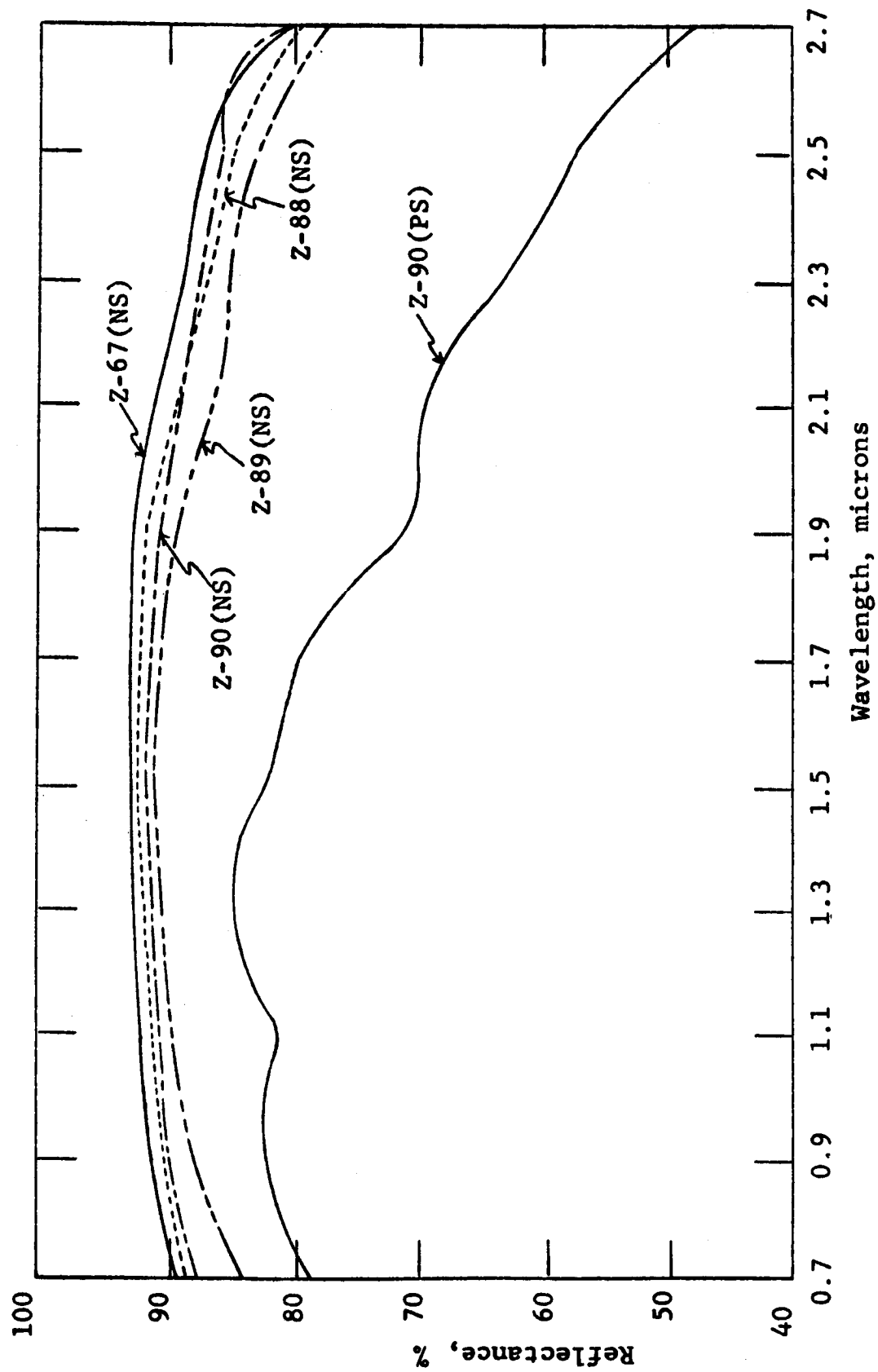Fig. 26 - SPECIFIC HEAT OF ZIRCON FOAM Z-90

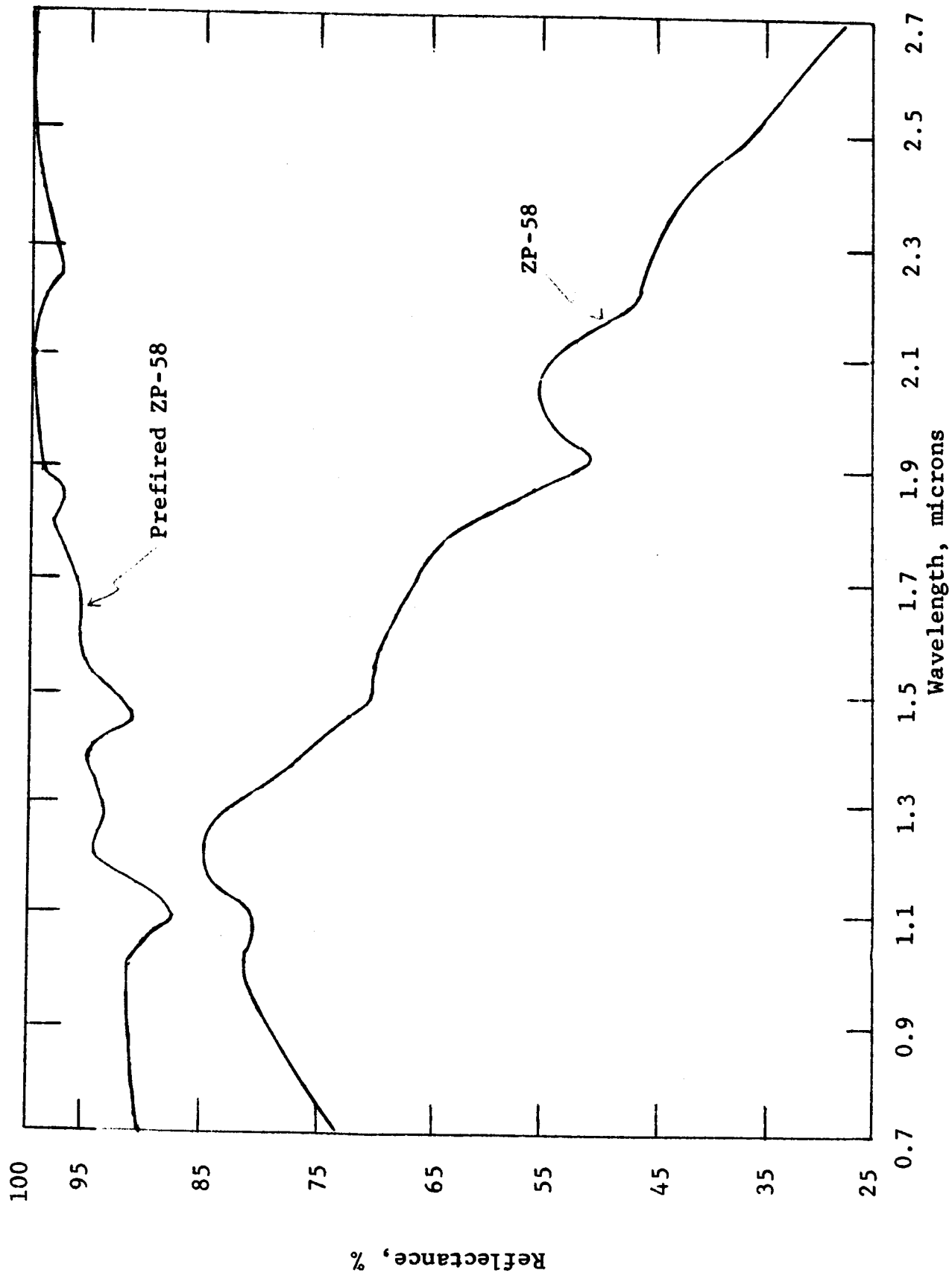Fig. 27 - ABSOLUTE REFLECTANCE OF SILICATE-BONDED ZIRCON FOAMS

Fig. 28 - ABSOLUTE REFLECTANCE OF PHOSPHATE-BONDED ZIRCON FOAMS, ZP-58 AND PREFIRED ZP-58

APPENDIX A

A DESCRIPTION OF THE STEPS INVOLVED
IN THE PREPARATION OF CASTABLE ZIRCON FOAMS

1. List of Materials

The raw materials used in the experimental foam formulations, along with the source of these materials, are shown below.

Material	Source
Albumin, egg Cat. No. A-388	Fisher Scientific Co. Fair Lawn, N. J.
Alumina, Tabular T61	Aluminum Co. of America 1501 Alcoa Building Pittsburgh, Pa.
Aluminum Hydrate, Hydral 710	Aluminum Co. of America 1501 Alcoa Building Pittsburgh, Pa.
AP Aluminum Phosphate, Mono 50% solution	Stauffer Chemical Co. Victor Division 380 Madison Ave. New York, N. Y.
Antaron FC-34	General Aniline Company 140 W. 51st St. New York, N. Y.
Armeen - Z	Armour and Co. 401 N. Wabash Chicago, Ill.
Calcium Aluminate, CA-25	Aluminum Co. of America 1501 Alcoa Building Pittsburgh, Pa.
Calcium Oxide Analytical Reagent	Mallinkrodt Chemical Works St. Louis, Mo.
Calcium Sulfate Powder (Plaster of Paris) Technical Code 1538 B & A	General Chemical Div. Morristown, N. J.

Ceric Oxide Purified	Fisher Scientific Co. Fairlawn, N. J.
Chromium Oxide, Sesqui Purified, B & A	General Chemical Div. Morristown, N. J.
Fiberfrax, long staple, medium and fine	Carborundum Co. Refractories and Electronics Div. P. O. Box 337 Niagara Falls, N. Y.
Gum Tragacanth, U.S.P.	E. H. Sargent & Co. 4647 W. Foster Chicago, Ill.
Clay: Kaolin, Ajax P	Georgia Kaolin Co. 1189 Mary St. Elizabeth, N. J.
Magnesium Oxide Powder Reagent ACS Code 1917 B & A	General Chemical Div. Morristown, N. J.
Mearl SW 2336	Mearl Chemical Corp. Roselle Park, N. J.
Mullite, -325 mesh	H. K. Porter & Co. 8708 S. Bennett Ave. Chicago, Ill.
Mullite, "Mullite B, 325F"	Norton Co. New Bond St. Worchester, Mass.
Nickel, metal, powder	Fisher Scientific Co. 1458 N. Lamon Ave. Chicago, Ill.
Potassium Silicate, PS-7	Sylvania Electric Product, Inc. Chemical & Metallurgical Div. Towanda, Pa.
Silicon Carbide Powder "Norton Crystolon B"	Norton Co. New Bond St. Worchester, Mass.

Sodium Silico Fluoride	Fisher Scientific Co. 1458 N. Lamon Ave. Chicago, Ill.
Titanium Oxide Sub micron, pigment grade	National Lead Co. Titanium Alloy Div. 111 Broadway New York, N. Y.
Titanium Oxide, Coarse, TAM Titanox T6	National Lead Co. Titanium Alloy Div. 111 Broadway New York, N. Y.
Zinc Oxide U.X.P. Code 2451 B & H	General Chemical Div. Morristown, N. J.

Zircon
(a) Zircon A
    "Tam Zircon Milled"
(b) Zircon
    "G" zircon milled
(c) Superpax
    "Superpax A"
(d) Granular Zircon
    "Tam Zircon Granular"
	National Lead Co.
	Titanium Alloy Div.
	111 Broadway
	New York, N. Y.

(e) "Ultrox 100"	Metal and Thermit Co. 415 E. 151st St. E. Chicago, Ind.

2. Surface Conditioning of Substrates

a. Honeycomb Substrates

The honeycomb with open face structure is first scrubbed and washed thoroughly with Alconox, rinsed with acetone, given a light sand blast, and then rinsed with acetone again.

The base coats are painted on with a brush. Different base coats are used for the silicate-bonded and phosphate-bonded foams. Each coat is about 6 mil thick.

The silicate base coat is applied in two coatings. The first coat is allowed to dry for 1 hr before the second coat is applied. After the second coat has dried at room temperature for 1 hr, the substrate is placed in the infra-dryer at a low temperature of 120°F for 15 hrs. A final cure at 260°F for 2 hrs is carried out.

The phosphate base coat is applied in a single coating, in a similar manner. A two hour air dry is followed by a 120°F heat cure in an infra-dryer for 15 hrs, after which it is subjected to a final cure at 260°F for 2 hrs.

b. Stainless Steel Plate Substrates
(12 x 12 x 0.093 in.)

A similar procedure is used for cleaning the plates and applying the base coat. The only difference is that prior to applying the base coat, the surface of the plates are lightly roughened with a disk sander, using Norton No. 36-E2 abrasive paper. The metal particles are blown off and the surface again rinsed with acetone.

3. Preparation of Base Coat

Base coat mixtures for both silicate and phosphate type foams were made by placing ingredients in the ball mill and wet milling for 2 hrs. For smaller amounts of base coat, mixing with a mortar and pestle is sufficient.

IIT RESEARCH INSTITUTE

Composition of Silicate Base Coat

Alcoa T61 Al_2O_3	500g
Potassium Silicate (PS-7)	150cc
Water	70cc
Gum Tragacanth	1.5g

Composition of Phosphate Base Coat

Alcoa T61 Al_2O_3	25g
Hydral 710	2.0g
AP	10cc
H_2O	5.0cc
Gum Tragacanth	0.15g
Cr_2O_3	1.0g

4. **Foaming of Scaled-Up Silicate-Bonded Castable Zircon Foam, Z-89**

The nominal composition and proportions of materials used are:

Item No.		
1	Zircon	1200g
2	Zircon A	1200g
3	Ajax P Kaolin	48g
4	Na_2SiF_6	101.6g
5	Albumin	5.1g
6	Water (distilled)	360cc
7	PS-7	792cc
8	Fiberfrax (medium)	240g

Na_2SiF_6 is lightly crushed in a motar and pestle and passed through a 100 mesh screen. Then, items 1 through 4 are V-blended for 15 min and ball-milled for 1 1/2 hrs. A Hobart C 100

type mixer with a stainless steel wire whip attachment was used for the foaming process. This mixer has a 3-speed action:

a. Low speed 144 rpm
b. Medium speed 248 rpm
c. High speed 450 rpm

The albumin is dissolved in water (approximately 20 mins); PS-7 is added and mixing in the Hobart mixer at low speed is continued for 1 min. Fiberfrax (cut into > 1/8 in. < 1/4 in. lengths) is added and low speed mixing is continued for another 2 min. The blended powder is added and mixing is continued at low speed for 2 min, medium speed for 2 min, and high speed for 1 min. A wet density measurement is taken at this point. If a wet density of 82 lb/ft^3 is not attained, mixing is continued until this density is reached. This wet-density is required to attain a final density of 60 lb/ft^3.

5. Foaming of Scaled-Up Phosphate-Bonded Castable Zircon Foam, ZP-58

The nominal composition and proportions of materials used are:

Item No.

1	Zircon A	1500g
2	Zircon	1200g
3	Ajax P Kaolin	30g
4	ZnO	120g
5	MgO	30g
6	Plaster of Paris	225g
7	Water (distilled)	750cc
8	Monoaluminum phosphate (solution 50%)	1425cc
9	Fiberfrax (long fiber medium)	150g
10	Albumin	7.5g

Items 1 through 6 were weighed and V-blended for 15 min and then ball-milled for 1 1/2 hrs.

Albumin powder (7.5g) was stirred into 750cc of distilled water and allowed to dissolve. Solution of the albumin was aided by gentle, intermittent stirring and breaking up of lumps, while keeping the formation of bubbles to a minimum. Complete dissolution of the albumin powder takes approximately 20 to 30 min. During the first 15 min most of the lumps were dispersed by hand. In the last 2 to 3 min the mixer was turned on low speed. Mono-aluminum phosphate is added to the albumin solution and the mixer turned on at speed No. 1 for 1 min.

Fiberfrax (cut to lengths of > 1/8 in. < 1/4 in.) is then added to the solution. The mixer is run on low for 3 min longer and stopped at 1 min intervals to remove any fibers that stick to the wire whip. After three minutes, the solution should be foamed.

While the mixer is still running, the blended powder (items 1 through 6) is then added. This takes approximately 1 min. Mixing is then continued with speeds of 2 min on low, 1 min on medium, and 1 min on high.

At this point a sample of the foam is taken out for a wet density measurement. For ZP-58 it was found that a wet density of approximately 88 lb/ft^3 gave a cured foam density near 60 lb/ft^3. Mixing is continued until the desired wet density is attained.

6. Casting and Curing of Foams

Before casting the foamed mix onto the substrate (honey-combs and/or plates), a mold has to be placed around it. This consists of wire reinforcements supporting the Saran Wrap plastic covered cardboard mold around the substrate.

For 1/2 in. thick silicate-bonded zircon foams, the wire support was flush with the top surface of the foam, as the plastic

wrapper is placed on the foam surface. This results in the NS (no skin) or PS (partial skin) types, depending on the total time the wrapper is used during curing.

In the case of 1/2 in. thick phosphate-bonded zircon foams, the wire supports (covered with a thick paper towel, "Scott Wipers") extend 4 1/2 in. above the surface of the foam for 12 x 12 in. areal dimensions, and 2 1/4 in. for foams of 9 x 9 in. areal dimensions. A cardboard cover is then placed on these wire supports above the surface of the foam. This results in CHCB type or controlled humidity cardboard type surface conditioned foams.

Prior to pouring the foamed mix on the substrate, base-coated substrates with wire attachments are preheated in the infra-dryer at 150°F for 1 hr.

The foam is poured to the height of the open face structure and the foam worked into the corners with a stiff brush. The remainder of the foam is then poured to the desired height which is 5/8 in.

Subsequent drying and curing for the silicate and phosphate-bonded zircon foams is carried out, as described in Section IV. In both cases, this consists of a curing schedule up to 220°F in the infra-dryer, followed by a final cure at 260°F in an oven.